

University of Vermont

UVM ScholarWorks

Graduate College Dissertations and Theses

Dissertations and Theses

2023

Dengue Virus Modulation Of Genome Instability In Vero E6 Cells

Erica Nicole Lamkin
University of Vermont

Follow this and additional works at: <https://scholarworks.uvm.edu/graddis>



Part of the [Biology Commons](#), [Genetics and Genomics Commons](#), and the [Virology Commons](#)

Recommended Citation

Lamkin, Erica Nicole, "Dengue Virus Modulation Of Genome Instability In Vero E6 Cells" (2023). *Graduate College Dissertations and Theses*. 1691.

<https://scholarworks.uvm.edu/graddis/1691>

This Thesis is brought to you for free and open access by the Dissertations and Theses at UVM ScholarWorks. It has been accepted for inclusion in Graduate College Dissertations and Theses by an authorized administrator of UVM ScholarWorks. For more information, please contact schwirks@uvm.edu.

DENGUE VIRUS MODULATION OF GENOME INSTABILITY IN VERO E6 CELLS

A Thesis Presented

by

Erica Nicole Lamkin

To

The Faculty of the Graduate College

of

The University of Vermont

In Partial Fulfilment of the Requirements
For the Degree of Master of Science
Specializing in Microbiology and Molecular Genetics

May, 2023

Defense Date: April 4, 2023
Thesis Examination Committee:

Nimrat Chatterjee, Ph.D., Advisor
Randall Holcombe, MD, MBA, Chairperson
Janet Murray, Ph.D.
Pei Zhou, Ph.D.
Cynthia J. Forehand, Ph.D., Dean of the Graduate College

ABSTRACT

Dengue virus (DENV) is the fastest-spreading arthropod-borne virus in the world. Dengue is characterized as a major global public health challenge in tropical and subtropical nations by the World Health Organization. The number of dengue cases globally has increased 8-fold in the past two decades, with 100 to 400 million cases occurring annually. While most patients with dengue fever are asymptomatic, dengue infection carries the possibility of severe and potentially fatal febrile illness. Approximately 1 in 4 individuals infected with dengue virus develop symptomatic dengue infection, often presenting as mild to moderate, nonspecific, acute febrile illness. A smaller subset of these individuals, about 1 in 20 infected with DENV, go on to develop severe dengue. Dengue fever is characterized by a high fever, headache, rash, myalgia, arthralgia, and stomachache. Dengue fever can progress into severe dengue, characterized by thrombocytopenia, vascular leakage, hypotension, and potentially fatal hypovolemic shock.

Given the COVID-19 pandemic, RNA virus research has been spotlighted across several fields, including DNA repair and genome instability. Recently, we have shown that SARS-CoV-2, an enveloped, positive sense RNA virus of the *Coronaviridae* family, triggers a DNA damage response in host cells and upregulates genome instability markers in human lung cells, Golden Syrian Hamster lung tissues, COVID-19 autopsy lung tissues, and blood sera from patients with acute COVID-19 and post-COVID. Specifically, we observed host cell genetic alterations, such as increased *HPRT*-mutagenesis, telomere length dysregulation, and elevated microsatellite instability (MSI).

In addition to this, emerging evidence has suggested that DENV-dependent modulation of host cell genome instability should be investigated. It is known that viruses of the *Flaviviridae* family, including DENV, trigger oxidative stress, which has been implicated in the pathogenesis of many diseases and cancers. Considering this, a recent preliminary study discovered a positive correlation between DNA damage, apoptosis, and oxidative stress during DENV infection. Epidemiologically, in 2020, a population-based cohort study through the National Health Insurance Research Databases in Taiwan provided the first epidemiologic evidence for the association between dengue virus infection and leukemia, suggesting a possible association between DENV infection and cancer incidence.

Here, we report host genome instability post-DENV infection in Vero E6 cells, as observed by global repression of DNA repair pathways. Specifically, we report suppression of essential homologous recombination, mismatch repair, Fanconi anemia, non-homologous end joining, base excision repair, nucleotide excision repair, DNA damage response, and cellular stress response genes. In addition, we see an increase in the mutagenic translesion synthesis polymerase, POL η . Strikingly, we discovered pre-treatment with JH-RE-06.NaOH, a small molecule inhibitor of the mutagenic translesion synthesis pathway, nearly completely suppresses DENV infection in Vero E6 cells. This result suggests a novel link between dengue virus and the translesion synthesis pathway and highlights the therapeutic potential of JH-RE-06 for patients with acute dengue infection.

DEDICATION

I dedicate this thesis to my father, Jon Lamkin, for his never-ending support and belief in my abilities; my mother, Diana Lamkin, for being a ferocious advocate for me and reminding me of my worth every day; my sister, Emily Lamkin PharmD, for always inspiring me and being my motivation to succeed alongside her; and my grandfather, John Duggan, for teaching me how to think like an engineer to innovate and improve the world around us.

ACKNOWLEDGMENTS

First and foremost, I would like to express my strongest gratitude to my mentor and advisor, Dr. Nimrat Chatterjee. Thank you for always supporting me and my passion for science. You have inspired me every day and have encouraged me to be the best that I can be. You have made me into the scientist I am today, and I couldn't thank you enough.

Next, I would like to thank the entire Chatterjee lab, both past and current members, for making my experience in the lab so incredible and rewarding. I especially want to thank Kanayo Ikeh, Andrew Crompton, Josh Victor, Alyssa Hurley, Hannah Koval, Lindsay Allen, and Anthony March. You all have inspired me, and I am so glad to have had the opportunity to work with you all. You all are the best team and lab family I could have ever asked for!

Next, I would like to thank my thesis committee members Dr. Randall Holcombe, Dr. Pei Zhou, Dr. Janet Murray, and Dr. Nimrat Chatterjee for all your support, guidance, and scientific insights this year.

Finally, I would like to thank the Department of Microbiology and Molecular Genetics for supporting me these past five years. Since joining MMG as a freshman in undergrad in 2018, I have found a home here.

TABLE OF CONTENTS

| | |
|---|-----|
| DEDICATION | ii |
| ACKNOWLEDGMENTS | iii |
| LIST OF TABLES | vi |
| LIST OF FIGURES | vii |
| CHAPTER 1: INTRODUCTION AND LITERATURE REVIEW | 1 |
| Dengue Virus..... | 1 |
| Prevalence | 1 |
| Mosquito Vectors and Transmission..... | 2 |
| Viral structure..... | 3 |
| Viral Life Cycle..... | 4 |
| Disease Pathology | 7 |
| Genome Instability | 9 |
| Mechanisms of DNA Damage and Mutagenesis | 10 |
| DNA Damage Response | 11 |
| Direct Reversal of DNA Damage | 11 |
| Homologous Recombination | 12 |
| Base Excision Repair | 13 |
| Nucleotide Excision Repair..... | 14 |
| Fanconi Anemia | 14 |
| Non-Homologous End Joining..... | 16 |
| Mismatch Repair | 17 |
| Translesion Synthesis..... | 19 |
| Telomere Biology and Instability..... | 20 |
| Chapter 1 Figures and Tables..... | 22 |
| Chapter 1 References | 35 |
| CHAPTER 2: DENGUE VIRUS INFECTION TRIGGERS GENOME INSTABILITY | 39 |
| Introduction and Project Rationale..... | 39 |
| Research Aims..... | 42 |
| Methodology | 42 |
| In Vitro Models of Dengue Virus Infection..... | 43 |
| Mammalian cell culture and DENV-4 infection | 44 |
| Immunoblotting..... | 45 |
| RT-qPCR Analysis..... | 46 |
| RNA-Sequencing Analysis | 48 |
| HPRT Mutagenesis | 48 |
| Relative Telomere Length Quantification..... | 49 |
| Results: Aim 1 | 50 |
| Dengue infection induces DNA damage in HUH-7 and Vero E6 cells | 50 |
| Dengue virus modulation of DNA damage response and cellular stress response genes | 51 |
| Dengue virus modulation of base excision repair transcript expression..... | 54 |
| Dengue virus modulation of mismatch repair transcript expression..... | 56 |
| Dengue virus modulation of homologous recombination transcript expression..... | 57 |
| Dengue virus modulation of non-homologous end joining transcript expression | 58 |
| Dengue virus modulation of Fanconi anemia transcript expression | 59 |
| Dengue virus modulation of nucleotide excision repair transcript expression | 60 |

| | |
|---|-----------|
| Dengue virus modulation of direct DNA damage reversal transcript expression..... | 60 |
| Dengue virus modulation of DNA repair-associated polymerases | 60 |
| Post-DENV infection RNA-Sequencing analysis..... | 61 |
| Results: Aim 2 | 61 |
| Dengue virus infection modulates the mutagenic translesion synthesis pathway..... | 61 |
| Therapeutic potential of JH-RE-06 in dengue virus infection | 62 |
| Results: Aim 3 | 63 |
| Dengue virus does not modulate host cell telomeres | 63 |
| HPRT mutagenesis post-dengue virus infection..... | 64 |
| Chapter 2 Figures and Tables..... | 66 |
| Chapter 2 References | 84 |
| CHAPTER 3: DISCUSSION AND FUTURE DIRECTIONS..... | 88 |
| Discussion and conclusions..... | 88 |
| Study Limitations | 90 |
| Future Directions..... | 90 |
| Chapter 3 References | 92 |
| COMPREHENSIVE BIBLIOGRAPHY | 93 |
| GLOSSARY | 99 |

LIST OF TABLES

| | |
|--|----|
| <i>Table 1. Dengue viral protein functions.</i> | 23 |
| <i>Table 2. RNA viruses and host cell DNA damage response.</i> | 66 |
| <i>Table 3. RT-qPCR primers.</i> | 68 |

LIST OF FIGURES

| | |
|----------------|----|
| Figure 1..... | 22 |
| Figure 2..... | 24 |
| Figure 3..... | 25 |
| Figure 4..... | 26 |
| Figure 5..... | 27 |
| Figure 6..... | 28 |
| Figure 7..... | 29 |
| Figure 8..... | 30 |
| Figure 9..... | 31 |
| Figure 10..... | 32 |
| Figure 11..... | 33 |
| Figure 12..... | 34 |
| Figure 13..... | 67 |
| Figure 14..... | 69 |
| Figure 15..... | 70 |
| Figure 16..... | 71 |
| Figure 17..... | 72 |
| Figure 18..... | 73 |
| Figure 19..... | 74 |
| Figure 20..... | 75 |
| Figure 21..... | 76 |
| Figure 22..... | 77 |
| Figure 23..... | 78 |
| Figure 24..... | 79 |
| Figure 25..... | 80 |
| Figure 26..... | 81 |
| Figure 27..... | 82 |
| Figure 28..... | 83 |

CHAPTER 1: INTRODUCTION AND LITERATURE REVIEW

Dengue Virus

Dengue virus is a mosquito-borne virus of the *Flavivirus* genus and *Flaviviridae* family. Dengue virus includes four serotypes (DENV-1, DENV-2, DENV-3, DENV-4) which share approximately 65% of their genomes and manifest the same disease and clinical symptomatology. Dengue virus is categorized as a single-stranded positive-sense RNA virus (+ssRNA virus), which can be directly translated into proteins by the host cell's ribosomes [2].

Prevalence

Dengue virus is the fastest-growing arthropod-borne virus in the world and is characterized as a major global public health challenge in tropical and subtropical nations by the World Health Organization. The number of dengue cases globally has increased 8-fold in the past two decades [3]. Globally, about 50 million cases and 22,000 deaths are reported to the World Health Organization annually [4]. However, this number is presumed to largely underestimate the true total cases and deaths per year, as many cases go unreported due to misdiagnosed febrile illnesses and asymptomatic or self-managed cases [3, 5]. Some estimates suggest there may be as many as 100 to 400 million cases annually. Further, over 2.5 billion people are estimated to live in areas that put them at risk of infection, including over 900 million individuals living in urban areas [5, 6]. In the

1970s, DENV-1 and DENV-2 circulated in Central America and Africa, while all four serotypes circulated in Southeast Asia. However, in the present day, all four serotypes (DENV-1, DENV-2, DENV-3, DENV-4) circulate the subtropical and tropical regions around the world [2]. Dengue virus is now endemic in over 100 countries, with some of the highest numbers of cases occurring in Bangladesh, Malaysia, the Philippines, and Vietnam. The most seriously affected regions include South America, South-East Asia, and the Western Pacific. Additionally, it is estimated that Asia represents approximately 70% of the global disease burden [3].

Mosquito Vectors and Transmission

Dengue virus is a mosquito-borne virus hypothesized to have evolved from sylvatic dengue strains previously transmitted through non-human primates in West Africa and Malaysia [6, 7]. Dengue viruses are transmitted by *Aedes* mosquitoes, most commonly *Aedes aegypti* mosquitoes and less frequently *Aedes albopictus* mosquitoes. Interestingly, despite being the most common transmission vector, *Aedes aegypti* mosquitoes are less susceptible to dengue infection than *Aedes albopictus*. It is hypothesized that this decreased susceptibility to dengue infection and the required increase of viral titer for infection could be a selection mechanism for more virulent dengue strains. Significant to the increased prevalence of dengue virus cases globally, *Aedes aegypti* mosquitoes are well adapted to live and survive in urban areas. This proximity of the *Aedes aegypti* mosquitoes to large populations further increases the spread of dengue in urban areas [6].

The primary mode of transmission of dengue virus begins with the infection of the female mosquito vector. Susceptible female mosquitoes ingest dengue virus during a blood meal from an infected and viremic human or non-human primate, and an infection of the mosquito midgut is established. Dengue spreads through the mosquito circulatory system during the intrinsic incubation period of about 5-7 days until the virus reaches the mosquito's salivary glands. After this intrinsic incubation period, the mosquito can be a life-long transmitter of dengue virus. The virus is transmitted from the mosquito vector when the infected mosquito, with infected salivary glands, bites the uninfected human or non-human primate. This cycle continues when an uninfected mosquito becomes infected from ingesting virus from the infected viremic human or non-human primate [6, 8]. This transmission cycle is depicted in **Figure 1**.

Viral structure

Dengue virus is a spherical, enveloped, single-stranded positive-sense RNA virus with a diameter of 50 nm [2, 9]. The virus contains an icosahedral nucleocapsid surrounded by a lipid bilayer retrieved from a host cell. The DENV genome is 11kb long and contains untranslated regions (UTRs) at the 5' and 3' ends on either side of the open reading frame (ORF). As a positive-sense RNA virus, the viral RNA acts as mRNA and can be directly translated into proteins by the host cell machinery [9].

The DENV genome encodes ten genes which are translated as one long polypeptide, called a polyprotein, and subsequently processed into ten separate proteins; three structural and seven non-structural [2]. The structural proteins include the Capsid (C),

Envelope (E), and pre-Membrane (prM) proteins. The non-structural proteins include the NS1, NS2A, NS2B, NS3, NS4A, NS4B, and NS5 proteins. The functions of each DENV protein are summarized in **Table 1** [10].

Viral Life Cycle

The skin is the first major barrier to infection. However, once a DENV-infected mosquito bites a susceptible host, DENV infects both the dermal and epidermal cells. Studies have shown that DENV can infect Langerhans cells, dermal macrophages, blood-derived monocytes, dermal dendritic cells, keratinocytes, endothelium, fibroblast, and mast cells. It was found that DENV can utilize several host-cell receptors to enter the cell, including glycosaminoglycans (heparan sulfate, lectins), DC-SIGN (adhesion molecule of dendritic cells), the mannose receptor of macrophages, and the lipopolysaccharide (LPS) receptor of CD14 and more. This suggests that DENV may not require a specific receptor for entry into the cell and is likely why the virus can infect many different cell types. Further, from a clinical standpoint, the liver, spleen, and lymph nodes are target organs for dengue infection [11]. With this, DENV infection of Langerhans cells is thought to be a main factor in pathogenesis. Langerhans cells are dendritic cells in the skin that produce interferons in response to infection. DENV can often cause systemic illness once infected Langerhans cells migrate to the lymph nodes and spread the virus systemically [12].

Early studies suggested, through single particle tracking, DENV exclusively enters host cells via clathrin-mediated endocytosis [13]. However, emerging evidence suggests that DENV may enter the cell via clathrin-mediated endocytosis, non-classical clathrin-

independent endocytosis or micropinocytosis, dependent upon the cell type and DENV serotype [14].

Despite this, clathrin-mediated endocytosis is recognized to be the most common mechanism of DENV entry [15]. Clathrin-mediated endocytosis is a molecular process in which extracellular cargo, in this case, dengue virus particles, are packaged into vesicles with the aid of a clathrin coat. Clathrin is a scaffold protein that polymerizes around invaginated portions of the plasma membrane and reinforces vesicle formation [16]. Typically, cargo proteins cluster around the coated region of the membrane, which further bends the membrane to form a clathrin-coated pit. In the case of DENV entry into the cell, the virus diffuses along the cell membrane until it is captured into a pre-existing clathrin pit [13]. This is followed by the scission process in which the neck of the membrane invagination is constricted, and the clathrin-coated vesicle is separated from the plasma membrane. Once the vesicle is inside the cell, DENV binds to the endosomal membrane and is subsequently released into the cytoplasm [2, 16]. Interestingly, for DENV to fuse to the endosomal membrane and be released from the endosomal vesicle, the vesicle must be in an acidic environment, and the membrane must gain a negative charge.

Once the virus has been released into the cytoplasm, the nucleocapsid opens and releases the viral RNA into the cytoplasm. As a positive sense RNA virus, the DENV genome can be directly translated into protein by the host cell machinery. The virus uses the host cell's ribosomes on the rough endoplasmic reticulum to translate its polypeptide. This polypeptide is then cleaved and creates the ten individual DENV proteins. The DENV capsid (C) protein then encloses the newly synthesized viral RNA and creates the new nucleocapsid. This newly formed nucleocapsid enters the rough endoplasmic reticulum,

where it is enveloped and surrounded by its membrane (M) and envelope (E) proteins for protection.

In addition to the translation of viral proteins, the viral genome is transported to the endoplasmic reticulum (ER) for replication. This replication is coupled to the translation of viral proteins to facilitate the use of newly synthesized viral proteins to aid in viral genome replication. DENV replicates with the aid of a replication complex which is a cytoplasmic compartment which protrudes into the ER. Of note, DENV's positive-sense RNA viral genome can directly serve as a template to synthesize the complementary negative RNA strand. The viral RNA genome can be in both linear and circular form whereby the linear genome is used to aid in translation while the circular form is used for transcription. Several of the viral proteins are involved in the replication of the dengue virus genome. Specifically, the C terminus of the NS3 proteins has 5' RNA-triphosphatase (RTP), nucleoside triphosphatase (NTPase), and helicase activity. Ultimately, NS3 can form a complex with NS5, the dengue RNA dependent RNA polymerase, which can aid in the unwinding of the viral RNA and dephosphorylation prior to 5'-end capping. The viral replication occurs in the replication complex which contains NS5 (RdRp), NS3 (helicase), 5' RNA-triphosphatase (RTP), nucleoside triphosphatase (NTPase), and several other host factors and dengue non-structural proteins which aid in RNA synthesis. The newly synthesized negative strand RNA remains attached to the positive strand RNA as a double-stranded RNA intermediate. This intermediate generates many copies, up to 10-fold more than the template, of the positive sense RNA genome. From here, the newly synthesized positive-sense RNA can be used for translation of viral proteins or encapsulated in newly synthesized viral proteins [9].

At the stage in which the newly synthesized viral genome is encapsulated, the virus is immature and travels through the Golgi apparatus as it matures. Once the virus is mature, the virus is released from the cell and infects other cells in the body leading to both local and systemic infection [2]. This viral life cycle is depicted in **Figure 2**. While this is dengue virus's main viral life cycle, the virus also disrupts other organelles, leading to severe pathobiological consequences. For example, DENV disrupts mitochondrial homeostasis, like many other viruses, to create an environment more conducive to viral replication. Dengue also selectively disrupts mitophagy, the cells' ability to tag damaged mitochondria for degradation, leading to an accumulation of damaged mitochondria and cellular injury [17]. Further, it is hypothesized that mitochondrial damage can lead to increased reactive oxygen species (ROS) and oxidative stress leading to severe pathobiological consequences [18-20].

Disease Pathology

Dengue virus is the causative agent of dengue fever, also known as breakbone fever. While most cases are asymptomatic, dengue infection carries the possibility of serious and potentially fatal febrile illness. Approximately 1 in 4 individuals infected with dengue virus develop symptomatic dengue infection, often presenting as mild to moderate, nonspecific, acute febrile illness [21]. A smaller subset of these individuals, about 1 in 20 infected with DENV, go on to develop severe dengue. Of note, infection with one of the four DENV serotypes confers lifelong immunity against only that specific serotype. Further, a second infection with a different DENV serotype is a risk factor for developing severe dengue.

In November 2009, the World Health Organization created a new standard for classifying cases into one of two groups: dengue or severe dengue. Currently, dengue is defined as having two or more of the following symptoms in a febrile individual who traveled to or lives in a dengue-endemic area: nausea, vomiting, rash, aches, pains, positive-tourniquet test, leukopenia. Often used specifically for diagnosing dengue, the tourniquet test assesses the fragility of capillaries by inflating a blood pressure cuff to the midway point between the patient's recorded systolic and diastolic blood pressure, waiting 2 minutes, and counting petechiae below the antecubital fossa. Ten or more petechiae indicate a positive tourniquet test. Warning signs in patients with the above signs of dengue which may indicate severe dengue include abdominal pain, persistent vomiting, clinical fluid accumulation, mucosal bleeding, lethargy, restlessness, postural hypotension, progressive increase in hematocrit, and liver enlargement. Further, severe dengue is defined as "dengue with any of the following symptoms: severe plasma leakage leading to shock or fluid accumulation with respiratory distress; severe bleeding; or severe organ impairment such as elevated transaminases $\geq 1,000$ IU/L, impaired consciousness, or heart impairment." It should be known that prior to this change of guidelines in 2009, dengue virus infections were classified as dengue fever (DF), dengue hemorrhagic fever (DHF), or dengue shock syndrome (DSS); these terms are still commonly used today [21].

The course of dengue infection begins after an incubation period of 5-7 days and contains three main phases: febrile, critical, and convalescent. The febrile phase consists of high, biphasic fevers, often up to 104°F, which lasts 2-7 days. The febrile phase is also when patients are viremic and can infect healthy mosquitos. Towards the end of the febrile phase, around defervescence, is when patients begin to develop warning signs of severe

dengue, as mentioned before. The critical phase in dengue infection follows the febrile phase at defervescence and lasts 1-2 days. During this time, most patients begin to improve. However, patients who experience serious plasma leakage can develop severe dengue during this period and exhibit early signs of hypovolemic shock. Patients developing severe dengue may exhibit pleural effusions, ascites, hypoproteinemia, hemoconcentration, or other hemorrhagic manifestations such as hematemesis during the critical phase. Once plasma leakage dissipates, patients enter the convalescent phase of infection in which extravasated fluids are reabsorbed and patients become hemodynamically stable [3, 21] .

Genome Instability

Genome instability is often referred to as the increased propensity for generating mutations in the DNA. Dysregulation of DNA damage checkpoints, DNA repair machinery, and mitotic checkpoints are implicated in causing genome instability. Differential expression of molecules in these pathways can be used as a marker for genome instability. Further, specific defects in DNA repair genes can lead to DNA damage accumulation and increase the propensity for mutagenesis, key hallmarks of genome instability [22, 23]. With this, genome instability is a hallmark of most cancers and several diseases, including Ataxia telangiectasia, Nijmegen breakage syndrome, Werner's syndrome, Bloom's syndrome, Rothmund-Thompson syndrome, Fanconi anemia, Xeroderma pigmentosa, and Cockayne's syndrome [24]. Often damaged DNA repair and cell cycle machinery, which lead to genome instability, are the drivers of cancer

development, allowing for the uncontrolled cell proliferation we see in cancer, despite DNA damage [25].

There are several forms of genome instability including, but not limited to, chromosomal instability (CIN), microsatellite instability (MSI), and telomere instability. Telomeres are the DNA-protein structures that cap the ends of chromosomes and protect the genome from degradation [25, 26]. The instability of the protective telomeres can lead to chromosomal instability. Chromosomal instability can be in the form of abnormal chromosome numbers and abnormal mitoses. Microsatellite instability is defined by the expansion or contraction of oligonucleotide repeats present in microsatellite sequences [25].

Mechanisms of DNA Damage and Mutagenesis

Mutagenesis is the mechanism by which changes in the DNA result in gene mutations. DNA is susceptible to both exogenous and endogenous sources of damage. Exogenous sources of DNA damage include environmental, physical, and chemical agents such as ionizing radiation, ultraviolet radiation, alkylating agents, and crosslinking agents. Endogenous DNA damage occurs from DNA interacting with agents present in the cell, such as reactive oxygen species (ROS). In **Figure 3**, the most common DNA-damaging agents are listed, alongside the damage to the DNA that is inflicted. Some of the most common DNA damages include base mismatches and replication errors, single-strand breaks, double-strand breaks, abasic (AP) sites, DNA adducts, intrastrand crosslinks, and interstrand crosslinks.

DNA Damage Response

Cells can detect DNA damage and promote its repair through a specialized set of sensor proteins, which make up the complex signal transduction pathway, the DNA damage response (DDR). The DDR, shown in **Figure 4**, is specifically comprised of sensors, transducers, and effectors. The main transducers of the DDR are the DNA-PK, ATM, and ATR kinases. Single-strand breaks (SSBs) typically engage the ATR kinase pathway. Double strand breaks (DSBs) typically engage the ATM and DNA-PK pathways [27]. Activation of these DDR transducers leads to the activation of their downstream effectors. ATM activates its downstream effector CHK2 while ATR activates its downstream effector CHK1. Ultimately, the DDR leads to several cellular responses including DNA repair, cell cycle arrest, apoptosis, or senescence through various signal transduction pathways.

The DDR can lead to DNA repair pathways including direct reversal of DNA damage, homologous recombination, base excision repair, nucleotide excision repair, Fanconi anemia, non-homologous recombination, mismatch repair, and translesion synthesis. Each of these pathways will be briefly summarized.

Direct Reversal of DNA Damage

Direct reversal of DNA damage is a mechanism that repairs UV photolesions, often pyrimidine dimers, and alkylated bases in a simplistic and error-free manner. The O⁶-

alkylguanine-DNA alkyltransferase (AGT/MGMT) enzyme can reverse O-alkylated lesions, pyridyloxobutyl adducts of guanine, and repair O⁶-G-alkyl-O⁶-G interstrand cross-links. AlkB-related α -ketoglutarate-dependent dioxygenases (AlkB) can reverse N-alkylated base adducts [28].

Deficiencies in molecules involved in this pathway may confer increased sensitivity to UV and alkylating agents. Clinically, decreased levels of the MGMT enzyme have been shown to sensitize tumors to temozolomide, a cancer chemotherapeutic that adds N-alkylation adducts (N7-methylguanine and N3-methyladenine) and some O6-methylguanine (O6mG) adducts [29, 30].

Homologous Recombination

Homologous recombination (HR) is a group of DNA repair pathways that aid in the repair of double-strand breaks (DSBs) in the DNA. HR is a high-fidelity mechanism of DNA repair that functions in a template-dependent manner [28]. In brief, HR is typically initiated when the MRN complex (composed of MRE11, RAD50, and NSB1) binds to the site of damage and engages in end-processing to form long 3' single-stranded regions which will invade the undamaged homologous DNA. This undamaged homologous DNA acts as a template to repair the double-strand break. A more comprehensive view of the sub-pathways involved in HR is shown in **Figure 5**.

As HR is a key pathway involved in maintaining genomic stability, defects, and deficiencies in several HR genes have been shown to increase cancer incidence. Most commonly, defects in the BRCA1 and BRCA2 genes have conferred increased cancer risk.

In fact, BRCA1 and BRCA2 genes are the strongest susceptibility genes for breast cancer, and further, 90% of hereditary breast cancers are caused by BRCA1 and BRCA2 mutations as well as a majority of hereditary cases of ovarian cancer [31].

Base Excision Repair

Base excision repair (BER) is a DNA repair process that helps maintain genome stability by correcting small base lesions, including damages from oxidation, deamination, and alkylation. The BER pathway, depicted in **Figure 6**, is initiated by one of eleven DNA glycosylases including UNG2, UNG1, SMUG1, TDG, MBD4, MPG, OGG1, MUTYH, NTHL1, NEIL1, NEIL2, and NEIL3. One of these specialized DNA glycosylases removes the damaged base and leaves an abasic site, also known as an AP site [32]. APE1 (APEX1) is a major AP endonuclease that cleaves the AP site and creates a 3' OH and 5' deoxyribose phosphate (dRP) terminus. Next, a DNA polymerase, usually Pol β , fills the gap in the DNA. Pol β has dRP lyase activity and cleaves off the 5' deoxyribose phosphate to generate a 5' phosphate. POL λ can also take over for POL β but is less efficient. A DNA ligase then ligates the ends together. This ligation is completed by LIG1 or the LIG3/XRCC1 complex [32-34]. With this, there are two main types of BER: short-patch BER and long-patch BER. A single nucleotide gap is generated, filled, and ligated in short-patch BER. On the other hand, long-patch BER generates a gap of 2-10 nucleotides which is subsequently filled and ligated [32].

Nucleotide Excision Repair

Nucleotide excision repair (NER) is the main pathway used to repair bulky, helix-distorting lesions in the DNA. Specifically, NER is used to repair lesions caused by UV radiation, such as CPDs and (6 – 4)PP, bulky chemical adducts, and certain forms of oxidative damage. As shown in **Figure 7**, there are four main steps to nucleotide excision repair: 1) recognition of damaged DNA, 2) removal of the damaged DNA fragment, 3) gap-filling DNA synthesis, and 4) ligation of DNA. In this process, XPC is the main DNA damage sensor that can recognize helix distortions in the DNA. Then, other NER factors are recruited to the site of damage. TFIIH can bind to the DNA and unwind the DNA. RPA and XPA can stabilize the DNA site, and XPG and XPF can cut on either side of the damaged DNA. Then, DNA polymerase can use the undamaged bases as a template to fill in the gap. Finally, LIG1 can ligate the DNA ends [35, 36].

Defects in the NER pathway can cause three rare recessive syndromes: xeroderma pigmentosum (XP), Cockayne syndrome (CS), and trichothiodystrophy (TTD). Each of these disorders results from defects in different NER genes and has severe detrimental effects. Most discussed, XP confers an increased UV sensitivity is linked to increased cancer risk. Increased cancer risk among DNA repair defects is extraordinarily common [37].

Fanconi Anemia

The Fanconi Anemia (FA) pathway is a key protector against genome instability. Interestingly, the FA pathway coordinates several classical repair pathways to remove interstrand crosslinks (ICLs) from the DNA. ICLs are particularly complex to repair as they involve both strands of the DNA double helix. Because of this, eukaryotes evolved the FA pathway to manage ICLs. Specifically, the FA pathway coordinates a response from proteins involved in the homologous recombination, nucleotide excision repair, and translesion synthesis pathways [1, 38].

There are 22 genes and thirteen FA complementation groups including FANCA, FANCB, FANCC, FANCD1, FANCD2, FANCE, FANCF, FANCG, FANCI, FANCI, FANCI, FANCI, FANCL, FANCM, and FANCN which help to facilitate the Fanconi anemia pathway [38]. As shown in **Figure 8**, eight FA proteins assemble to form the FA core complex in response to DNA damage from either an exogenous or endogenous source. These proteins which form the FA core complex include FANCA, FANCB, FANCC, FANCE, FANCF, FANCG, FANCL, and FANCM. This FA core complex functions as a nuclear E3 ubiquitin ligase complex, which monoubiquitinates the FANCD2/FANCI heterodimer, also known as the I-D heterodimer. The I-D monoubiquitinated heterodimer localizes to the damaged DNA and interacts with several DNA repair proteins and other FA proteins including FANCD1, FANCDN, FANCI, and FANCS, to repair the DNA via homologous recombination. Translesion synthesis polymerases REV1 and POL ζ are also involved in the ICL repair here. Then, the monoubiquitin can be removed from the I-D complex by USP1 (ubiquitin specific peptidase 1). It should be noted that these FA genes overlap several other DNA repair pathways. For example, FANCD1 is also known as BRCA2, a key protein in the homologous recombination pathway [1, 38].

Fanconi anemia, the disease after which the Fanconi anemia pathway is named, is a genomic instability disorder characterized by chromosomal instability, bone marrow failure, congenital malformations, and a predisposition to developing several cancer types. Deficiencies in FA genes increase sensitivity to cross-linking agents, and chromosome breakage and cytogenetic abnormalities are possible upon exposure to crosslinking agents with FA deficiencies [39]. Interestingly, deficiencies in the FA pathway have been shown to decrease the efficiency of homologous recombination repair of double-strand breaks. Further studies suggested that FANCD2 functions independently from BRCA2 and RAD51-associated HR to facilitate the repair of DSBs [40, 41].

Non-Homologous End Joining

Non-homologous end joining, also known as NHEJ, is the primary pathway in which cells repair double-strand breaks (DSBs). In contrast to homologous recombination, non-homologous end joining does not require a homologous template to repair the lesion in the DNA and is an intrinsically mutagenic pathway [42, 43]. By not requiring a homologous template, NHEJ can occur in all cell cycle phases, whereas homologous recombination can only occur during the S and G2 phases of the cell cycle. As expected, defects in the NHEJ pathway increase sensitivity to DNA-damaging agents which cause DSBs, including ionizing radiation. Additionally, deficiencies in NHEJ can lead to (Severe) combined immunodeficiency, (S)CID. NHEJ deficiency can cause SCID by failing to carry out V(D)J recombination, which is involved in generating diverse T cells and B cells using programmed double-strand breaks [44].

There are four main steps to non-homologous end joining, as shown in **Figure 9**. First, the end of DNA at the site of a double-strand break is recognized, and the NHEJ complex is assembled and stabilized. Specifically, the Ku70 protein, encoded by the XRCC6 gene, forms a heterodimer with the Ku80 protein, encoded by the XRCC5 gene. This Ku70-Ku80 heterodimer binds to DSBs and allows NHEJ machinery to assemble at the site of damage. DNA-PKcs, XRCC4, LIG4, XLF, and APLF are some factors recruited to the site of damage by the Ku heterodimer. These core NHEJ factors form a stable complex at the DSB. Second, the two broken ends of DNA are bridged together by XRCC4 and XLF to stabilize the DNA. Third, to create ligatable ends, the ends of the DNA are processed. There are several enzymes involved in this process. Some proteins that resect the DNA ends include Artemis, WRN, and APLF. Some of the enzymes that fill the DNA gaps are of the family X polymerases including POL μ and POL λ . Fourth and finally, LIG4 ligates the broken ends of the DNA, and the NHEJ complex is dispersed [42].

Mismatch Repair

Mismatch repair is a key pathway in maintaining genome stability and decreasing the mutational burden on cell populations. The key function of the mismatch repair pathway (MMR), shown in **Figure 10**, is to repair spontaneous base mismatches and small insertion-deletion loops (indels) [45]. Eukaryotic replicative polymerases make errors every 10^4 - 10^5 nucleotides polymerized, which equates to approximately 100,000 to 1,000,000 errors each time a diploid cell replicates. Post-replicatively, these base mispairs and indels caused by primer-template slippages can be repaired by mismatch repair [46].

Strikingly, MMR increases replication fidelity by 50-1000 fold and hence significantly protects genome stability, especially at microsatellite regions in the DNA [47].

In humans, there are eight genes that encode for the MMR machinery including MSH2, MSH3, MSH5, MSH6, MLH1, PMS1 (MLH2), MLH3, and PMS2 (MLH4). MSH2 can form heterodimers with MSH6 and MSH3. The MSH2-MSH6 heterodimer is known as MutS α and detects single base mismatches and dinucleotide distortions. The MSH2-MSH3 heterodimer is known as MutS β and detects indel loops. These heterodimers scan the post-replicative DNA and bind to mismatches [45]. MLH1 forms a heterodimer with PMS2, PMS1, or MLH3 to form MutL α , MutL β , or MutL γ . This MutL complex then activates PMS2 endonuclease activity which nicks the strand on either side of the mismatch. EXO1 excises the damaged portion of the DNA. POL δ resynthesizes the damaged DNA and the strands are ligated [47].

Deficient MMR, also referred to as dMMR, is associated with several pathobiological phenotypes including microsatellite instability (MSI), with an increased risk of cancer development. MMR deficiency is most common in colorectal, gastrointestinal, and endometrial cancer; however, it has also been implicated in breast, prostate, bladder, and thyroid cancers [48]. Of note, Lynch syndrome, also known as hereditary nonpolyposis colorectal cancer, is a disorder caused by germline mutations in mismatch repair genes. Lynch syndrome clearly exemplifies the importance of MMR in maintaining genome stability and further how MMR protects against MSI. Strikingly, MSI can be detected in 90% of colorectal cancers in individuals with Lynch syndrome compared to 15% of sporadic colorectal cancer cases [49].

Translesion Synthesis

Translesion synthesis (TLS) is a DNA damage tolerance mechanism that allows for the error-prone and mutagenic bypass of DNA damage. As shown in **Figure 11**, the replication fork stalls when it encounters an unrepaired lesion in the DNA. To avoid deleterious consequences, TLS polymerases assemble to bypass the damage in the DNA. REV1 is the key scaffolding molecule of TLS and allows the other TLS polymerases to assemble. First, an inserter polymerase, usually POL η , POL ι , or POL κ inserts a nucleotide opposite the lesion in the DNA. The inserted base can often be incorrect and lead to mutations in the next round of replication. This increased propensity for mutation generation is a characteristic of genome instability. This step is followed by an extender polymerase, usually POL ζ (Rev3/Rev7/PoID2/PoID3 complex), which replaces the inserter polymerase and begins to extend the template. REV1, a polymerase with a unique scaffolding function, facilitates this process. REV1 binds to POL η , POL ι , or POL κ via their REV1 interacting region (RIR) or to POL ζ via its REV3/REV7 interface [28, 50].

Currently, the mainstay cancer therapies, such as chemotherapy and radiation therapy, are designed to damage the DNA of cancer cells beyond repair in an attempt to kill cancer cells. Recently, TLS has been implicated in causing cancer resistance to chemotherapy, where TLS polymerases enable damage bypass of cancer therapy-induced DNA damage [50]. Additionally, by targeting one of the key TLS proteins, REV1, with small molecule inhibitors, cancer cells can be sensitized to chemotherapeutic drugs [51-54].

Along with TLS implication in cancer resistance to therapy, DNA viruses, including oncogenic viruses, have been shown to interact with the translesion synthesis pathway. Recently, it was observed that HPV 16 (human papillomavirus 16, oncogenic virus) oncogene E7 activates the translesion synthesis pathway. This study also reported that cervical cancers have significantly elevated TLS expression compared to the 15 other cancer types evaluated in this study [55]. Epstein-Barr virus (EBV), a known oncogenic virus, was reported to require TLS polymerase POL η for efficient infectivity [56].

Of interest to this thesis work, recently, a novel connection between TLS and the RNA virus SARS-CoV-2 was made whereby SARS-CoV-2 instigated the upregulation of mutagenic translesion synthesis. Further, pre-treatment with JH-RE-06.NaOH, a small molecule inhibitor of the mutagenic translesion synthesis pathway, was shown to suppress SARS-CoV-2 proliferation, suggesting a link between SARS-CoV-2 replication and the translesion synthesis pathway [57, 58].

Telomere Biology and Instability

Telomeres are the DNA-protein structures that cap the ends of chromosomes and protect the genome from degradation. More specifically, telomeres consist of TTAGGG repeats with a G-rich leading strand and a C-rich lagging strand. The shelterin complex protects the telomere, comprised of the telomeric repeat binding factors TRF1 (TERF1) and TRF2 (TERF2), the TRF2 binding factor RAP1, bridging molecules TIN2 and TPP1, and the telomeric protection factor POT1. These proteins aid in the formation of the telomeric loop, also called the T-loop, which is the protective structure that protects the

ends of chromosomes [26]. A diagram of the human telomere T-loop is shown in **Figure 12** [26].

To prevent successive shortening of telomeres with replication, telomeres employ the telomerase complex to extend the telomeres. The human telomerase complex contains TERT, TR, and Dyskerin. TERT, telomerase reverse transcriptase, is a catalytic reverse transcriptase that utilizes TR, telomerase template RNA, to extend telomeric repeats. Dyskerin, DKC1, is a key auxiliary protein. While TERT is rarely expressed in somatic cells, aberrant regulation of the telomerase complex or other telomeric proteins can lead to genome instability and cancer development [26, 59].

Chapter 1 Figures and Tables

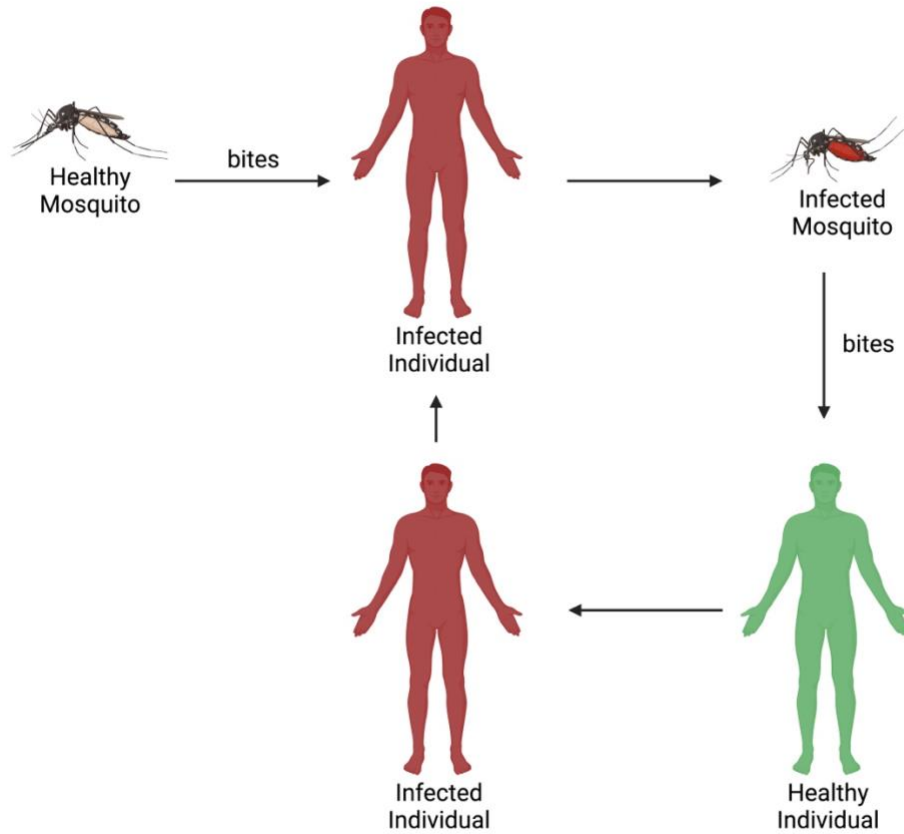


Figure 1. Model of dengue virus transmission cycle.

Figure made with BioRender.com

Table 1. Dengue viral protein functions.

| Protein | Structural/Non-Structural | Function(s) |
|-------------------------------|----------------------------------|---|
| Capsid (C) | Structural | Genome encapsidation |
| Pre-Membrane/Membrane (prM/M) | Structural | Cap-like structure that protects the envelope protein from undergoing premature fusion before virus release |
| Envelope (E) | Structural | Mediates virus binding, fusion to host cell membrane, determines host range, tropism, virulence |
| NS1 | Non-Structural | Viral RNA replication complex, viral defense through inhibition of complement activation |
| NS2A | Non-Structural | Coordination between RNA packaging and replication and antagonism of interferon |
| NS2B | Non-Structural | NS2B associates with NS3 to form the DENV protease complex, serves as a cofactor in the structural activation of the DENV serine protease of NS3 |
| NS3 | Non-Structural | Chymotrypsin-like serine protease, RNA helicase, RNA triphosphatase enzyme activity, also cleaves the DENV polyprotein as well as RNA replication |
| NS4A | Non-Structural | Membrane alterations |
| NS4B | Non-Structural | Membrane alterations, assists viral RNA replication through direct interaction with NS3 and blocks IFN-induced signal transduction |
| NS5 | Non-Structural | Methyltransferase and RNA-dependent RNA polymerase activity |

Table adapted from Harapan et al., 2020 [10].

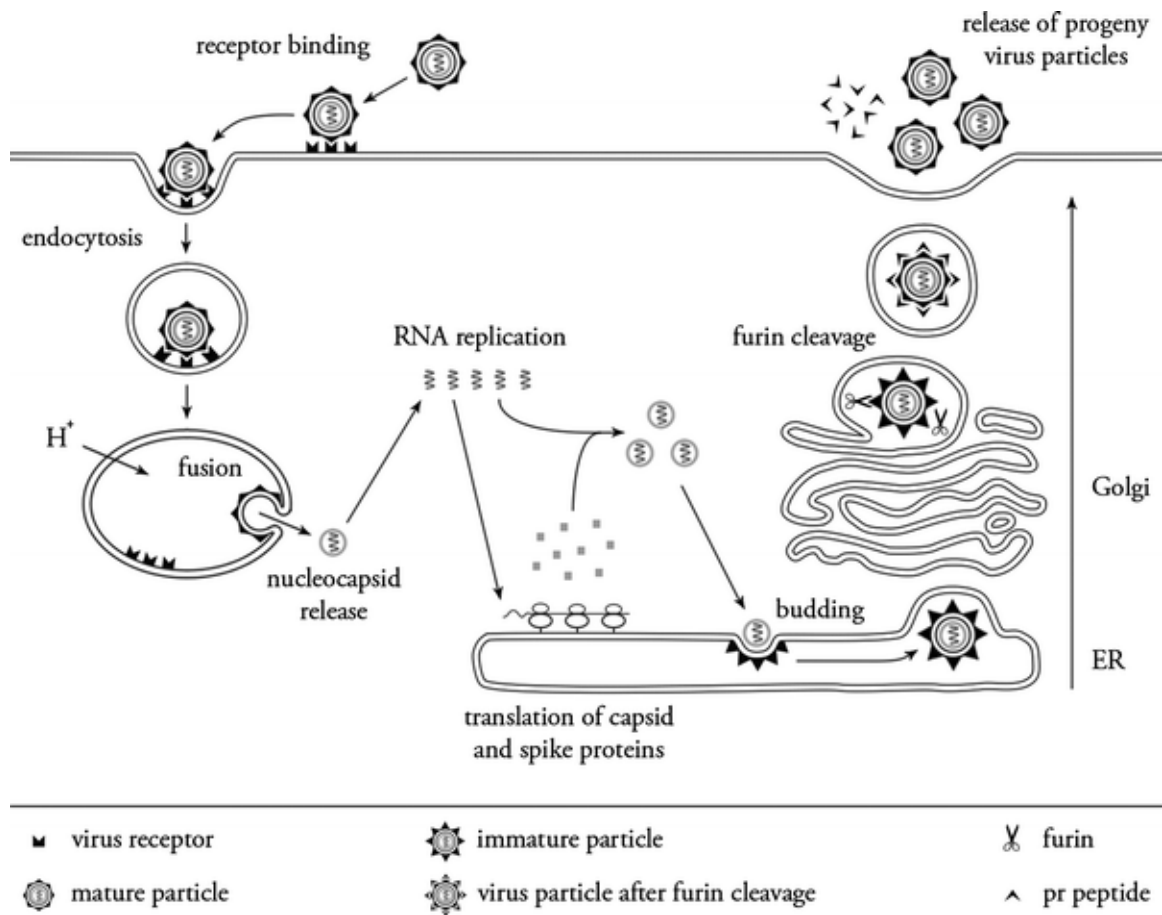


Figure 2. Dengue virus life cycle.

Reprinted from *Cellular and Molecular Life Sciences*, Rodenhuis-Zybert, I.A., Wilschut, J. & Smit, J.M. Dengue virus life cycle: viral and host factors modulating infectivity. *Cell. Mol. Life Sci.* 67, 2773–2786 (2010). <https://doi.org/10.1007/s00018-010-0357-z>, with permission from Springer Nature [60]

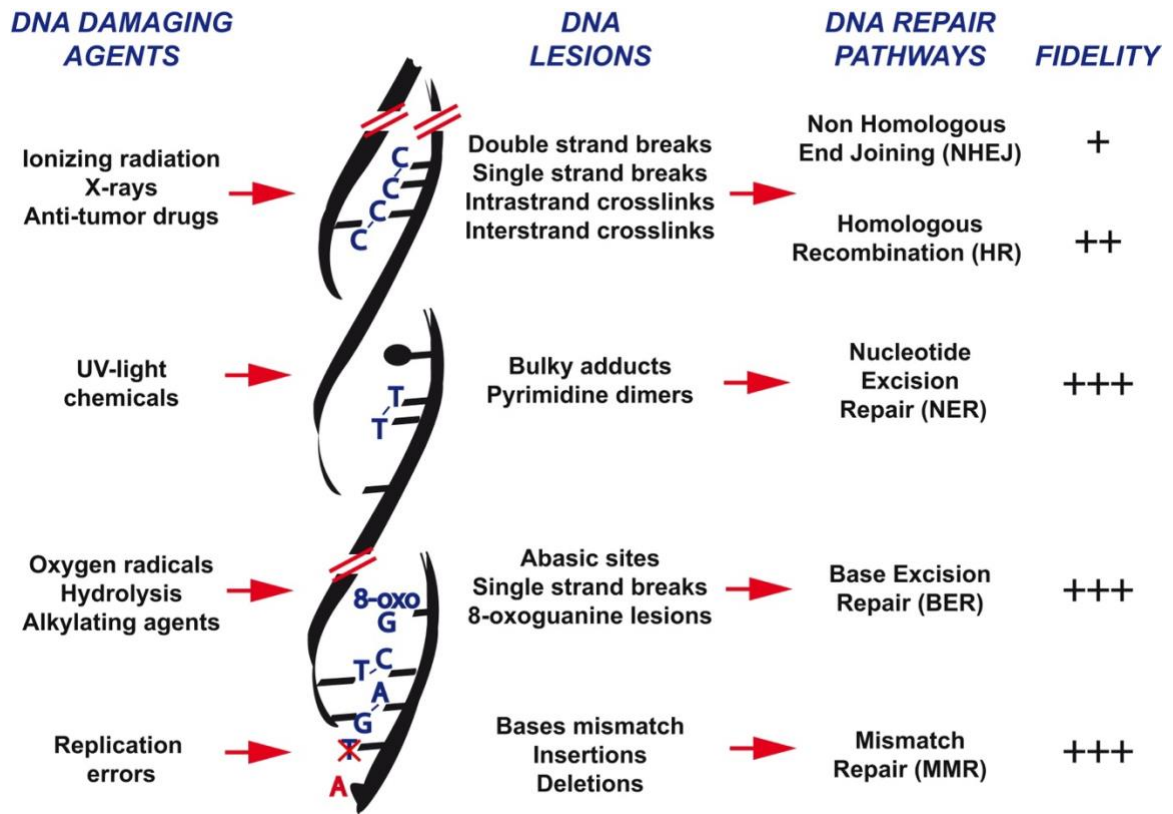


Figure 3. DNA damaging agents and corresponding DNA lesions.

Reprinted from *Cell Stem Cell*, Volume 8, Issue 1, Authors: Cedric Blanpain, Mary Mohrin, Panagiota A. Sotiropoulou, and Emmanuelle Passegué, "DNA-Damage Response in Tissue-Specific and Cancer Stem Cells," 2011, with permission from Elsevier [39].

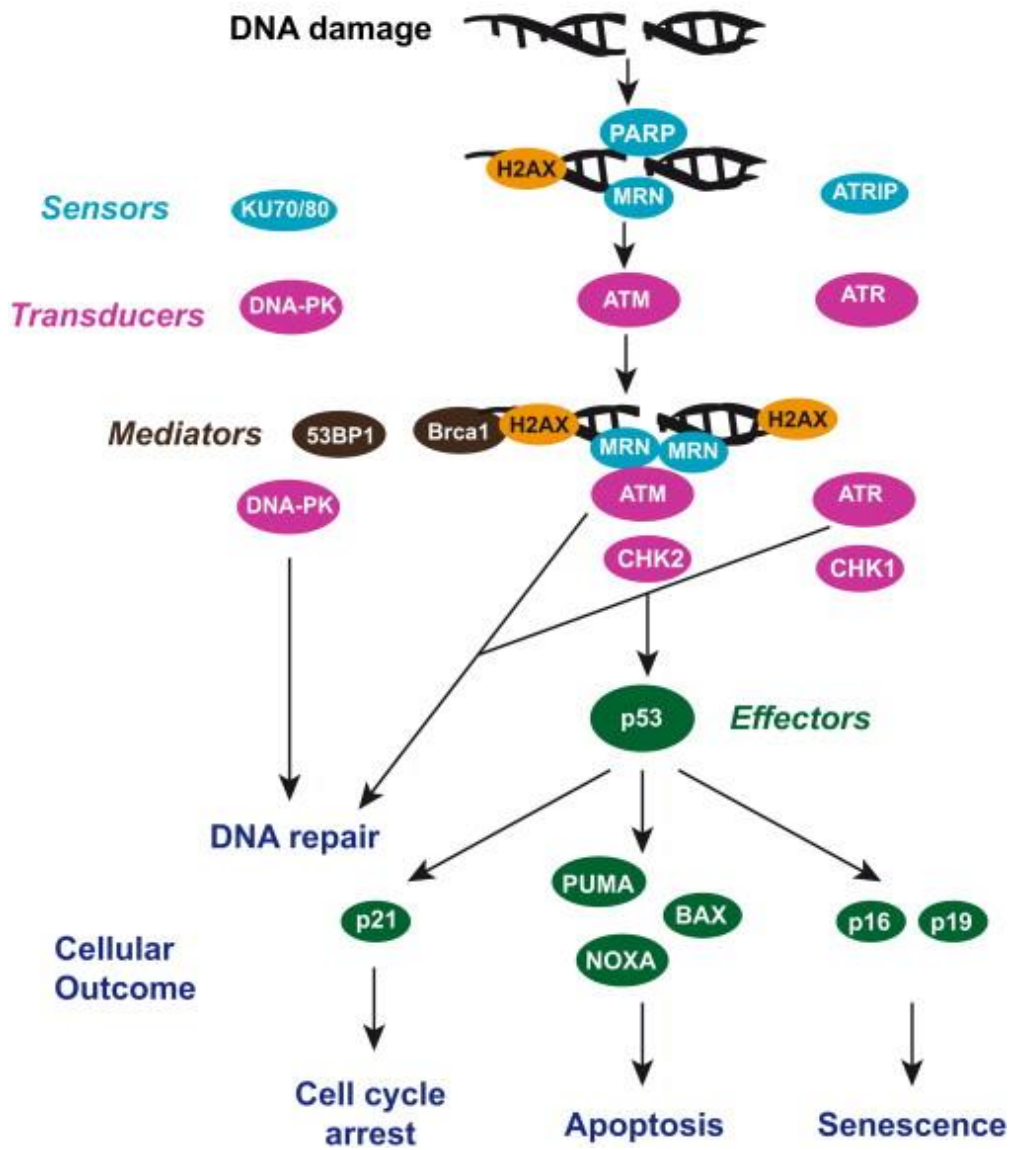


Figure 4. Model of the DNA Damage Response.

Reprinted from Cell Stem Cell, Volume 8, Issue 1, Authors: Cedric Blanpain, Mary Mohrin, Panagiota A. Sotiropoulou, and Emmanuelle Passegué, "DNA-Damage Response in Tissue-Specific and Cancer Stem Cells," 2011, with permission from Elsevier [39].

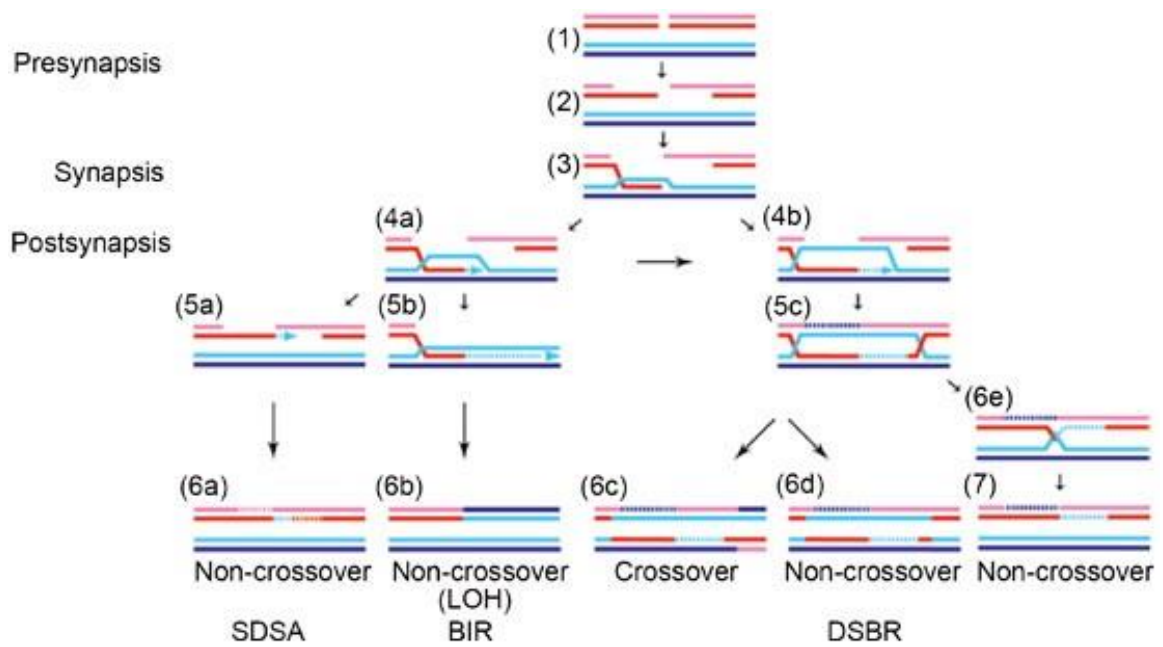


Figure 5. Model of the homologous recombination pathway.

Reprinted from Cell Research, 18, pages 99–113 (2008), Authors: Xuan Li and Wolf-Dietrich Heyer, "Homologous recombination in DNA repair and DNA damage tolerance," 2008, with permission from Springer Nature [28].

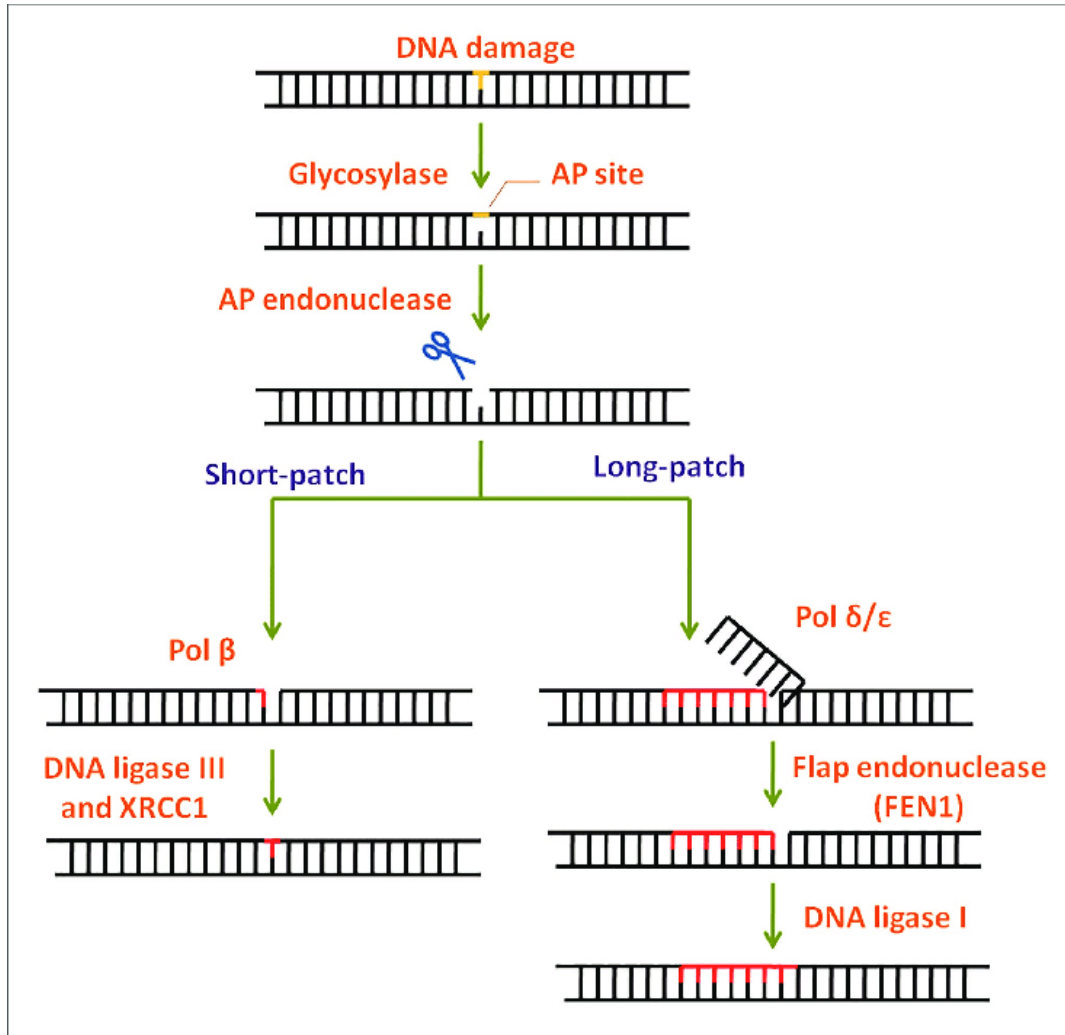


Figure 6. Model of the base excision repair pathway.

Reprinted from Frontiers in Genetics, volume 12, Authors: Barve, Galande, Ghaskadbi and Ghaskadbi, "DNA Repair Repertoire of the Enigmatic Hydra," 2021, Copyright © 2021 Barve, Galande, Ghaskadbi and Ghaskadbi, distributed under the terms of the Creative Commons Attribution License, which permits unrestricted use, distribution, and reproduction in any medium, provided the original author and source are credited [61].

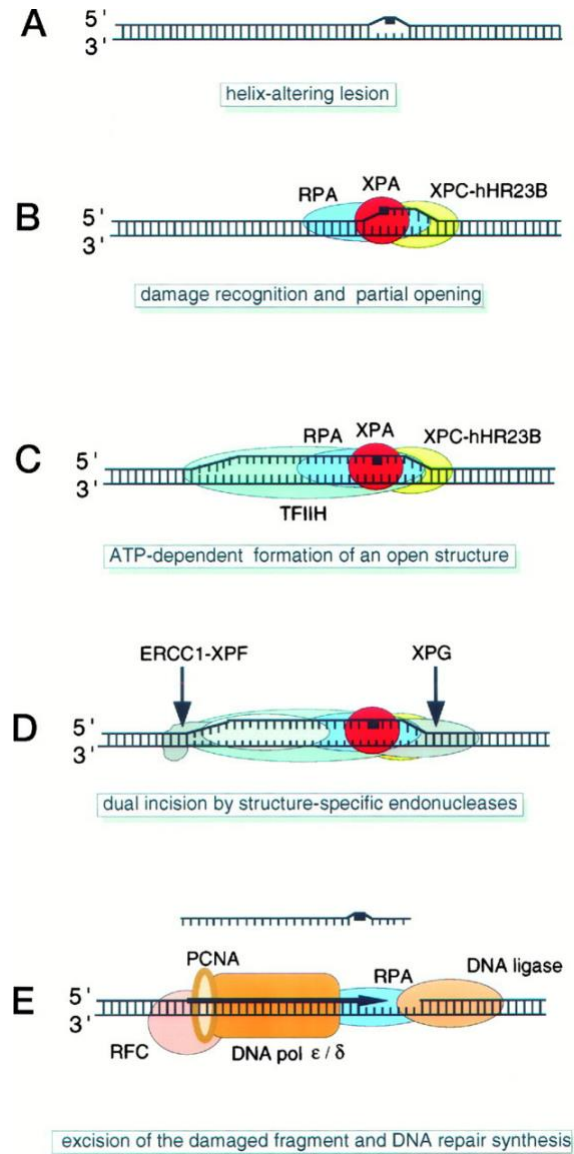


Figure 7. Model of the nucleotide excision repair pathway.

Reprinted from Wood, R. D. (1997). "Nucleotide excision repair in mammalian cells." J Biol Chem 272(38): 23465-23468, distributed under the terms of the Creative Commons Attribution License, which permits unrestricted use, distribution, and reproduction in any medium, provided the original author and source are credited [62].

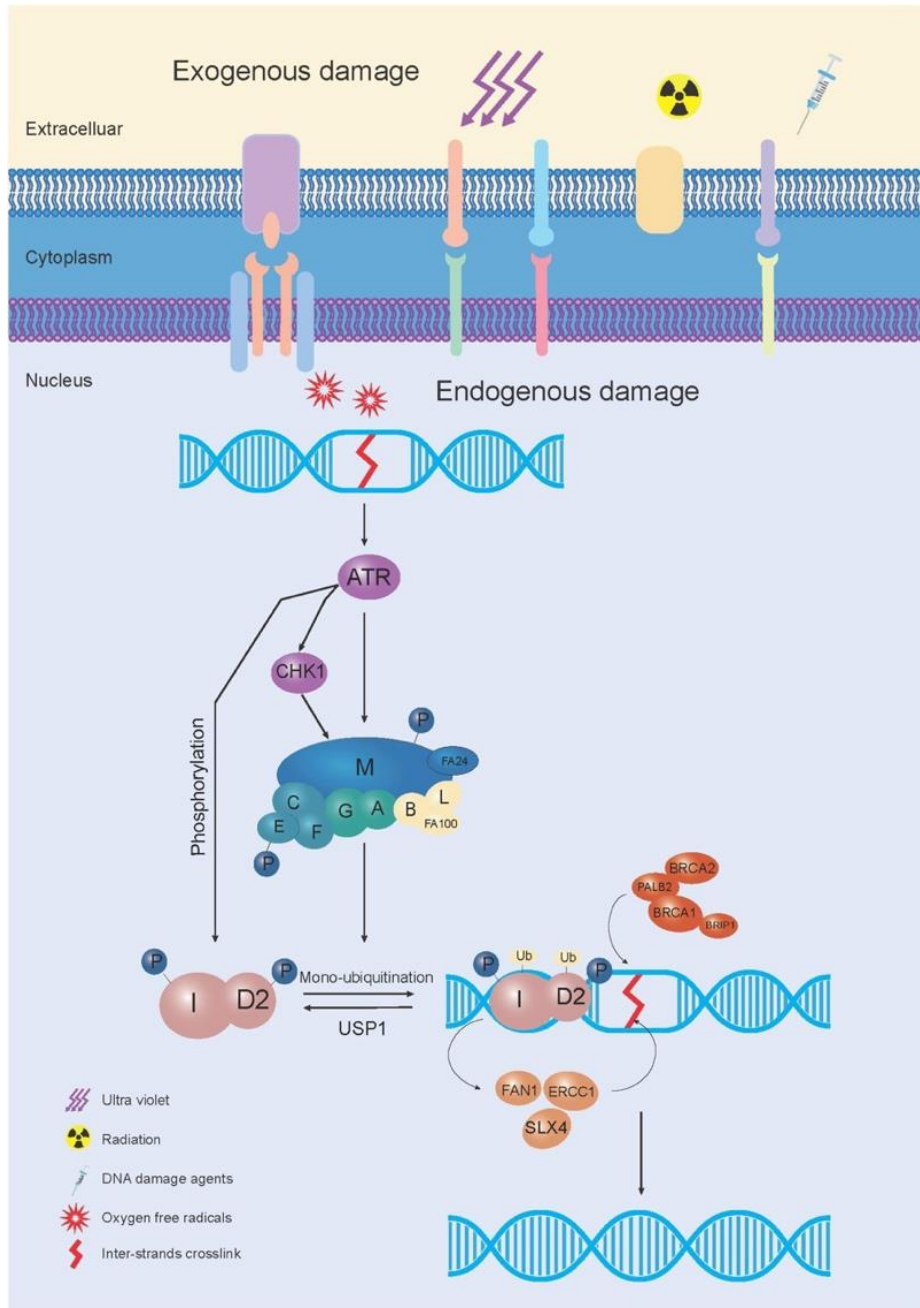


Figure 8. Model of the Fanconi anemia pathway.

Reprinted from Fang C-B, Wu H-T, Zhang M-L, Liu J and Zhang G-J (2020) Fanconi Anemia Pathway: Mechanisms of Breast Cancer Predisposition Development and Potential Therapeutic Targets. *Front. Cell Dev. Biol.* 8:160. doi: 10.3389/fcell.2020.00160. Copyright © 2020 Fang, Wu, Zhang, Liu and Zhang., distributed under the terms of the Creative Commons Attribution License, which permits unrestricted use, distribution, and reproduction in any medium, provided the original author and source are credited [1]

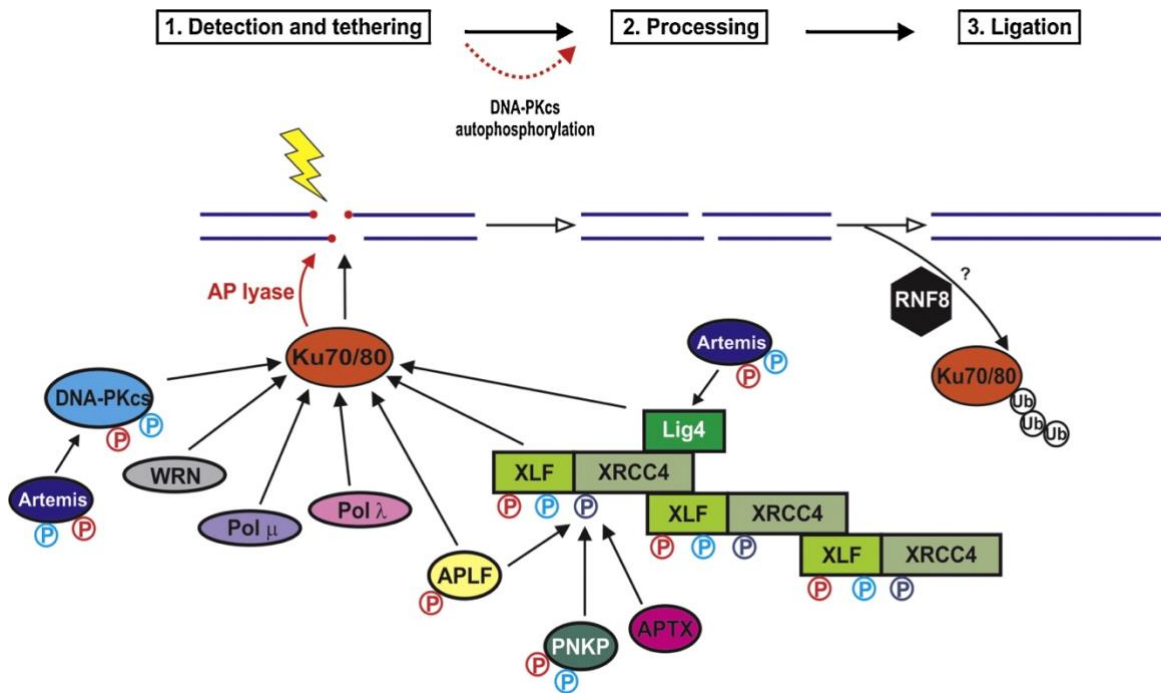


Figure 9. Model of the non-homologous end joining pathway

Reprinted from DNA Repair, Vol 17, Authors: Williams, G. J., Hammel, M., Radhakrishnan, S. K., Ramsden, D., Lees-Miller, S. P., Tainer, J. A., "Structural insights into NHEJ: Building up an integrated picture of the dynamic DSB repair super complex, one component and interaction at a time, Pages No., Copyright (2014), with permission from Elsevier [63].

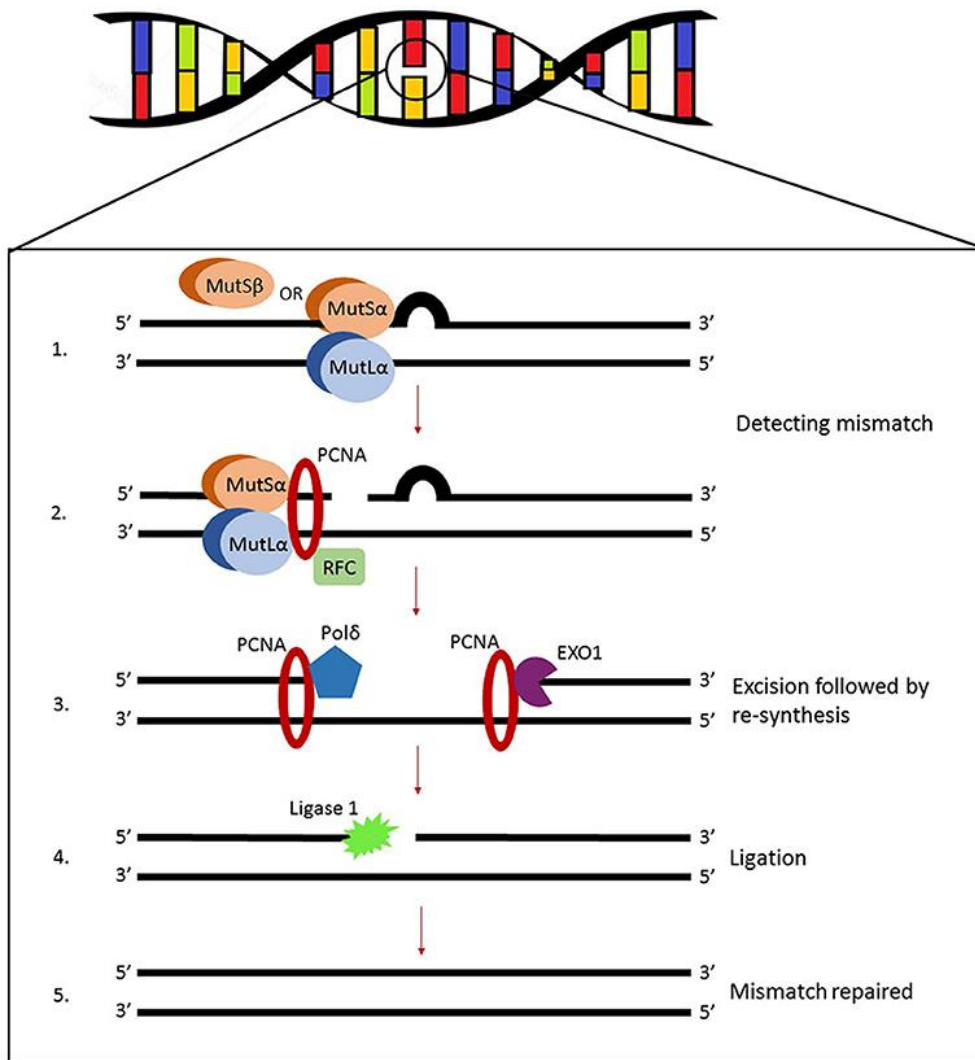
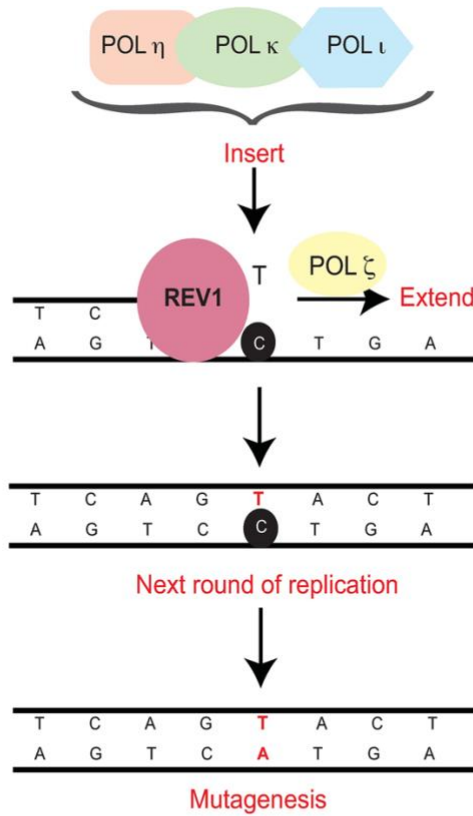


Figure 10. Model of the mismatch repair pathway.

Reprinted from Pećina-Šlaus, N., et al. (2020). "Mismatch Repair Pathway, Genome Stability and Cancer." Front Mol Biosci 7: 122. Copyright © 2020 Pećina-Šlaus, Kafka, Salamon and Bukovac., distributed under the terms of the Creative Commons Attribution License, which permits unrestricted use, distribution, and reproduction in any medium, provided the original author and source are credited [45].

1A



1B



Figure 11. Model of the translesion synthesis pathway.

Reprinted from Yamanaka K, Chatterjee N, Hemann MT, Walker GC (2017) Inhibition of mutagenic translesion synthesis: A possible strategy for improving chemotherapy? *PLoS Genet* 13(8): e1006842. <https://doi.org/10.1371/journal.pgen.1006842>. Copyright: © 2017 Yamanaka et al., distributed under the terms of the Creative Commons Attribution License, which permits unrestricted use, distribution, and reproduction in any medium, provided the original author and source are credited. [50].

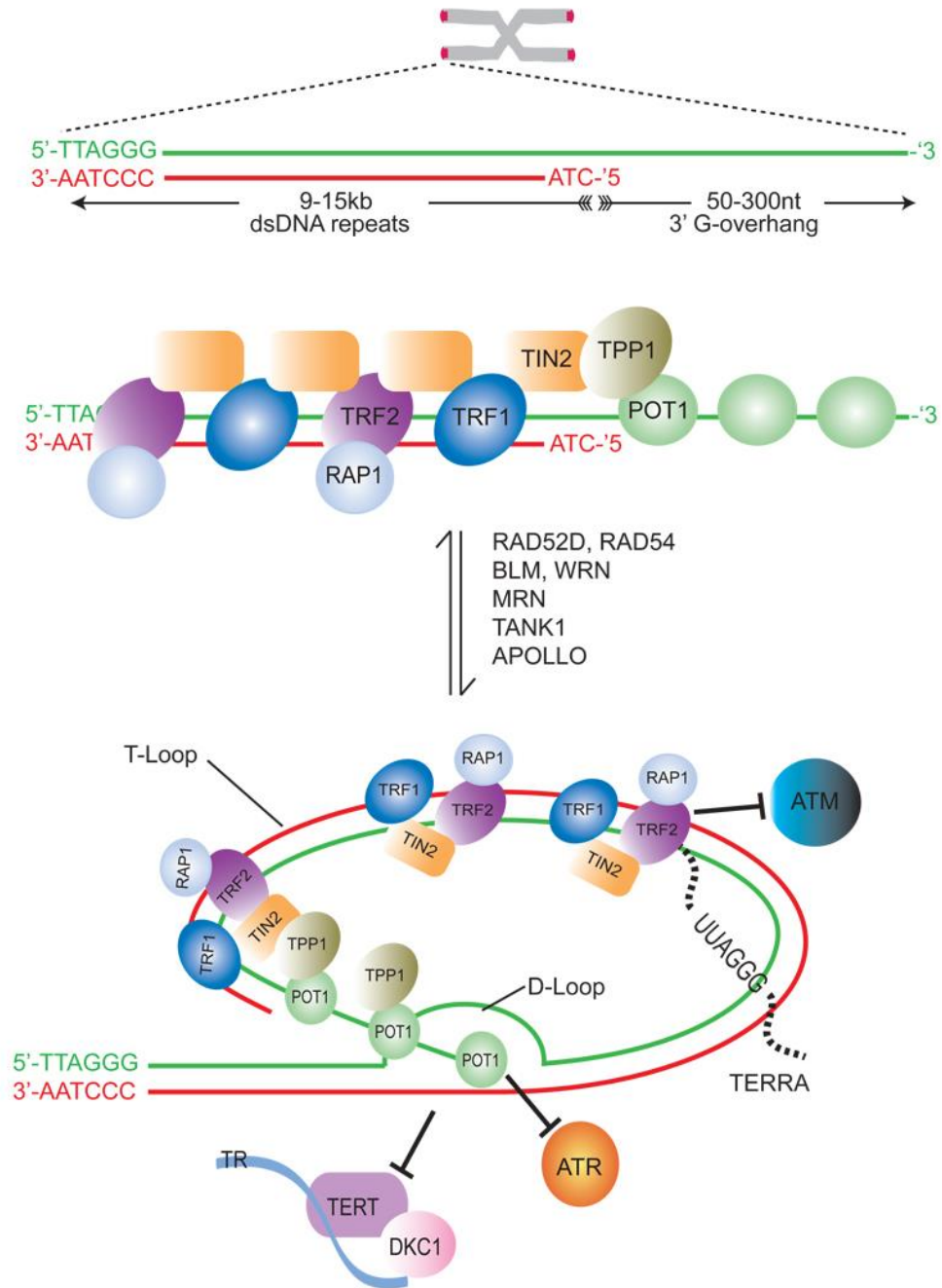


Figure 12. Model of telomere structure.

Reprinted from *Nat Rev Mol Cell Biol*, 11, 171–181 (2010). <https://doi.org/10.1038/nrm2848> Authors: O'Sullivan, R., Karlseder, J. "Telomeres: protecting chromosomes against genome instability." with permission from Springer Nature [26].

Chapter 1 References

1. Fang, C.-B., et al., *Fanconi Anemia Pathway: Mechanisms of Breast Cancer Predisposition Development and Potential Therapeutic Targets*. *Frontiers in Cell and Developmental Biology*, 2020. **8**.
2. Education, N. *Dengue Viruses*. Scitable; Available from: <https://www.nature.com/scitable/topicpage/dengue-viruses-22400925/#:~:text=Discovery%20of%20the%20Dengue%20Viruses&text=In%201943%2C%20Ren%20Kimura%20and,independently%20isolated%20the%20dengue%20virus.>
3. *Dengue and severe dengue*. 2022 January 10, 2022; Available from: <https://www.who.int/news-room/fact-sheets/detail/dengue-and-severe-dengue>.
4. NIAID. *Dengue Fever*. Available from: <https://www.niaid.nih.gov/diseases-conditions/dengue-fever#:~:text=Worldwide%2C%20about%2050%20million%20cases,who%20have%20recently%20traveled%20abroad.>
5. Hasan, S., et al., *Dengue virus: A global human threat: Review of literature*. *J Int Soc Prev Community Dent*, 2016. **6**(1): p. 1-6.
6. Back, A.T. and A. Lundkvist, *Dengue viruses - an overview*. *Infect Ecol Epidemiol*, 2013. **3**.
7. Wang, E., et al., *Evolutionary relationships of endemic/epidemic and sylvatic dengue viruses*. *J Virol*, 2000. **74**(7): p. 3227-34.
8. Hanley, K.A.W., S.C., *Frontiers in dengue virus research*, ed. K.A.W. Hanley, S.C. 2010: Caister Academic Press.
9. Nanaware, N., et al., *Dengue Virus Infection: A Tale of Viral Exploitations and Host Responses*. *Viruses*, 2021. **13**(10).
10. Harapan, H., et al., *Dengue: A Minireview*. *Viruses*, 2020. **12**(8).
11. Póvoa, T.F., et al., *The pathology of severe dengue in multiple organs of human fatal cases: histopathology, ultrastructure and virus replication*. *PLoS One*, 2014. **9**(4): p. e83386.
12. Begum, F., et al., *Insight into the Tropism of Dengue Virus in Humans*. *Viruses*, 2019. **11**(12).
13. van der Schaar, H.M., et al., *Dissecting the cell entry pathway of dengue virus by single-particle tracking in living cells*. *PLoS Pathog*, 2008. **4**(12): p. e1000244.
14. Cruz-Oliveira, C., et al., *Receptors and routes of dengue virus entry into the host cells*. *FEMS Microbiol Rev*, 2015. **39**(2): p. 155-70.
15. Ang, F., et al., *Small interference RNA profiling reveals the essential role of human membrane trafficking genes in mediating the infectious entry of dengue virus*. *Virol J*, 2010. **7**: p. 24.
16. Kaksonen, M. and A. Roux, *Mechanisms of clathrin-mediated endocytosis*. *Nat Rev Mol Cell Biol*, 2018. **19**(5): p. 313-326.
17. Singh, B., et al., *Defective Mitochondrial Quality Control during Dengue Infection Contributes to Disease Pathogenesis*. *J Virol*, 2022. **96**(20): p. e0082822.

18. Simula, M.P. and V. De Re, *Hepatitis C virus-induced oxidative stress and mitochondrial dysfunction: a focus on recent advances in proteomics*. *Proteomics Clin Appl*, 2010. **4**(10-11): p. 782-93.
19. Dan Dunn, J., et al., *Reactive oxygen species and mitochondria: A nexus of cellular homeostasis*. *Redox Biol*, 2015. **6**: p. 472-485.
20. Zhang, Z., L. Rong, and Y.P. Li, *Flaviviridae Viruses and Oxidative Stress: Implications for Viral Pathogenesis*. *Oxid Med Cell Longev*, 2019. **2019**: p. 1409582.
21. Prevention, C.f.D.C.a. *Dengue Clinical Presentation*. For Healthcare Providers; Available from: <https://www.cdc.gov/dengue/healthcare-providers/clinical-presentation.html>.
22. Institute, N.C., in *NCI Dictionary of Cancer Terms*. cancer.gov.
23. Yao, Y. and W. Dai, *Genomic Instability and Cancer*. *J Carcinog Mutagen*, 2014. **5**.
24. Terabayashi, T. and K. Hanada, *Genome instability syndromes caused by impaired DNA repair and aberrant DNA damage responses*. *Cell Biology and Toxicology*, 2018. **34**(5): p. 337-350.
25. Negrini, S., V.G. Gorgoulis, and T.D. Halazonetis, *Genomic instability — an evolving hallmark of cancer*. *Nature Reviews Molecular Cell Biology*, 2010. **11**(3): p. 220-228.
26. O'Sullivan, R.J. and J. Karlseder, *Telomeres: protecting chromosomes against genome instability*. *Nat Rev Mol Cell Biol*, 2010. **11**(3): p. 171-81.
27. Yang, J., et al., *ATM, ATR and DNA-PK: initiators of the cellular genotoxic stress responses*. *Carcinogenesis*, 2003. **24**(10): p. 1571-80.
28. Chatterjee, N. and G.C. Walker, *Mechanisms of DNA damage, repair, and mutagenesis*. *Environ Mol Mutagen*, 2017. **58**(5): p. 235-263.
29. Fuchs, R.P., et al., *Crosstalk between repair pathways elicits double-strand breaks in alkylated DNA and implications for the action of temozolomide*. *eLife*, 2021. **10**: p. e69544.
30. Kulke, M.H., et al., *O6-methylguanine DNA methyltransferase deficiency and response to temozolomide-based therapy in patients with neuroendocrine tumors*. *Clin Cancer Res*, 2009. **15**(1): p. 338-45.
31. Mehrgou, A. and M. Akouchekian, *The importance of BRCA1 and BRCA2 genes mutations in breast cancer development*. *Med J Islam Repub Iran*, 2016. **30**: p. 369.
32. Krokan, H.E. and M. Bjørås, *Base excision repair*. *Cold Spring Harb Perspect Biol*, 2013. **5**(4): p. a012583.
33. Hegde, M.L., T.K. Hazra, and S. Mitra, *Early steps in the DNA base excision/single-strand interruption repair pathway in mammalian cells*. *Cell Research*, 2008. **18**(1): p. 27-47.
34. Kim, Y.J. and D.M. Wilson, 3rd, *Overview of base excision repair biochemistry*. *Curr Mol Pharmacol*, 2012. **5**(1): p. 3-13.
35. Kusakabe, M., et al., *Mechanism and regulation of DNA damage recognition in nucleotide excision repair*. *Genes and Environment*, 2019. **41**(1): p. 2.

36. Gomez, V. and A. Hergovich, *Chapter 14 - Cell-Cycle Control and DNA-Damage Signaling in Mammals*, in *Genome Stability*, I. Kovalchuk and O. Kovalchuk, Editors. 2016, Academic Press: Boston. p. 227-242.
37. de Boer, J. and J.H.J. Hoeijmakers, *Nucleotide excision repair and human syndromes*. *Carcinogenesis*, 2000. **21**(3): p. 453-460.
38. Moldovan, G.L. and A.D. D'Andrea, *How the fanconi anemia pathway guards the genome*. *Annu Rev Genet*, 2009. **43**: p. 223-49.
39. Rageul, J. and H. Kim, *Fanconi anemia and the underlying causes of genomic instability*. *Environ Mol Mutagen*, 2020. **61**(7): p. 693-708.
40. Ohashi, A., et al., *Fanconi anemia complementation group D2 (FANCD2) functions independently of BRCA2- and RAD51-associated homologous recombination in response to DNA damage*. *J Biol Chem*, 2005. **280**(15): p. 14877-83.
41. Liu, W., et al., *Fanconi anemia pathway as a prospective target for cancer intervention*. *Cell & Bioscience*, 2020. **10**(1): p. 39.
42. Davis, A.J. and D.J. Chen, *DNA double strand break repair via non-homologous end-joining*. *Transl Cancer Res*, 2013. **2**(3): p. 130-143.
43. Mao, Z., et al., *Comparison of nonhomologous end joining and homologous recombination in human cells*. *DNA Repair (Amst)*, 2008. **7**(10): p. 1765-71.
44. Woodbine, L., A.R. Gennery, and P.A. Jeggo, *The clinical impact of deficiency in DNA non-homologous end-joining*. *DNA Repair (Amst)*, 2014. **16**: p. 84-96.
45. Pećina-Šlaus, N., et al., *Mismatch Repair Pathway, Genome Stability and Cancer*. *Front Mol Biosci*, 2020. **7**: p. 122.
46. Preston, B.D., T.M. Albertson, and A.J. Herr, *DNA replication fidelity and cancer*. *Semin Cancer Biol*, 2010. **20**(5): p. 281-93.
47. Hsieh, P. and K. Yamane, *DNA mismatch repair: molecular mechanism, cancer, and ageing*. *Mech Ageing Dev*, 2008. **129**(7-8): p. 391-407.
48. Institute, N.C., *mismatch repair deficiency*, in *NCI Dictionary of Cancer Terms*. National Cancer Institute: cancer.gov.
49. Pino, M.S., et al., *Deficient DNA mismatch repair is common in Lynch syndrome-associated colorectal adenomas*. *J Mol Diagn*, 2009. **11**(3): p. 238-47.
50. Yamanaka, K., et al., *Inhibition of mutagenic translesion synthesis: A possible strategy for improving chemotherapy?* *PLoS Genet*, 2017. **13**(8): p. e1006842.
51. Wojtaszek, J.L., et al., *A Small Molecule Targeting Mutagenic Translesion Synthesis Improves Chemotherapy*. *Cell*, 2019. **178**(1): p. 152-159 e11.
52. Sail, V., et al., *Identification of Small Molecule Translesion Synthesis Inhibitors That Target the Rev1-CT/RIR Protein-Protein Interaction*. *ACS Chem Biol*, 2017. **12**(7): p. 1903-1912.
53. Dash, R.C., et al., *Virtual Pharmacophore Screening Identifies Small-Molecule Inhibitors of the Rev1-CT/RIR Protein-Protein Interaction*. *ChemMedChem*, 2019. **14**(17): p. 1610-1617.
54. Chatterjee, N., et al., *REVI inhibitor JH-RE-06 enhances tumor cell response to chemotherapy by triggering senescence hallmarks*. *Proc Natl Acad Sci U S A*, 2020. **117**(46): p. 28918-28921.
55. Wendel, S.O., et al., *HPV 16 E7 alters translesion synthesis signaling*. *Virology*, 2022. **19**(1): p. 165.

56. Dyson, O.F., J.S. Pagano, and C.B. Whitehurst, *The Translesion Polymerase Pol η Is Required for Efficient Epstein-Barr Virus Infectivity and Is Regulated by the Viral Deubiquitinating Enzyme BPLF1*. J Virol, 2017. **91**(19).
57. Victor, J., et al., *SARS-CoV-2 triggers DNA damage response in Vero E6 cells*. Biochem Biophys Res Commun, 2021. **579**: p. 141-145.
58. Victor, J., et al., *SARS-CoV-2 hijacks host cell genome instability pathways*. Res Sq, 2022.
59. Lu, W., et al., *Telomeres-structure, function, and regulation*. Exp Cell Res, 2013. **319**(2): p. 133-41.
60. Rodenhuis-Zybert, I.A., J. Wilschut, and J.M. Smit, *Dengue virus life cycle: viral and host factors modulating infectivity*. Cellular and Molecular Life Sciences, 2010. **67**(16): p. 2773-2786.
61. Barve, A., et al., *DNA Repair Repertoire of the Enigmatic Hydra*. Front Genet, 2021. **12**: p. 670695.
62. Wood, R.D., *Nucleotide excision repair in mammalian cells*. J Biol Chem, 1997. **272**(38): p. 23465-8.
63. Williams, G.J., et al., *Structural insights into NHEJ: building up an integrated picture of the dynamic DSB repair super complex, one component and interaction at a time*. DNA Repair (Amst), 2014. **17**: p. 110-20.

CHAPTER 2: DENGUE VIRUS INFECTION TRIGGERS GENOME INSTABILITY

Introduction and Project Rationale

Given the COVID-19 pandemic, RNA virus research has been gaining traction and provides significant motivation behind researching DENV. Recently, we have shown that SARS-CoV-2, an enveloped, positive sense RNA virus of the *Coronaviridae* family, triggers a DNA damage response in host cells and upregulates genome instability markers in human lung cells, Golden Syrian Hamster lung tissues, COVID-19 autopsy lung tissues, and blood sera from patients with acute COVID-19 and post-COVID. Specifically, we observed host cell genetic alterations, such as increased *HPRT*-mutagenesis, telomere length dysregulation, and elevated microsatellite instability (MSI) [57, 58]. With this, inhibition of REV1, the key scaffolding molecule of the mutagenic translesion synthesis pathway, via JH-RE-06, strongly suppressed SARS-CoV-2 proliferation in cells and organoids. While there are several differences between SARS-COV-2 and DENV, both SARS-CoV-2 and DENV establish severe systemic illnesses affecting multiple organ systems throughout its host, warranting further investigation of DENV-dependent host-cell damage.

While the activation and manipulation of host cell DNA damage response (DDR) and genome instability by DNA viruses have been extensively studied, the study of RNA viruses and their ability to cause DNA damage is gaining traction. In alignment with our previous work on SARS-CoV-2-dependent host cell genome instability, several other RNA

viruses have been documented to activate a host cell DNA damage response. Most interestingly, viruses that complete most of their viral life cycle in the cytoplasm, like DENV, can also cause DNA damage in the host. Shown in **Table 2** is an overview of several RNA viruses and their previously studied impact on the host cell DDR [64]. Previously studied viruses that impact the host cell DNA damage response include HIV-1, HTLV-1, HCV, IBV, Influenza A virus, Chikungunya virus, Sindbis virus, La crosse virus, Rift Valley Fever virus, Avian Reovirus, Zika virus (ZIKV) and SARS-Cov-2 [64].

Further, it is known that viruses of the *Flaviviridae* family, including DENV, trigger oxidative stress, which has been implicated in the pathogenesis of many diseases and cancers [20, 65]. Oxidative stress has been linked to cancer development and, more specifically, has been shown to initiate cancer development by increasing mutagenesis and genome instability [65]. In the field of dengue research, there has been emerging evidence that there is a positive correlation between DNA damage, apoptosis, lipid peroxidation, and oxidative stress during DENV infection [66]. Importantly, DNA damage post-dengue infection in patient peripheral blood mononuclear cells (PBMCs) was assessed using image analysis of comet assays and it was found that patients post-dengue infection had increased DNA damage when compared to OFI (other-febrile illness) and NFI (non-febrile illness) controls [66]. This study also found an increase in Malondialdehyde (MDA, a key marker of oxidative stress) levels in dengue-infected individuals compared to the OFI and NFI controls and an increase in apoptotic cells in the dengue-infected individuals [66]. Each aspect – oxidative stress, DNA damage, and apoptosis can be linked to genome instability mechanisms.

In alignment with the aforementioned observations, oxidative damage to the DNA is a direct mechanism of mutagenesis whereby the low oxidative potential of guanine makes the base susceptible to ROS, leading to the formation of 8-oxo-7,8-dihydroguanine (8-oxoG) which has the potential to incorrectly pair with adenine and lead to mutagenesis in following rounds of DNA replication [67]. Oxidative stress not only can damage host cell DNA, lipids, and proteins but it can also damage protein-coding RNA and cause dysregulation of gene expression [68]. Dysregulation of genes related to the maintenance of the cell cycle and DNA repair are hallmarks of genome instability and cancer development.

Also of note, one of the documented oncogenic viruses, Hepatitis C Virus (HCV), is a related Hepacivirus of the *Flaviviridae* family, which also causes oxidative stress in the host cell. It has been shown that the oxidative stress caused by chronic HCV infection can lead to HCV-induced liver carcinogenesis [69]. However, a key factor in HCV infection leading to liver carcinogenesis is its ability to establish chronic infections [69]. It is unknown whether DENV can establish chronic infections in humans.

From an epidemiological perspective, in 2020, a population-based cohort study through the National Health Insurance Research Databases in Taiwan provided the first epidemiologic evidence for the association between dengue virus infection and leukemia, suggesting a possible association between DENV infection and cancer incidence [70]. However, it should be noted that this study points out that solid cancers typically take at least ten years to develop, whereas leukemias may develop within 2-3 years of a detrimental exposure. The study's median time to follow-up was 8.22 years, short of the 10-year minimum expected of solid tumor development [70]. It remains unknown whether

DENV infection may increase the risk of solid tumors when evaluated over a longer time period following detrimental exposure and infection.

Research Aims

To evaluate host genome instability mechanisms post-dengue virus infection, the following aims were set for this thesis project:

1. Characterize genome instability mechanisms post-dengue infection by analyzing the expression of a broad panel of genome instability markers within the DNA damage response and DNA repair pathways
2. Investigate DENV-dependent modulation of translesion synthesis and verify therapeutic potential via JH-RE-06.NaOH
3. Investigate genome instability post-DENV infection through HPRT mutagenesis and relative telomere length quantification assays

Methodology

Experimental design

In order to ascertain DENV-dependent modulation of host cell DNA repair and genome instability pathways, a time-course analysis post-DENV-4 infection was carried out. Vero E6 and HUH-7 cells were infected with DENV-4, and cell lysates were collected 24 hours post-infection (HPI), 48 HPI, and 5 days post-infection (DPI), as shown in **Figure**

13. Most studies with viral time course analyses often use 48 hours for an endpoint, and this endpoint is often due to limiting factors such as the cytotoxicity of the virus used. An example of this is our recent work studying SARS-CoV-2-dependent modulation of genome instability pathways [57, 58]. However, in this work with DENV-4 in Vero E6 and HUH-7 cells, we were able to evaluate a more comprehensive time course analysis, which included 5-days post-infection. This expanded time course allowed us to fully capture and evaluate DENV-dependent modulation of host cell genome instability pathways.

***In Vitro* Models of Dengue Virus Infection**

Two cell lines, Vero E6 and HUH-7, were chosen as cellular models for DENV-4 infection. DENV-4 was chosen as the dengue virus serotype for this project due to resource availability.

Vero E6 cells were derived from the kidney of an African green monkey (*Chlorocebus sabaues*, AGM) in the 1960s and have since become one of the most widely used mammalian cell lines, especially in the field of virology [71]. Vero E6 cells have been widely utilized in virology research due to their high susceptibility to an array of viruses, including dengue virus. This high susceptibility to viruses is due to a deficiency in interferon expression. Of interest to this study on genome instability, Vero E6 cells were derived from a normal, non-diseased AGM kidney and retain most normal cell characteristics. Most notably, Vero E6 cells have not lost contact inhibition and follow similar growth patterns to normal cells. Further, this continuous cell line allows for the

passaging of the cells over extended periods of time without acquiring the tumorigenic functions seen in most cancer cell lines [72].

HUH-7 cells were derived from male hepatocellular carcinoma, also known as hepatoma, tissue in the 1980s. HUH-7 cells have been predominantly used in the study of hepatitis C virus (HCV), a member of the *Flaviviridae* family, which highly infects hepatocytes. Similarly, HUH-7 cells are highly susceptible to DENV infection, as the liver is a target organ of DENV infection. Of note to this study, HUH-7, being a tumor cell line, contains highly heterogenous cell populations [73].

Initial results, discussed later in this thesis, suggested that genome instability mechanisms in Vero E6 cells and HUH-7 cells may be similar. For this preliminary study with a 1-year timeframe, a majority of genome instability markers were assessed using only the Vero E6 cell line. In addition, the maintenance of normal cellular characteristics was beneficial as we addressed genome instability mechanisms in this cellular model.

Mammalian cell culture and DENV-4 infection

Vero E6 (African Green Monkey Kidney cells) were grown at 37°C with 5% CO₂ in DMEM (Gibco), 10 mM non-essential amino acids (Gibco), 10 mM HEPES (Gibco), 1% penicillin-streptomycin antibiotic (Gibco), and 2% (v/v) fetal bovine serum (FBS, Gibco). HUH-7 (human hepatocellular carcinoma cells) were grown at 37°C with 5% CO₂ in DMEM (Gibco), 1% Penicillin-Streptomycin antibiotic (Gibco), 1% HEPES (Gibco), and 10% fetal bovine serum (FBS, Gibco). The cells were plated into 6-well cell culture plates.

As shown in **Figure 13**, 24 hours after plating the cells, the cells were pre-treated with 10 μ M of the REV1 inhibitor JH-RE-06.NaOH (provided by Drs. Pei Zhou and Jiyong Hong, Duke University). After a 1-hour incubation with JH-RE-06.NaOH, the media was removed, and the cells were infected with DENV-4 at an MOI of 0.1 and fresh, serum-free media was added to the cells (Vero E6: DMEM, 10 mM non-essential amino acids, 10 mM HEPES, 1% penicillin-streptomycin antibiotic; HUH-7: DMEM, 1% Penicillin-Streptomycin antibiotic, 1% HEPES). Dengue virus serotype 4 was kindly provided by the Kirkpatrick lab (University of Vermont) and previously propagated in African green monkey kidney cells (Vero E6).

Cell lysates were collected 24 hours post-infection (HPI), 48 HPI, and 5 DPI after checking cytopathic effect (CPE) under the microscope. Of note, there was visible CPE in infected cells versus the mocks as published previously [74]; and no enhanced CPE in drug-treated versus the non-treated cells. Media was aspirated from the cells and the cells were collected directly in 600 μ L of RLT buffer (Qiagen) and β ME or directly in Laemmli Buffer + β ME.

Immunoblotting

After-infection, protein lysates from Vero E6 and HUH-7 cells were collected directly in 2X Laemmli sample buffer (Bio-Rad) and β ME. Samples were separated on a Novex WedgeWell 4-20% Tris-Glycine gel (Invitrogen). Proteins were transferred onto a polyvinylidene difluoride membrane (Thermo Scientific) at 100V for 90 minutes using the Mini Trans-Blot Electrophoretic Transfer Cell (Bio-Rad). Membranes were blocked using

Pierce StartingBlock (PBS) Blocking Buffer (Thermo Scientific) for one hour and blotted with primary antibody at 4°C overnight. Actin (Invitrogen, MA1744, Mouse mAb) at 1:1000, γ H2AX [p Ser139] (Novus Biologicals, Edgewood, CO, USA; NB100-384, Rabbit pAb) at 1:1000, MLH1 (Cell Signaling Technology, Danvers, MA, USA; 3515S, Mouse mAb) at 1:1000, and TRF2 (Abcam, ab108997, rabbit mAb) at 1:1000 were used as primary antibodies. Membranes were washed three times for 15 minutes each with PBS (Corning) with 0.1% Tween-20 (Sigma-Aldrich) before and after incubating with secondary antibody for 1 hour at ambient temperature, with donkey anti-mouse (IRDye 680RD, Li-COR BioSciences) or goat anti-rabbit (IRDye 800CW, LiCOR Biosciences), at 1:20,000 with 0.01% SDS and 0.1% Tween-20. Membranes were imaged with the Li-COR Odyssey CLx, and images were analyzed with Image Studio software. Bands indicating our proteins of interest were normalized to actin and DENV-infected results were further normalized to the mock controls.

RT-qPCR Analysis

RT-qPCR analysis was used to assess DNA repair gene expression post-DENV infection. Total RNA was extracted from Vero E6 cells post-DENV-4 infection using the AllPrep DNA/RNA/Protein Kit (Qiagen). Two RT-qPCR methods were used in this thesis work.

Method 1:

RNA concentration was quantified using Nanodrop 2000 (ThermoFisher) and diluted to 10 ng/ μ L using RNase/Dnase Free Molecular Grade H₂O (Cytiva). The qPCR reaction was performed using the iTaq Universal SYBR Green One-Step Kit (Bio-Rad, #1725151). The reaction was set as follows: reverse transcription reaction for 10 minutes at 50°C, polymerase activation and denaturation for 1 minute at 95°C followed by 35-40 cycles of amplification. Each amplification cycle consisted of denaturation for 15 seconds at 95°C and annealing/extension and plate read at 60°C for 60 seconds. All primer sequences are provided in **Table 3**. GAPDH was used as the housekeeping gene.

Method 2:

Total RNA was extracted as mentioned above. Using the High Capacity RNA-to-cDNA kit (Applied Biosystems), 2000 ng of total RNA was converted to 2000 ng of cDNA. Specifically, a 9 μ L mix of total RNA and H₂O containing 2000 ng of RNA was added to 10 μ L of 2X RT Buffer Mix and 1.0 μ L of RT Enzyme Mix for a total reaction volume of 20 μ L. Cycling conditions were followed per the manufacturer's instructions using the MiniAmp Plus Thermal Cycler (Applied Biosystems). A panel of 95 DNA repair genes was tested using the TaqMan Array Human DNA Repair Mechanism plate (Applied Biosystems). The TaqMan Fast Advanced Master Mix (Applied Biosystems) with the following cycling conditions: 95°C for 20 seconds and 40 cycles of 95°C for 1 second followed by 60°C for 20 seconds. TaqMan® Primers used are listed in **Table 3**. 18S rRNA was used as the housekeeping gene.

All qPCR data was collected using the QuantStudio 3 Real Time PCR system (ThermoFisher) and analyzed using the QuantStudio Design and Analysis Software v1.5.1 using the $\Delta\Delta CT$ method. Statistical analysis was performed using GraphPad Prism version 9.4.1. Multiple unpaired t-tests were performed to compare the mock control to each post-infection timepoint. * $P < 0.05$, ** $P < 0.01$, *** $P < 0.001$, **** $P < 0.0001$.

RNA-Sequencing Analysis

Total RNA was extracted from Vero E6 cells post-DENV-4 infection using the AllPrep DNA/RNA/Protein Kit (Qiagen). Standard RNA-Sequencing was performed by Genewiz Azenta Life Sciences RNA Sequencing services and followed their documented workflow. Preliminary analysis was carried out by normalizing transcripts per million (TPM) counts of specific genes to the mock control for n=1 biological replicate. The following two biological replicates had not resulted at the time of this thesis submission.

HPRT Mutagenesis

The HPRT mutagenesis assay was conducted on 20 ng of DNA extracted from Vero E6 cells post-DENV infection using the AllPrep DNA/RNA/Protein Kit (Qiagen). DNA concentration was quantified using Nanodrop 2000 (ThermoFisher). Exon 6 of the HPRT gene was amplified using the Platinum SuperFi II Master Mix from ThermoFisher Scientific using the primers listed below. PCR amplification was conducted on the MiniAmp Plus Thermal Cycler using the following cycling conditions: 98°C for 30

seconds; 35 cycles of 98°C for 10 seconds, followed by 60°C for 10 seconds, and then 72°C for 1 minute; 72°C for 5 minutes ending with a 4°C hold until the samples are ready to be used. The PCR reactions were run with 4 technical replicates per each treatment condition. The PCR products were purified using the QIAquick PCR Purification Kit (Qiagen). Sanger sequencing was conducted at Azenta Life Sciences. Data generated was analyzed using Geneious version 2022.0.2.

HPRT Primers:

HPRT FWD: GACAGTATTGCAGTTATACATGGGG

REV/SEQ: CCAAATCCTCTGCCATGCTATTC

Relative Telomere Length Quantification

DNA was extracted from Vero E6 cells post-DENV infection using the AllPrep DNA/RNA/Protein Kit (Qiagen) and quantified using Nanodrop 2000 (ThermoFisher). The DNA was diluted to 2 ng/μL using RNase/DNase Free Molecular Grade H₂O (Cytiva). Two primers were used from the Relative Telomere Length Quantification qPCR kit from ScienCell: a primer designed to recognize telomeric repeats (Tel) and a primer for a single copy reference control on chromosome 17 (SCR). Each reaction contained 2 ng of DNA mixed with 2 μL of primer (Tel or SCR), 10 μL of the PowerTrack SYBR Green Master Mix (ThermoFisher), and Q.S. to 20 μL with RNase/DNase Free Molecular Grade H₂O. The reaction conditions were set to 95°C for 2 minutes, followed by 40 cycles of 95°C for

15 seconds and 60°C for 1 minute on the QuantStudio 3 Real Time PCR system (ThermoFisher) and analyzed using the QuantStudio Design and Analysis Software v1.5.1.

Results: Aim 1

Dengue infection induces DNA damage in HUH-7 and Vero E6 cells

γ H2AX, phosphorylated H2AX, is a key sensor of DNA damage and has been widely used as a quantitative marker for double-strand breaks in the DNA [75]. Here, we assessed the expression level of γ H2AX via western blot on a time course analysis of HUH-7 and Vero E6 cells post-DENV infection (**Figure 14**). We see a significant increase in H2AX phosphorylation with increased time post-DENV infection, indicative of DNA damage and the accumulation of double-strand breaks in the DNA. Strikingly, the 5-day post-infection time point shows a significantly increased level of phosphorylated H2AX, suggesting that this is a key time point to be assessed.

Given the similar results in γ H2AX expression in both Vero E6 and HUH-7 cells, the 1-year timeframe for this master's thesis project, and the maintenance of normal cellular characteristics in Vero E6 cells, we decided to continue analysis solely in Vero E6 cells to lay the groundwork for the understanding of DENV modulation of host cell genome instability pathways.

After determining that there was an accumulation of DNA damage in cells post-DENV infection, as shown by increased phosphorylation of H2AX, we assessed the gene transcript expression of a panel of DNA damage response and DNA repair genes post-

DENV infection. While many of the DNA repair genes are closely related and overlap several pathways, here we categorize several DNA repair and DNA damage response genes into their primary pathways to further delineate which pathways DENV infection may modulate.

Dengue virus modulation of DNA damage response and cellular stress response genes

To assess DENV-dependent modulation of host cell DNA damage response (DDR) and related cellular stress response genes, RT-qPCR analysis of ATM, ATR, CHEK1, CHEK2, PARP1, TP53, RAD17, HUS1, PSMA3, PSMB10, MDM2, GADD45A, and GADD45B in Vero E6 cells 24 HPI, 48 HPI, and 5 DPI was performed (**Figure 15**).

Interestingly, there is a significant decrease in ATM and ATR transcript expression at 5 DPI. Both ATM and ATR are key transducers of the DNA damage response (DDR). The ATM and ATR signaling pathways are activated in response to DNA damage and signal their downstream effectors to initiate cell cycle arrest, DNA repair, apoptosis, senescence, or other cellular response to DNA damage. Specifically, the downstream effectors of ATM and ATR are CHEK2 and CHEK1, respectively [76]. A decrease in ATM and ATR transcript expression may result in deficient DDR and minimize the cell's ability to initiate processes to combat DNA damage.

Interestingly, we saw an increase of phosphorylated H2AX via western blot, indicative of double-strand breaks in the DNA, yet here we observe a decrease in ATR gene expression post-DENV infection. These results, in combination, suggest that DENV-dependent suppression of the DDR and its downstream effectors may lead to the

accumulation of unrepaired double-strand breaks we have observed, as indicated by increased γ H2AX. Further, the significant repression of ATR's downstream effector CHEK1, is also a significant factor leading to the accumulation of DSBs. Additionally, we observed no change in CHEK2 expression.

With this, we observed a significant decrease in PARP1 at 48 HPI and 5 DPI. One of the earliest events in the DDR is the recruitment of PARP1 (Poly (ADP-ribose) polymerase 1) to the site of DNA damage, usually single-strand and double-strand breaks [77]. Deficient pathways which lead to the repair of single-strand breaks may be leading to the accumulation of unrepaired single-strand breaks, which are unstable and can lead to double-strand breaks [78].

Next, we observed that there was not a significant change in TP53 transcript expression. TP53, also referred to as tumor protein p53, promotes cell cycle arrest to allow for DNA repair or apoptosis. The tumor protein p53 is a tumor suppressor protein and maintains genome stability by initiating cell cycle arrest and allowing for DNA repair or apoptosis. It has previously been reported that DENV infection can trigger host cell p53-dependent apoptosis [79]. Our results further support this observation by suggesting there are sufficient p53 levels post-DENV infection to engage the p53-dependent apoptosis pathway.

In conjunction with this result, we examined MDM2 expression post-DENV infection. We observed a slight decrease in MDM2 transcript expression levels at 48 HPI. The MDM2 levels were unchanged at all other time points. MDM2 is a known inhibitor of p53. When MDM2 binds to p53, MDM2 stimulates the nuclear export and degradation of

p53. This is of interest as any decrease in MDM2 may increase p53's ability to carry out its functions to initiate cell cycle arrest and DNA repair [80].

Next, we evaluated the expression of HUS1 and RAD17, checkpoint proteins and sensors of DNA damage. We observed a significant decrease in HUS1 at 48 HPI and a significant decrease in both HUS1 and RAD17 at 5 DPI. HUS1 is a protein that is a part of the heterotrimeric complex with RAD9 and RAD1, often termed the 9-1-1 complex. RAD17 can bind to chromatin and can be phosphorylated by ATR if the chromatin becomes damaged. RAD17 can then recruit the 9-1-1 complex, which initiates downstream cellular responses, such as DNA-damage-induced cell cycle G2 arrest [81].

After this, we evaluated PSMA3 and PSMB10 expression. PSMB10 expression was significantly repressed at 24 HPI, 48 HPI, and 5 DPI. PSMA3 expression was significantly repressed at 48 HPI and 5 DPI. Both PSMA3 and PSMB10 are proteasome subunits.

Next, we assessed the transcript expression of GADD45A and GADD45B. We observed a significant decrease in GADD45B at 5 DPI. In contrast, there was only a decrease of GADD45A at 48 HPI, with transcript levels unchanged at 24 HPI and 5 DPI. Both GADD45A and GADD45B are growth arrest and DNA damage-inducible proteins and downstream effectors of p53. Specifically, the GADD45 genes have been implicated in initiating cellular responses to stress and DNA damage, most often in response to UV radiation. Both GADD45A and GADD45B have been implicated in several cellular stress responses including G2/M cell cycle arrest, G1 cell cycle arrest, DNA repair (NER), apoptosis, and senescence [82]. GADD45 genes are important to the maintenance of genome stability. It has been reported that GADD45-null cells often exhibit chromosomal

abnormalities and further, GADD45-deficient mice show increased radiation carcinogenesis [83, 84]. Repression of GADD45A and GADD45B transcripts post-DENV infection may increase genome instability in the host cells.

Finally, we assessed several MAPK genes associated with pathways in response to cellular stress and DNA damage (**Figure 16**). JNK is a MAPK family protein that is activated in response to cellular stress. Three of the JNK isoforms are JNK1 (MAPK8), JNK2 (MAPK9), and JNK3 (MAPK10). This signaling pathway ultimately leads to several cellular processes. However, the JNK pathway most commonly leads to apoptosis [85]. Here we observed a significant decrease in MAPK8 at 48 HPI and MAPK8 and MAPK9 at 5 DPI. Interestingly, although not significant, there appears to be an increase in MAPK10. This could be indicative of the aforementioned pro-apoptotic signaling. We also assessed MAPK11, MAPK12, and MAPK14, which are the p38 MAPKs. The p38 MAPKs respond to stressful stimuli including LPS, heat shock, UV light, and even oncogenic activation. The p38 MAPK pathway can lead to several cellular outcomes including apoptosis and senescence. Here we report decreased MAPK12 transcript expression at 48 HPI and decreased transcription of MAPK12 and MAPK14 at 5 DPI. There is no change in MAPK11 expression post-DENV infection.

Dengue virus modulation of base excision repair transcript expression

Knowing that DENV, like other viruses of the *Flaviviridae* family, can cause oxidative stress in host cells, which can lead to oxidative DNA damage, we tested the transcript expression of base excision repair (BER) genes. Base excision repair is the main

pathway in which oxidative base damage is repaired. To assess base excision repair gene expression, RT-qPCR analysis of MBD4, XRCC1, NTHL1, OGG1, APEX1, PNKP, FEN1, LIG3, and POL β transcript expression in Vero E6 cells 24 HPI, 48 HPI, and 5 DPI was performed (**Figure 17**). Here we observe a significant decrease in MBD4, OGG1, APEX1, FEN1, and POL β expression at 48 HPI and a significant decrease in OGG1, APEX1, XRCC1, LIG3, FEN1, and PNKP expression at 5 DPI. Interestingly MBD4 and POL β decreased expression is not sustained at 5 DPI. Additionally, there is no change in the expression of the NTHL1 gene.

MBD4 (MED1), OGG1, and NTHL1 are DNA glycosylases used in BER. PNKP (polynucleotide kinase/phosphatase) is a bifunctional end-processing enzyme with 5' kinase and 3' phosphatase activity. XRCC1 helps to coordinate BER by binding to abasic (AP) sites in the DNA and binding to BER intermediates [32]. APEX1, also known as APE1, is an AP endonuclease that mainly functions in the BER pathway but also has been shown to protect against oxidative damage by inhibiting reactive oxygen species (ROS) production [32, 86]. POL β is the key polymerase that fills in the gaps at the AP sites. FEN1, also known as flap endonuclease 1, is important in long-patch BER. FEN1 contains 5' flap endonuclease, 5'-3' exonuclease, and gap endonuclease activities [87]. LIG3 is an important ligase in BER. Through BER, oxidative base damage can be converted to double-stranded breaks to be repaired and ligated by LIG3 [88]. Like many DNA repair pathways, BER plays a key role in maintaining genome stability. The BER pathway allows cells to cope with damages from oxidation, alkylation, and deamination. However, this decrease in BER expression post-dengue infection may indicate a decreased tolerance to these agents,

including the oxidative damage caused by DENV, and further increase in genome instability.

Dengue virus modulation of mismatch repair transcript expression

To assess mismatch repair gene expression, RT-qPCR analysis of MSH2, MSH3, and MSH6 transcript expression in Vero E6 cells 24 HPI, 48 HPI, and 5 DPI was performed. Strikingly, we see a significant decrease in MSH2, MSH3, and MSH6 transcript expression at 5 DPI (**Figure 18**). In addition, there is also a significant decrease in MSH2 and MSH6 transcript expression at 48 HPI. MSH2 is a mismatch repair protein that forms heterodimers with both MSH3 (MSH2-MSH3, MutS β) and MSH6 (MSH2-MSH6, MutS α). These heterodimers recognize and bind to mismatches in the DNA to facilitate mismatch repair. Specifically, the MSH2-MSH6 heterodimer can recognize single base mismatches and dinucleotide indel (insertion-deletion) loops, and the MSH2-MSH3 heterodimer can recognize larger indel loops that are about 13 nucleotides long [45, 89]. Deficient mismatch repair is directly linked to microsatellite instability (MSI), causing genome instability. Deficient mismatch repair post-DENV infection is indicative that there may be an increased mutational rate and potentially MSI in these cells.

A western blot was performed to assess MLH1 protein levels post-DENV infection to accompany this MMR transcript expression assessment. Visually, there appears to be no change in MLH1 protein levels. However, preliminary quantification shows there may be a decrease at 5 DPI. More analysis must be completed before a conclusion can be made on MLH1 protein expression post-DENV infection.

Dengue virus modulation of homologous recombination transcript expression

To assess homologous recombination (HR) gene expression, RT-qPCR analysis of BRCA1, BRCA2, BARD1, MRE11A, NBN, and RAD51 transcript expression in Vero E6 cells 24 HPI, 48 HPI, and 5 DPI was performed (**Figure 19**).

Most strikingly, there is a significant decrease in BRCA1, BRCA2, and BARD1 at 5 DPI. In addition, there is a significant decrease in BRCA2 at 48 HPI. Both BRCA1 and BRCA2 are tumor suppressor genes and key proteins in maintaining genome stability. While BRCA1 and BRCA2 have functions outside of homologous recombination, their main functions are their role in homologous recombination. Homologous recombination repairs double-strand breaks in the DNA in a relatively error-free fashion. Without HR, the cell will attempt to repair the DSB, often in an error-prone fashion, leading to genome instability. BARD1 interacts with BRCA1 and aids in BRCA1's function to maintain genome stability by forming a stable BARD1/BRCA1 complex [90]. A deficiency in BRCA1 and BRCA2 has been shown to induce severe genome instability [91, 92]. Clinically, women in the general population have a lifetime risk of breast cancer of 13%. However, 55-72% of women with BRCA1 germline mutations and 45-69% of women with BRCA2 germline mutations will develop breast cancer by 70-80 years old [93]. This significant decrease in BRCA1, BRCA2, and BARD1 we have observed post-DENV infection may indicate genome instability in these cells.

Next, we tested MRE11A, NBN, and RAD51. Here, we observed decreased NBN transcript expression at 48 HPI and 5 DPI. Interestingly, we see a decrease in MRE11a

transcript expression at 48 HPI but unchanged at all other time points. Finally, we see no significant difference in RAD51 expression. However, there was significant biological variability in RAD51 expression post-DENV infection. NBN, also referred to as NSB1, is the gene that encodes nibrin. Nibrin can form a complex with MRE11A and RAD50, which is recruited to the site of DSBs by γ H2AX and RAD17. Further, this complex can interact with ATM. The MRN complex has nuclease activity which carries out DNA end resection. This DNA end resection helps to facilitate HR [94]. RAD51 is key to homologous recombination as it directly connects the DNA substrate with the homologous template, which creates the heteroduplex DNA (D-loop) [95].

Dengue virus modulation of non-homologous end joining transcript expression

After assessing homologous recombination genes, we assessed the other most common double-strand break repair pathway, non-homologous end joining (NHEJ). To assess NHEJ gene expression, RT-qPCR analysis of LIG4, PRKDC, XRCC4, XRCC5, and XRCC6 transcript expression in Vero E6 cells 24 HPI, 48 HPI, and 5 DPI was performed (**Figure 20**). Here we observed a significant decrease in transcript expression of LIG4 and XRCC4 at 48 HPI. We also see a significant decrease in LIG4, PRKDC, XRCC4, XRCC5, and XRCC6 expression at 5 DPI.

NHEJ repairs double-strand breaks in an error-prone manner. While NHEJ in and of itself has the potential to be mutagenic and cause genome instability, there remains a benefit to repairing DSBs as they are extremely toxic to the cell. The decrease in NHEJ expression, combined with our previous observation of a DENV-dependent decrease in HR

expression, suggests that double-strand breaks in the DNA may be left unrepaired. This aligns with our previous result showing the accumulation of DSBs by quantifying γ H2AX expression.

Dengue virus modulation of Fanconi anemia transcript expression

To assess Fanconi anemia (FA) gene expression, RT-qPCR analysis of FANCA, FANCC, FANCD2, FANCE, FANCF, FANCG, and DCLRE1A transcript expression in Vero E6 cells 24 HPI, 48 HPI, and 5 DPI was performed (**Figure 21**). Strikingly, we see decreased transcript expression of FANCA, FANCC, FANCD2, FANCE, FANCG, and DCLRE1A at 5 DPI. We also see a decrease in FANCG expression at 48 HPI. Interestingly, FANCF expression is unchanged.

The Fanconi Anemia (FA) pathway is a key protector against genome instability by coordinating several classical repair pathways to remove interstrand crosslinks (ICLs) from the DNA. Fanconi anemia, the disease after which the Fanconi anemia pathway is named, is a rare genetic disorder in which symptomatology (bone marrow failure, developmental abnormalities, high cancer risk) is a result of genome instability from deficient interstrand crosslink repair [39]. The decreased expression of FA genes post-DENV infection suggests that DENV may induce genome instability in these cells.

Dengue virus modulation of nucleotide excision repair transcript expression

To assess nucleotide excision repair gene expression, RT-qPCR analysis of ERCC1, ERCC2, ERCC3, ERCC4, ERCC5, ERCC6, ERCC8, GTF2H3, GTF2H1, LIG1, XAB2, and XPC transcript expression in Vero E6 cells 24 HPI, 48 HPI, and 5 DPI was performed (**Figure 22**). Here we observe a significant decrease in ERCC8 at 24 HPI, ERCC4, ERCC5, ERCC8, GTF2H1, LIG1, and XAB2 at 48 HPI, and ERCC1, ERCC2, ERCC3, ERCC4, ERCC5, ERCC6, ERCC8, GTF2H3, GTF2H1, LIG1, and XAB2. Interestingly, we do not see a change in the expression of XPC.

Nucleotide excision repair plays a key role in maintaining genomic stability by repairing bulky DNA lesions. Here, we see a significant decrease in the expression of several NER genes. This is indicative of an increased susceptibility to bulky, helix-distorting lesions in the DNA.

Dengue virus modulation of direct DNA damage reversal transcript expression

Briefly, to assess direct reversal of DNA damage gene expression, RT-qPCR analysis of MGMT transcript expression in Vero E6 cells 24 HPI, 48 HPI, and 5 DPI was performed (**Figure 23**). We observed a slight decrease in MGMT transcript expression at 48 HPI while all other time points were unchanged.

Dengue virus modulation of DNA repair-associated polymerases

To assess several DNA repair-associate polymerases which had not previously been assessed, RT-qPCR analysis of POLA1, POLR2A, POLR2B, POLR2C, POLR1B, POLD1, POLG, and POLQ transcript expression in Vero E6 cells 24 HPI, 48 HPI, and 5 DPI was performed (**Figure 24**). Here we observed a significant decrease in POLA1, POLR1B, and POLG expression at 48 HPI. We also observed a significant decrease in POLA1, POLR2A, POLR2B, POLR1B, POLG, and POLQ at 5 DPI.

Post-DENV infection RNA-Sequencing analysis

Finally, to further validate gene expression, we performed standard RNA-Sequencing. However, at the time of this thesis submission, only one out of three biological replicates have resulted. Therefore, we will share our preliminary data (**Figure 25**). The other two biological replicates will be required to make formal conclusions based on this data. Overall, we continue to see a pattern of global repression of DNA repair genes in post-DENV samples compared to the mock.

Results: Aim 2

Dengue virus infection modulates the mutagenic translesion synthesis pathway

The second aim of this project was to assess the novel link between the mutagenetic translesion synthesis pathway and viral infection in the context of dengue virus infection. Recently, we discovered a link between translesion synthesis and SARS-CoV-2 whereby

SARS-CoV-2 infection increased expression of the mutagenic translesion synthesis pathway, accompanied by increased genetic alterations and mutagenesis.

Because of this, we sought to assess whether DENV infection similarly increases mutagenic translesion synthesis expression (**Figure 26**). Despite significant variability in the expression of TLS genes, there was no significant difference in REV1 and REV7 transcript expression. There is a slight decrease in POL η and POL κ at 48 HPI and POL η at 5 DPI. However, there is a significant increase in POL ι expression at 5 DPI. This increased expression of POL ι is also noted in the preliminary RNA-Seq data (**Figure 25**). This is of interest as we previously observed a significant decrease in Fanconi anemia expression. Interestingly, POL ι has been shown to compensate for deficiencies in the Fanconi anemia pathway [96]. Additionally, evidence suggests POL ι plays a protective role against oxidative damage [97]. Whether POL ι plays a role in protecting host cells from DENV-dependent oxidative damage remains unknown.

Therapeutic potential of JH-RE-06 in dengue virus infection

Recently, we observed that JH-RE-06 pre-treatment suppresses SARS-CoV-2 proliferation, suggesting a link between RNA viral infection and the translesion synthesis pathway. JH-RE-06.NaOH is a small molecule inhibitor that inhibits REV1, the key scaffolding molecule of translesion synthesis. This inhibition of REV1 prevents the assembly of other TLS polymerases, suppressing lesion bypass. JH-RE-06.NaOH specifically works by dimerizing REV1, preventing REV1/REV7 (subunit of POL ζ) binding. Given JH-RE-06.NaOH's therapeutic effect in SARS-CoV-2 infection, we

decided to test pre-treatment with JH-RE-06.NaOH in Vero E6 cells prior to DENV infection.

In order to assess the relative DENV-4 level, RT-qPCR was used to detect DENV RNA specific to serotype 4. We used previously designed and validated primers to detect DENV-4 by Mun et al., 2019 [98] .

Here we report a near-complete suppression of DENV-4 proliferation in Vero E6 cells with pre-treatment with JH-RE-06.NaOH at 5 DPI (**Figure 27**). This is indicative that there may be a link between functional translesion synthesis and the dengue virus life cycle. Further, JH-RE-06 may hold significant therapeutic potential for patients infected with DENV.

Results: Aim 3

Dengue virus does not modulate host cell telomeres

To assess whether DENV infection may be causing telomere instability in host cells, we assessed the relative telomere length in Vero E6 cells post-DENV infection at 24 HPI, 48 HPI, and 5 DPI. A key indicator of telomere instability is the lengthening and shortening of telomeres. Here, we did not observe a significant change in telomere lengths post-DENV infection (**Figure 28A**).

In addition to this, we assessed TRF2 protein expression post-DENV infection in Vero E6 cells. In the representative western blot shown in **Figure 28B**, there does not appear to be a significant difference in TRF2 expression post-DENV infection.

Finally, we assessed preliminary RNA-sequencing data of one biological replicate on 15 telomere genes (DKC1, GAR1, NHP2, NOP10, POT1, RAP1A, RAP1B, RTEL1, RUVBL1, RUVBL2, TERF1, TERF2, TERT, TINF2, and TPP1) in **Figure 28C**. Preliminarily, all these telomere genes are not differentially expressed post-DENV infection. More experimentation must be completed to conclude any results on these genes via RNA-sequencing analysis and determine significance once all biological replicates have been analyzed.

HPRT mutagenesis post-dengue virus infection

Next, we aimed to assess mutation formation in cells post-DENV infection due to the deficient DNA repair pathways observed and our hypothesized association between DENV infection and the mutagenic translesion synthesis pathway. HPRT mutagenesis assays are the main method of assessing mutation formation in cells. However, the typical HPRT mutagenesis assay uses a colony formation assay to assess HPRT mutagenesis. Given the restraints of DENV cytopathic effect (CPE) and the original experimental design, we decided to assess mutation formation using Sanger sequencing of exon 6 of the HPRT gene. We performed Sanger sequencing on eight treatment conditions: mock, 24 HPI, 48 HPI, and 5 DPI, both with and without JH-RE-06.NaOH treatment. The PCR for this experiment was performed four separate times however, only one biological replicate was completed during the timeframe of this project. All genetic alterations which occur in more than 1% of the population were categorized as single nucleotide polymorphisms (SNPs). More biological replicates will be needed to conclude these results. Preliminarily, we

observe a deletion at base 44 of HPRT exon 6 in 24 HPI and 48 HPI post-DENV infection samples.

Chapter 2 Figures and Tables

Table 2. RNA viruses and host cell DNA damage response.

| Virus | Family | RNA Genome Conformation | DDR Consequences | References |
|--|-------------------------|----------------------------|--|------------|
| Human immunodeficiency Virus 1 (HIV-1) | <i>Retroviridae</i> | + single strand (2 copies) | Activation of ATR, replication stress, activation of nucleases and formation of DDR foci by Vpr | [99-102] |
| Human T-cell lymphotropic virus 1 (HTLV-1) | <i>Retroviridae</i> | + single strand (2 copies) | Genome instability and DNA damage; attenuation of BER, NER, MMR, HR, NHEJ pathways by Tax. Generation of ROS | [103-105] |
| Hepatitis C virus (HCV) | <i>Flaviviridae</i> | + single strand | Generation of ROS and NO, reduced expression of MMR, BER and NER components, interaction of viral proteins with ATM and modulation of ATM pathway activity | [106-110] |
| Infectious bronchitis virus (IBV) | <i>Coronaviridae</i> | + single strand | Activation of ATR pathway and DNA replication stress | [111] |
| Influenza A virus | <i>Orthomyxoviridae</i> | - single strand | Direct DNA damage (comet assay) Induction of γ H2AX foci | [112, 113] |
| Chikungunya virus | <i>Togaviridae</i> | + single strand | Induction of GADD34 expression | [114] |
| Sindbis virus | <i>Togaviridae</i> | + single strand | Activation of PARP-1 | [115] |
| La Crosse virus | <i>Bunyaviridae</i> | - single strand | Increased phosphorylation of H2AX | [116] |
| Rift valley fever virus (RVFV) | <i>Bunyaviridae</i> | - single strand | Activation of ATM signaling; inhibition of ATR | [117] |
| Avian Reovirus (ARV) | <i>Reoviridae</i> | double strand | Genome instability and activation of ATR signaling | [118] |
| Borna disease virus 1 (BoDV-1) | <i>Bornaviridae</i> | - single strand | Downregulation of ATR/CHK1 signaling pathway, impairing DNA repair, increasing DSBs | [119] |
| Zika virus (ZIKV) | <i>Flaviviridae</i> | + single strand | Activation of ATM/CHK2 signaling pathway, suppression of ATR/CHK1 signaling pathway, induction of DSBs. | [120] |
| Severe acute respiratory syndrome coronavirus 2 (SARS-CoV-2) | <i>Coronaviridae</i> | + single strand | Activation of ATR signaling, increased phosphorylation of H2AX. | [57] |

Table adapted from Ryan et al., 2016 [64].

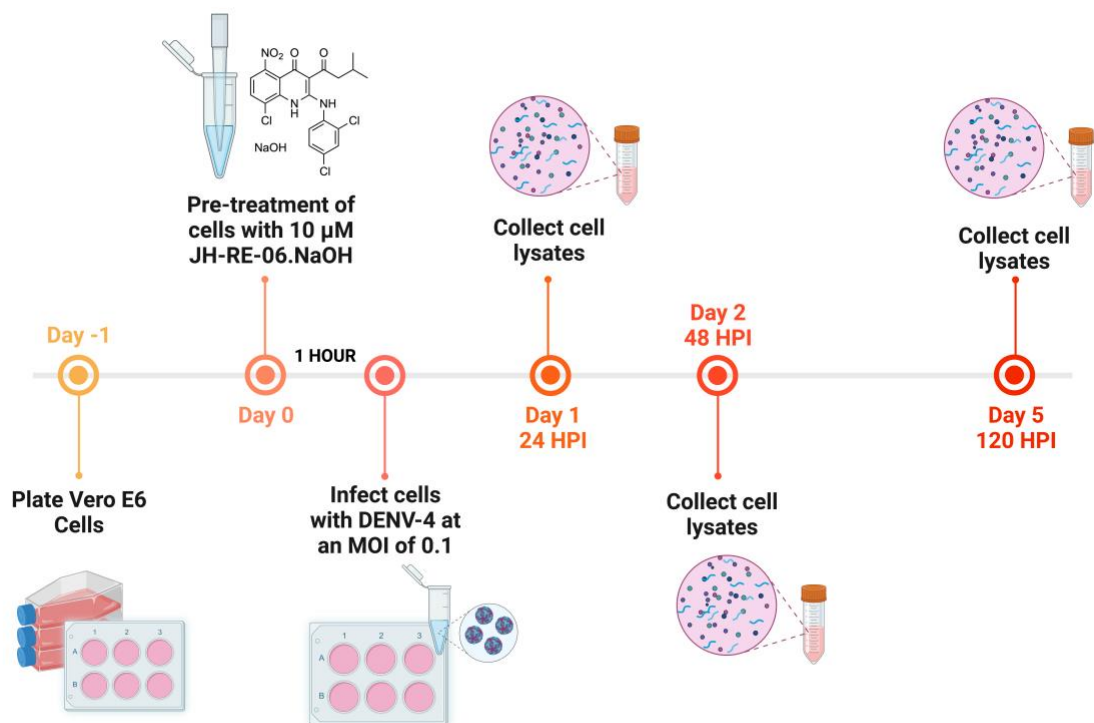


Figure 13. Model of experimental design. Vero E6 cells were plated in 6-well cell culture dishes on day -1. On day 0, cells were pre-treated with 10 μM of JH-RE-06.NaOH. The cells were incubated with the drug for one hour, then the media replaced. Cells were infected with DENV-4 at an MOI of 0.1. Cell lysates were collected 24 hours post-infection (HPI), 48 HPI, and 5 days post-infection (DPI).

Table 3. RT-qPCR primers.

| TaqMan® Primers | | | |
|-----------------|-----------------------------|--------|---------------|
| 18S | Hs99999901_s1 | MAPK9 | Hs00177102_m1 |
| APEX1 | Hs00172396_m1 | MBD4 | Hs00187498_m1 |
| ATM | Hs01112307_m1 | MDM2 | Hs99999008_m1 |
| ATR | Hs00354807_m1 | MGMT | Hs01037698_m1 |
| BARD1 | Hs00184427_m1 | MRE11A | Hs00967437_m1 |
| BRCA1 | Hs01556193_m1 | MSH2 | Hs00953523_m1 |
| BRCA2 | Hs01037414_m1 | MSH3 | Hs00989003_m1 |
| CCNO | Hs00221731_m1 | MSH6 | Hs00264721_m1 |
| CHEK1 | Hs00967506_m1 | NBN | Hs00159537_m1 |
| CHEK2 | Hs00200485_m1 | NTHL1 | Hs00267385_m1 |
| DCLRE1A | Hs00384872_m1 | OGG1 | Hs00213454_m1 |
| ERCC1 | Hs01012158_m1 | PARP1 | Hs00242302_m1 |
| ERCC2 | Hs00361161_m1 | PNKP | Hs00892544_m1 |
| ERCC3 | Hs00164475_m1 | POLA1 | Hs00213524_m1 |
| ERCC4 | Hs00193342_m1 | POLB | Hs00160263_m1 |
| ERCC5 | Hs00164482_m1 | POLD1 | Hs00172491_m1 |
| ERCC6 | Hs00972920_m1 | POLG | Hs00160298_m1 |
| ERCC8 | Hs00163958_m1 | POLH | Hs00197814_m1 |
| FANCA | Hs01116668_m1 | POLK | Hs00211965_m1 |
| FANCC | Hs00984538_m1 | POLQ | Hs00198196_m1 |
| FANCD2 | Hs00276992_m1 | POLR1B | Hs00219263_m1 |
| FANCE | Hs00222482_m1 | POLR2A | Hs00172187_m1 |
| FANCF | Hs00256030_s1 | POLR2B | Hs00265358_m1 |
| FANCG | Hs00184947_m1 | POLR2C | Hs00160308_m1 |
| FEN1 | Hs00748727_s1 | PRKDC | Hs00179161_m1 |
| GADD45A | Hs00169255_m1 | PSMA3 | Hs00541059_m1 |
| GADD45B | Hs00169587_m1 | PSMB10 | Hs00160620_m1 |
| GTF2H1 | Hs00366525_g1 | RAD17 | Hs00607830_m1 |
| GTF2H3 | Hs00231000_m1 | RAD51 | Hs00153418_m1 |
| HUS1 | Hs00189595_m1 | TP53 | Hs01034249_m1 |
| LIG1 | Hs01553527_m1 | TREX2 | Hs00273080_s1 |
| LIG3 | Hs00242692_m1 | XAB2 | Hs00220205_m1 |
| LIG4 | Hs00172455_m1 | XPC | Hs01104206_m1 |
| MAPK10 | Hs00373461_m1 | XRCC1 | Hs00959834_m1 |
| MAPK11 | Hs00177101_m1 | XRCC4 | Hs00243327_m1 |
| MAPK12 | Hs00268060_m1 | XRCC5 | Hs00221707_m1 |
| MAPK14 | Hs00176247_m1 | XRCC6 | Hs01922652_g1 |
| MAPK8 | Hs01548508_m1 | | |
| Custom Primers | | | |
| REV1 | Fwd: CTTCGCTGAGGAATTGAGAAA | | |
| | Rev: GGAGAGGAGTCGTCAGCTT | | |
| REV7 | Fwd: TAGGGATCTGAGCCTGCGG | | |
| | Rev: CTGGGTGGTGAGAGACAGG | | |
| POLI | Fwd: ACAAACCGGGATTTCCTACC | | |
| | Rev: TCACACTCCTTTCCCTTGAA | | |
| GAPDH | Fwd: CTGTTGCTGTAGCCAAATTCGT | | |
| | Rev: ACCCACTCCTCCACCTTTGAC | | |

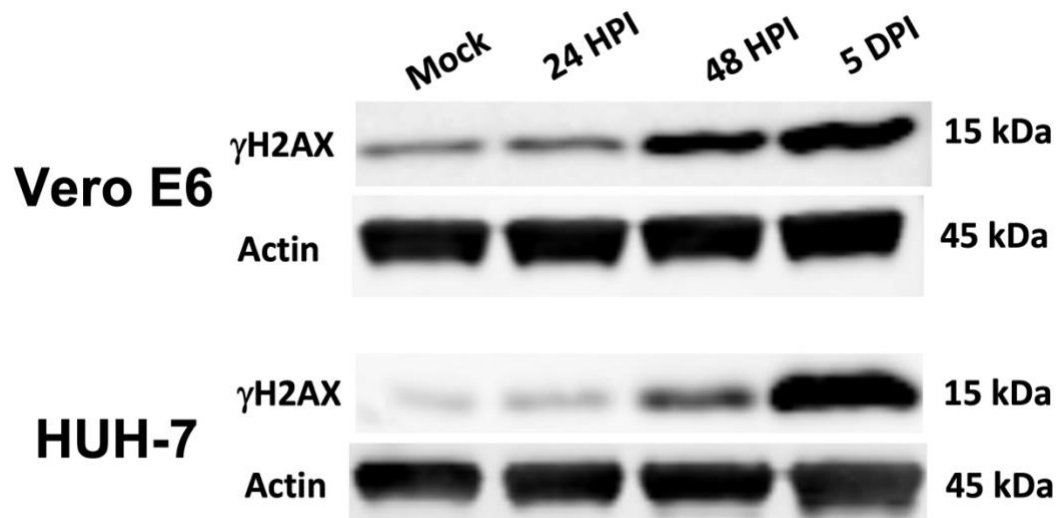


Figure 14. Representative western blots of γ H2AX expression in a time-course analysis of Vero E6 and HUH-7 cells post-DENV-4 infection. Shown are representative western blots of γ H2AX expression in Vero E6 and HUH-7 cells 24 hours post-infection (HPI), 48 hours post-infection (HPI) and 5 days post-infection (DPI) with DENV-4 (MOI 0.1). Actin was used as a loading control.

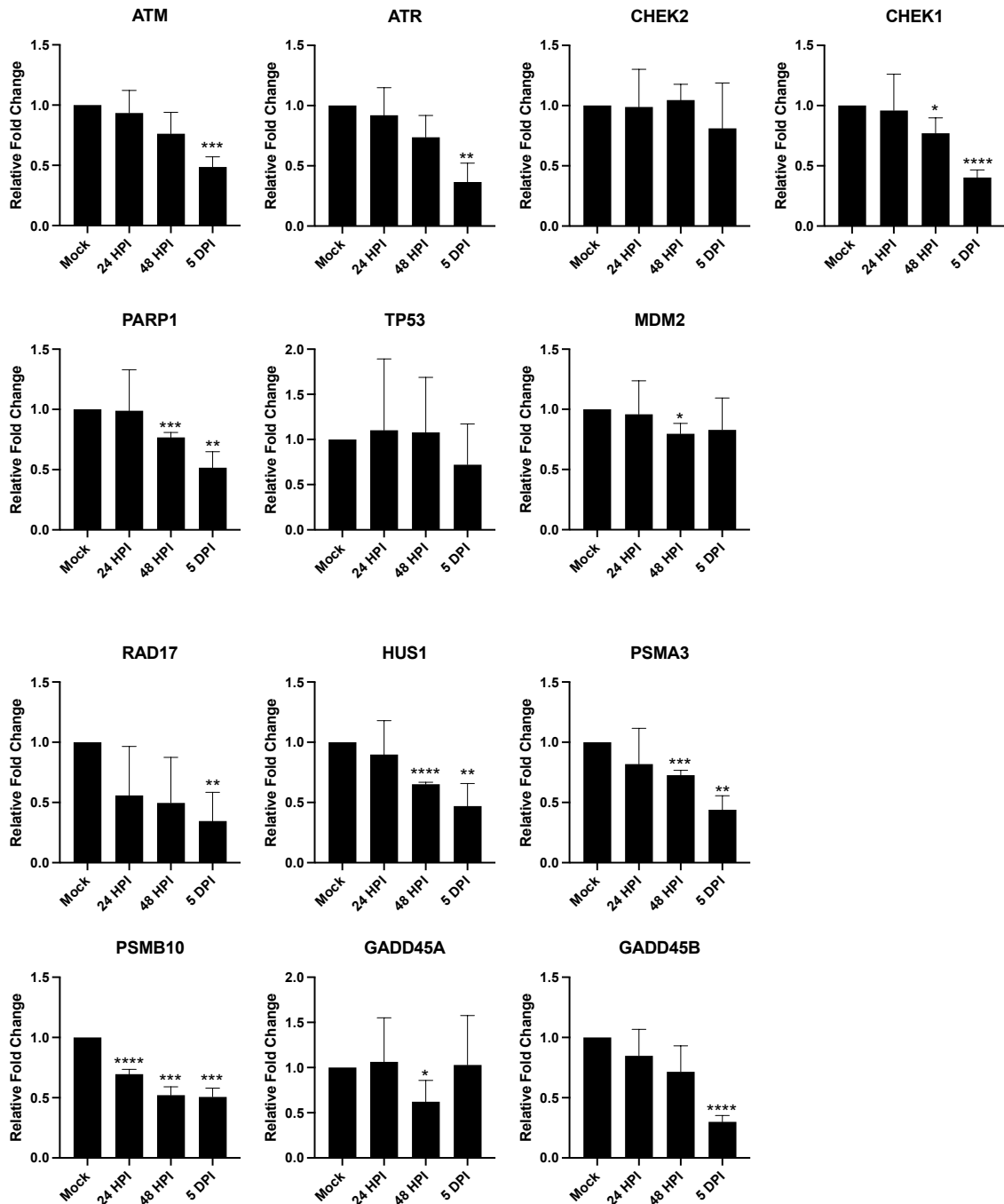


Figure 15. Relative transcript expression of DNA damage response and cellular stress response genes in a time-course analysis of Vero E6 cells post-DENV-4 infection. Shown here are the relative fold changes in transcript levels of ATM, ATR, CHEK2, CHEK1, PARP1, TP53, MDM2, RAD17, HUS1, PSMA3, PSMB10, GADD45A, and GADD45B. n=3 for all genes. Error bars represent standard deviation. Multiple unpaired t-tests were performed to compare the mock control to each post-infection timepoint. * P<0.05, ** P<0.01, *** P<0.001, ****P<0.0001.

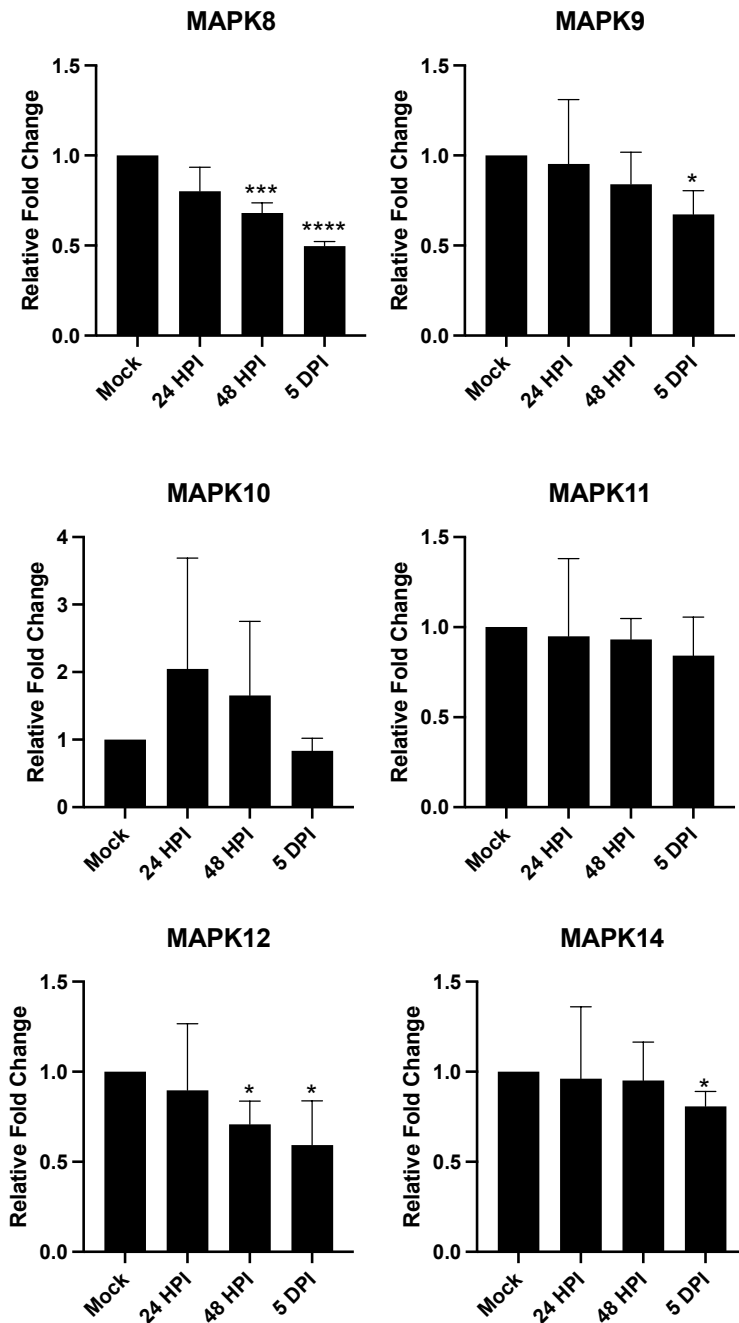


Figure 16. Relative transcript expression of MAPK cellular stress response genes in a time-course analysis of Vero E6 cells post-DENV-4 infection. Shown here are the relative fold changes in transcript levels of MAPK8, MAPK9, MAPK10, MAPK11, MAPK12, and MAPK14. n=3 for all genes. Error bars represent standard deviation. Multiple unpaired t-tests were performed to compare the mock control to each post-infection timepoint. * P<0.05, ** P< 0.01, *** P<0.001, ****P<0.0001.

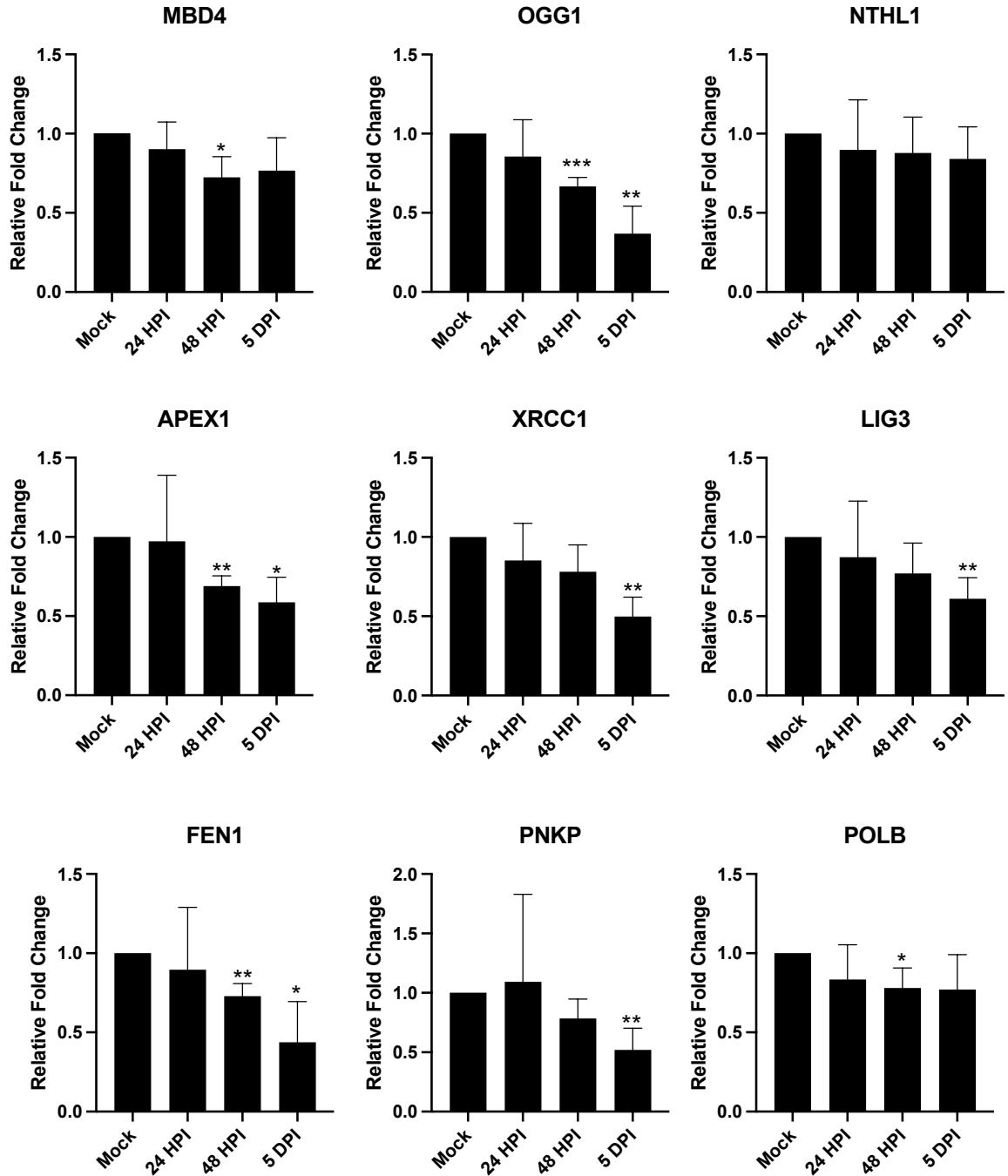


Figure 17. Relative transcript expression of base excision repair genes in a time-course analysis of Vero E6 cells post DENV-4 infection. Shown here are the relative fold changes in transcript levels of MBD4, OGG1, NTHL1, APEX1, XRCC1, LIG3, FEN1, PNKP, and POLB. n=3 for all genes. Error bars represent standard deviation. Multiple unpaired t-tests were performed to compare the mock control to each post-infection timepoint. * P<0.05, ** P< 0.01, *** P<0.001, ****P<0.0001.

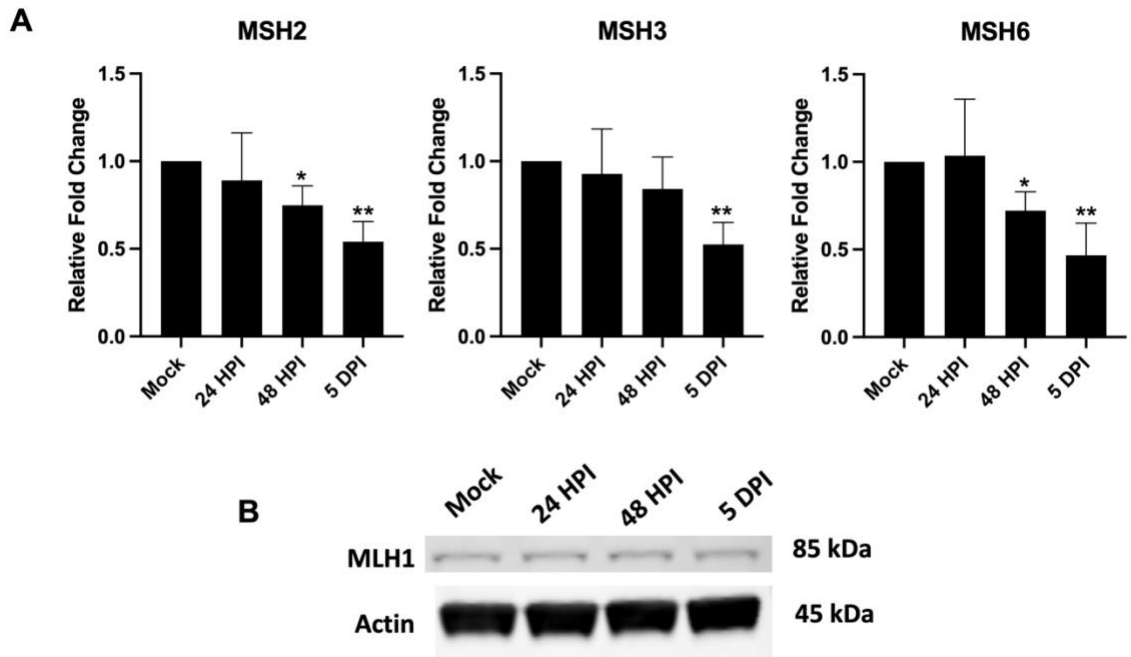


Figure 18. Expression of mismatch repair genes in a time-course analysis of Vero E6 cells post DENV-4 infection. (A) Shown here are the relative fold changes in transcript levels of MSH2, MSH3, MSH6. $n=3$ for all genes. Error bars represent standard deviation. Multiple unpaired t-tests were performed to compare the mock control to each post-infection timepoint. * $P<0.05$, ** $P<0.01$, *** $P<0.001$, **** $P<0.0001$. (B) Representative western blot showing MLH1 protein expression post-DENV-4 infection.

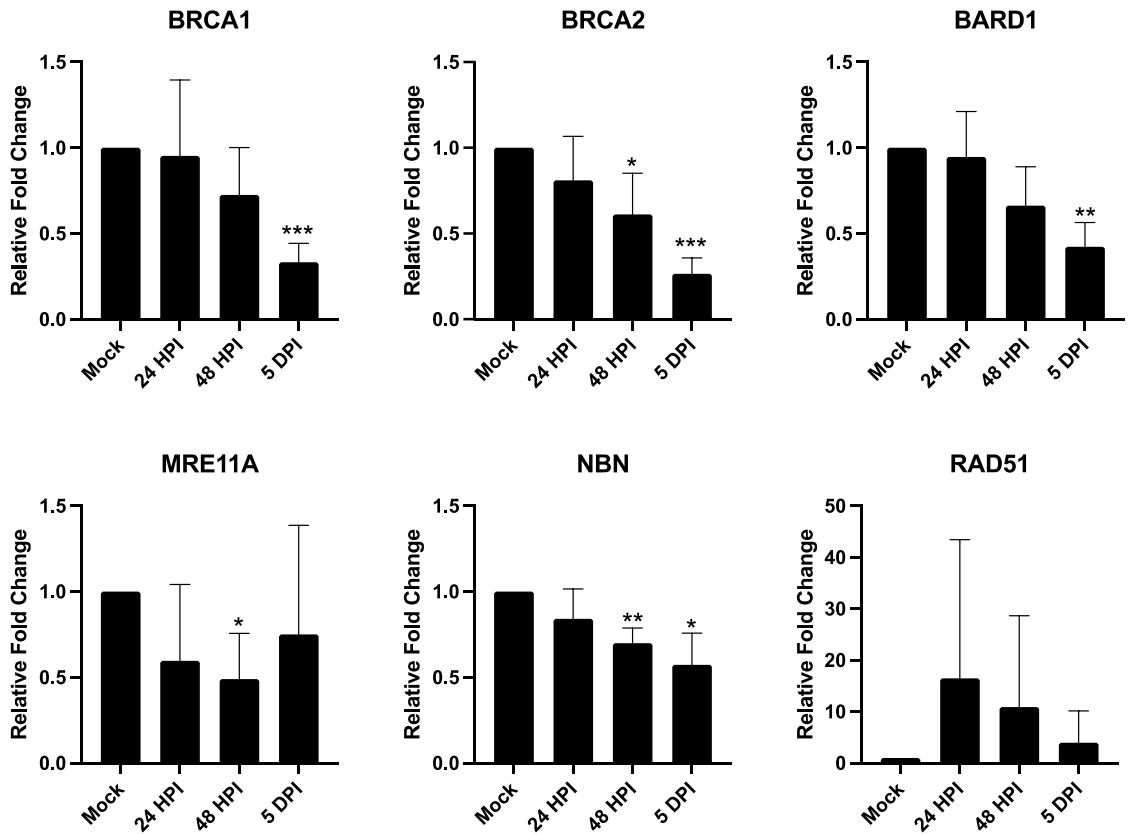


Figure 19. Relative transcript expression of homologous recombination genes in a time-course analysis of Vero E6 cells post DENV-4 infection. Shown here are the relative fold changes in transcript levels of BRCA1, BRCA2, BARD1, MRE11A, NBN, and RAD51. n=3 for all genes. Error bars represent standard deviation. Multiple unpaired t-tests were performed to compare the mock control to each post-infection timepoint. * P<0.05, ** P< 0.01, *** P<0.001, ****P<0.0001.

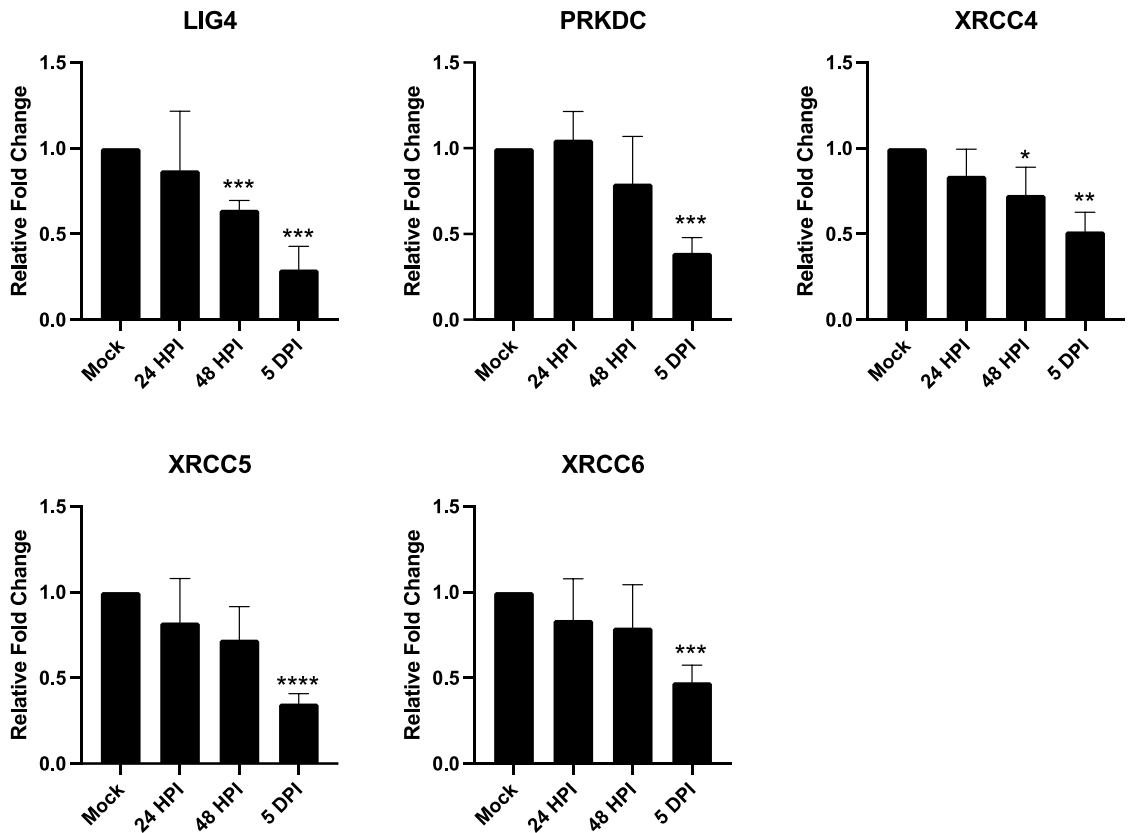


Figure 20. Relative transcript expression of non-homologous end joining genes in a time-course analysis of Vero E6 cells post DENV-4 infection. Shown here are the relative fold changes in transcript levels of LIG4, PRKDC, XRCC4, XRCC5, and XRCC6. n=3 for all genes. Error bars represent standard deviation. Multiple unpaired t-tests were performed to compare the mock control to each post-infection timepoint. * P<0.05, ** P< 0.01, *** P<0.001, ****P<0.0001.

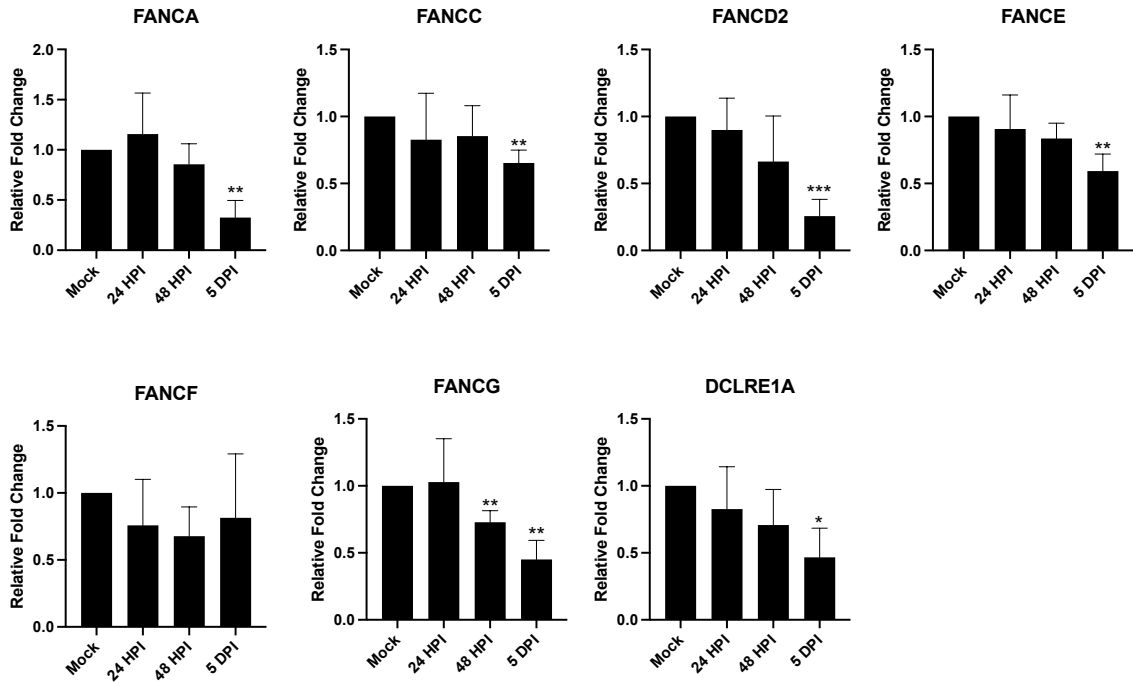


Figure 21. Relative transcript expression of Fanconi anemia genes in a time-course analysis of Vero E6 cells post DENV-4 infection. Shown here are the relative fold changes in transcript levels of FANCA, FANCC, FANCD2, FANCE, FANCF, FANCG, and DCLRE1A. n=3 for all genes. Error bars represent standard deviation. Multiple unpaired t-tests were performed to compare the mock control to each post-infection timepoint. * P<0.05, ** P< 0.01, *** P<0.001, ****P<0.0001.

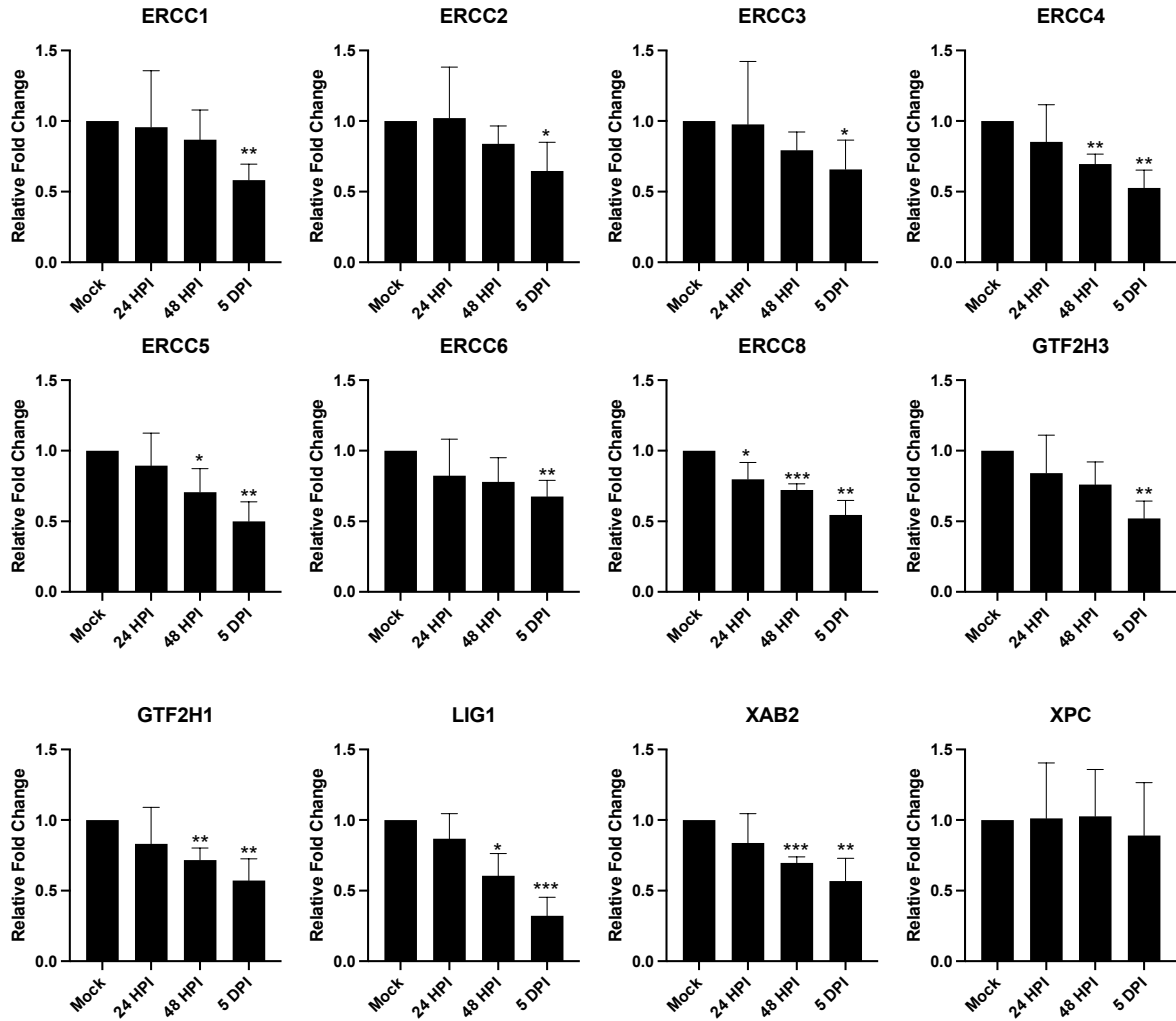


Figure 22. Relative transcript expression of nucleotide excision repair genes in a time-course analysis of Vero E6 cells post DENV-4 infection. Shown here are the relative fold changes in transcript levels of ERCC1, ERCC2, ERCC3, ERCC4, ERCC5, ERCC6, ERCC8, GTF2H3, GTF2H1, LIG1, XAB2, and XPC. n=3 for all genes. Error bars represent standard deviation. Multiple unpaired t-tests were performed to compare the mock control to each post-infection timepoint. * P<0.05, ** P<0.01, *** P<0.001, ****P<0.0001.

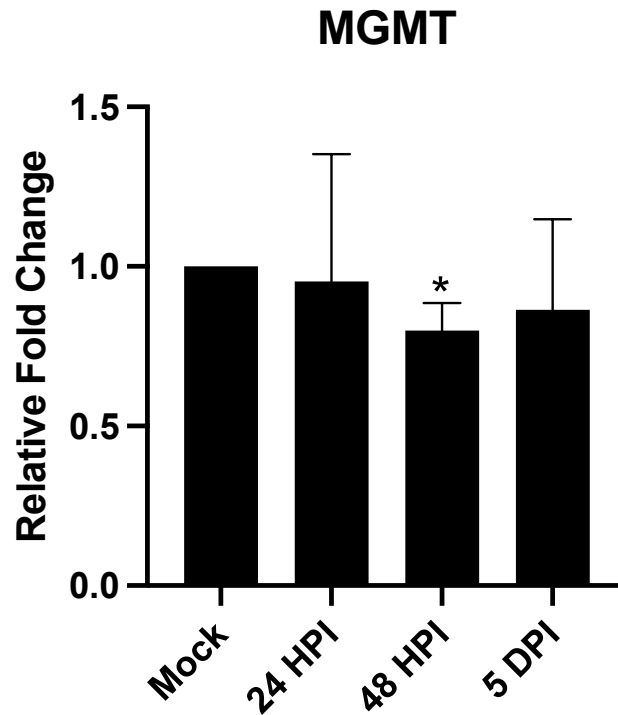


Figure 23. Relative transcript expression of direct reversal of DNA damage gene in a time-course analysis of Vero E6 cells post DENV-4 infection. Shown here is the relative fold change in transcript level of MGMT, n=3. Error bars represent standard deviation. Multiple unpaired t-tests were performed to compare the mock control to each post-infection timepoint. * P<0.05, ** P< 0.01, *** P<0.001, ****P<0.0001.

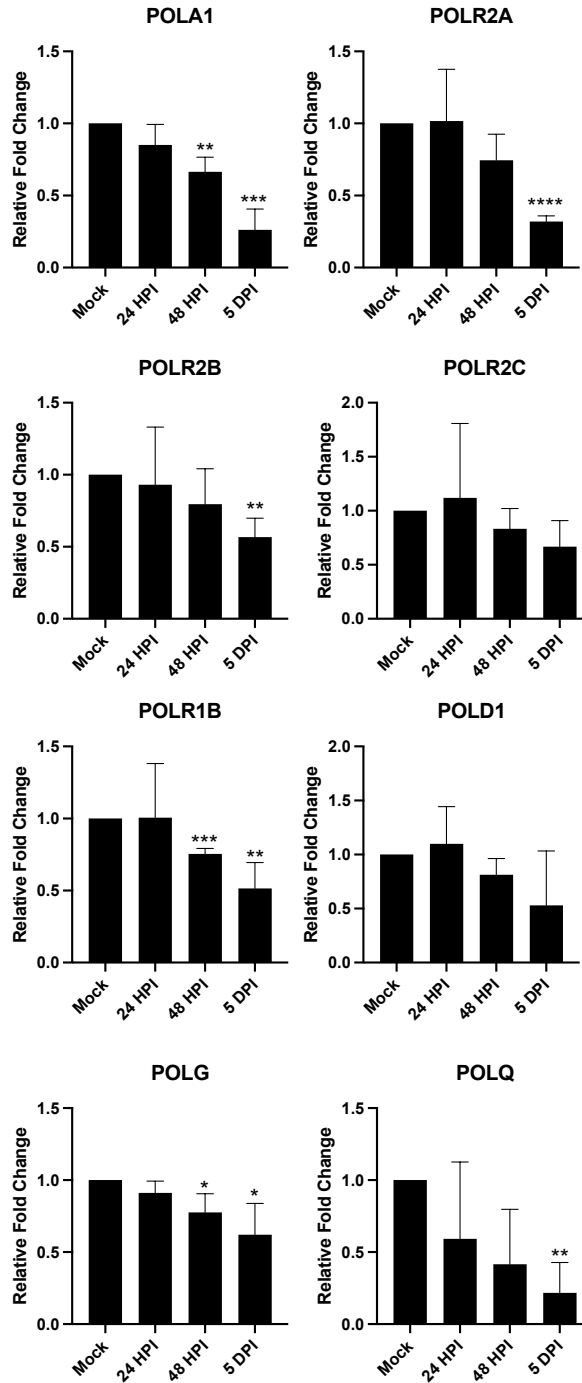


Figure 24. Relative transcript expression of DNA repair associated polymerase genes in a time-course analysis of Vero E6 cells post DENV-4 infection. Shown here are the relative fold changes in transcript levels of POLA1, POLR2A, POLR2B, POLR2C, POLR1B, POLD1, POLG, POLQ. n=3 for all genes. Error bars represent standard deviation. Multiple unpaired t-tests were performed to compare the mock control to each post-infection timepoint. * P<0.05, ** P<0.01, *** P<0.001, ****P<0.0001.

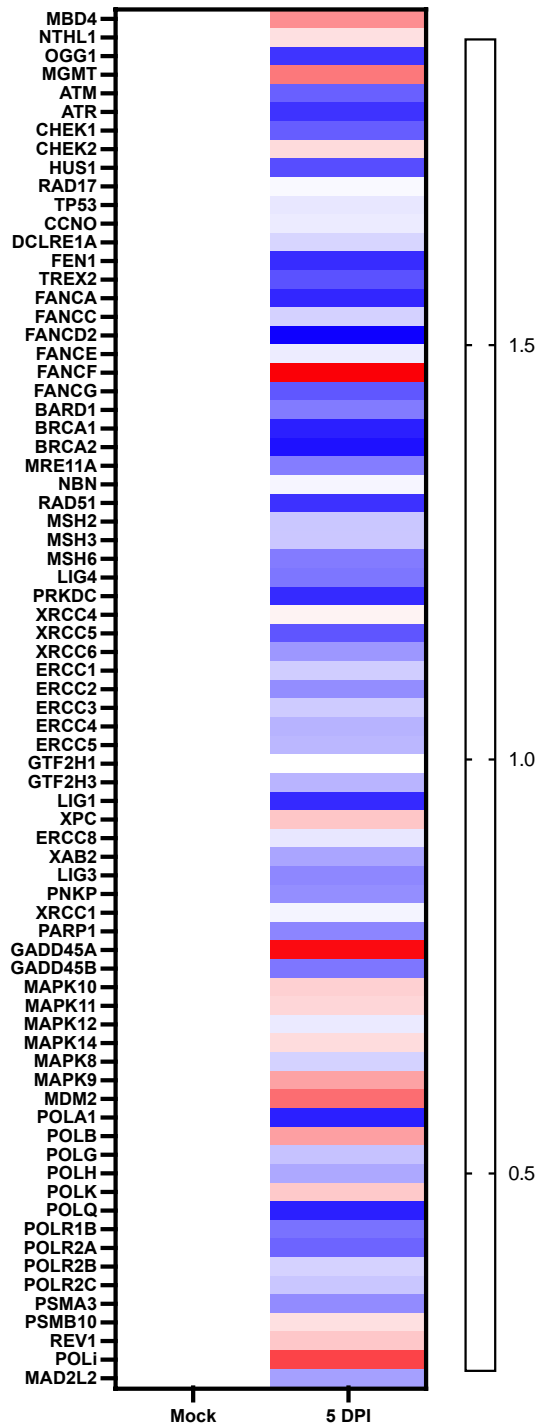


Figure 25. Preliminary RNA-sequencing analysis of DNA repair and DNA damage response gene expression 5 days post-DENV-4 infection. Shown here are normalized transcript per million (TPM) counts of key DNA repair genes. Each gene was normalized to the mock control, n=1.

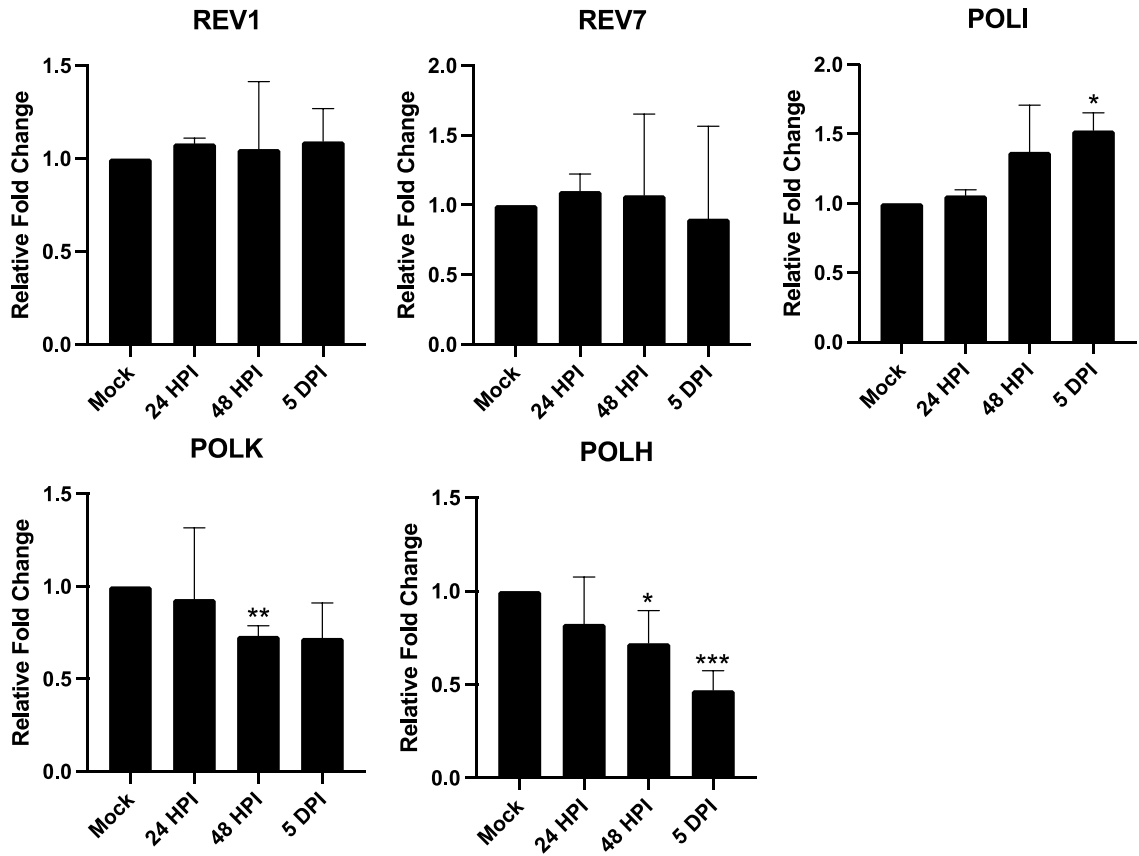


Figure 26. Relative transcript expression of translesion synthesis genes in a time-course analysis of Vero E6 cells post DENV-4 infection. Shown here are the relative fold changes in transcript levels of REV1, REV7, POLI, POLK, POLH. $n=3$ for all genes. Error bars represent standard deviation. Multiple unpaired t-tests were performed to compare the mock control to each post-infection timepoint. * $P<0.05$, ** $P<0.01$, *** $P<0.001$, **** $P<0.0001$.

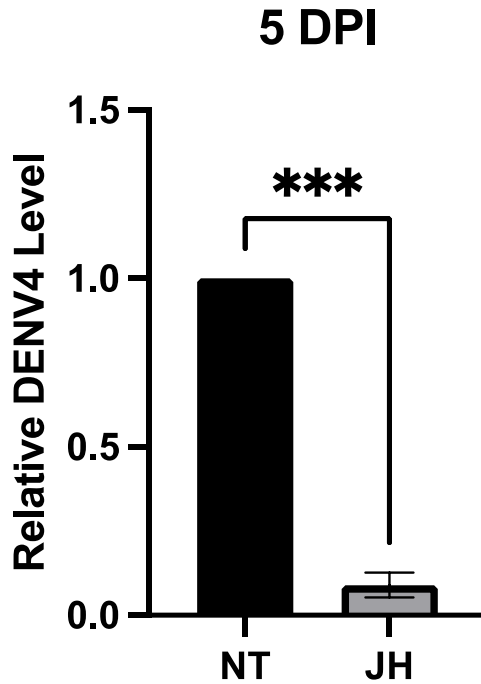


Figure 27. Relative DENV-4 level in Vero E6 cells 5 days post-infection in cells treated with JH-RE-06.NaOH. Shown here is the relative DENV-4 level in Vero E6 cells post-DENV-4 infection and pre-treatment with JH-RE-06. n=3. A paired t-test was performed to compare the non-treated 5-day post-infection sample to the JH-treated 5-day post-infection sample. * P<0.05, ** P< 0.01, *** P<0.001, ****P<0.0001.

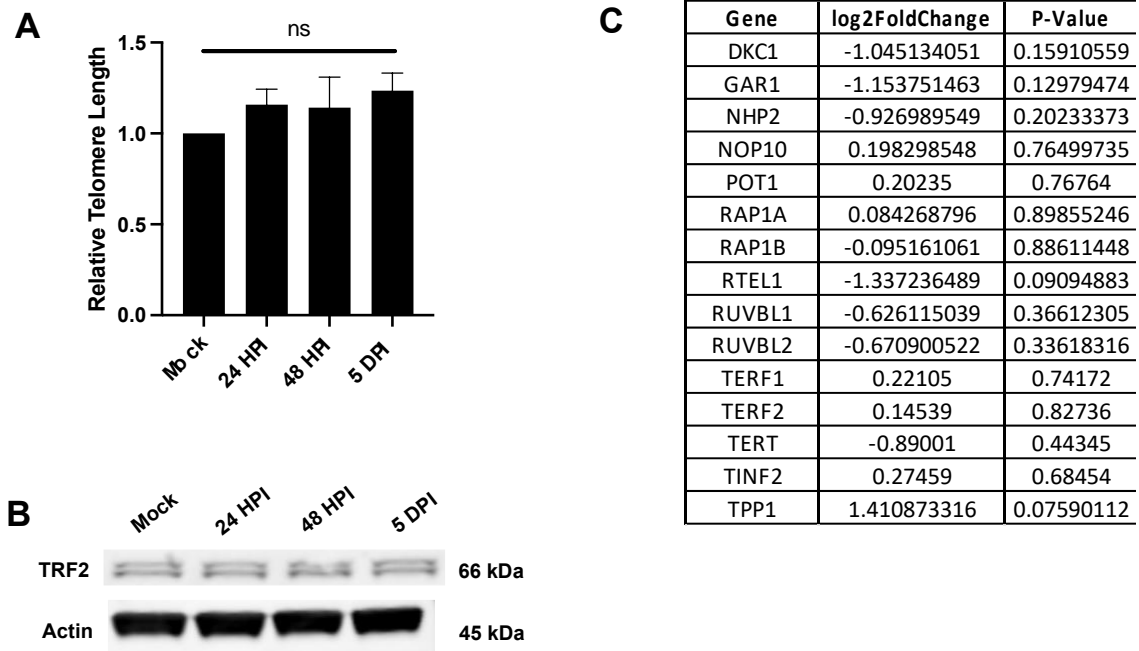


Figure 28. Evaluation of telomeres in Vero E6 cells in a time-course analysis post-DENV-4 infection. (A) Relative telomere length in Vero E6 cells post-DENV-4 infection at 24 HPI, 48 HPI, and 5 DPI. n=3, ordinary one-way ANOVA. (B) Representative western blot of TRF2 protein expression in Vero E6 cells post-DENV-4 infection. (C) Preliminary RNA-Sequencing gene expression of key telomere genes, n=1.

Chapter 2 References

20. Zhang, Z., L. Rong, and Y.P. Li, *Flaviviridae Viruses and Oxidative Stress: Implications for Viral Pathogenesis*. Oxid Med Cell Longev, 2019. **2019**: p. 1409582.
32. Krokan, H.E. and M. Bjørås, *Base excision repair*. Cold Spring Harb Perspect Biol, 2013. **5**(4): p. a012583.
39. Rageul, J. and H. Kim, *Fanconi anemia and the underlying causes of genomic instability*. Environ Mol Mutagen, 2020. **61**(7): p. 693-708.
45. Pećina-Šlaus, N., et al., *Mismatch Repair Pathway, Genome Stability and Cancer*. Front Mol Biosci, 2020. **7**: p. 122.
57. Victor, J., et al., *SARS-CoV-2 triggers DNA damage response in Vero E6 cells*. Biochem Biophys Res Commun, 2021. **579**: p. 141-145.
58. Victor, J., et al., *SARS-CoV-2 hijacks host cell genome instability pathways*. Res Sq, 2022.
64. Ryan, E.L., R. Hollingworth, and R.J. Grand, *Activation of the DNA Damage Response by RNA Viruses*. Biomolecules, 2016. **6**(1): p. 2.
65. Reuter, S., et al., *Oxidative stress, inflammation, and cancer: how are they linked?* Free Radic Biol Med, 2010. **49**(11): p. 1603-16.
66. Cherupanakkal, C., et al., *Lipid peroxidation, DNA damage, and apoptosis in dengue fever*. IUBMB Life, 2018. **70**(11): p. 1133-1143.
67. Poetsch, A.R., *The genomics of oxidative DNA damage, repair, and resulting mutagenesis*. Comput Struct Biotechnol J, 2020. **18**: p. 207-219.
68. Klaunig, J.E., L.M. Kamendulis, and B.A. Hocevar, *Oxidative stress and oxidative damage in carcinogenesis*. Toxicol Pathol, 2010. **38**(1): p. 96-109.
69. Ivanov, A.V., et al., *Oxidative stress, a trigger of hepatitis C and B virus-induced liver carcinogenesis*. Oncotarget, 2017. **8**(3): p. 3895-3932.
70. Chien, Y.W., et al., *Risk of Leukemia after Dengue Virus Infection: A Population-Based Cohort Study*. Cancer Epidemiol Biomarkers Prev, 2020. **29**(3): p. 558-564.
71. Ammerman, N.C., M. Beier-Sexton, and A.F. Azad, *Growth and maintenance of Vero cell lines*. Curr Protoc Microbiol, 2008. **Appendix 4**: p. Appendix 4E.
72. Sène, M.-A., Y. Xia, and A.A. Kamen, *Overview of recent advances in Vero cells genomic characterization and engineering for high-throughput vaccine manufacturing*. Clinical and Translational Discovery, 2022. **2**(2): p. e40.
73. Kasai, F., et al., *HuH-7 reference genome profile: complex karyotype composed of massive loss of heterozygosity*. Hum Cell, 2018. **31**(3): p. 261-267.
74. McCormick, K.D., et al., *Development of a robust cytopathic effect-based high-throughput screening assay to identify novel inhibitors of dengue virus*. Antimicrob Agents Chemother, 2012. **56**(6): p. 3399-401.
75. Kuo, L.J. and L.X. Yang, *Gamma-H2AX - a novel biomarker for DNA double-strand breaks*. In Vivo, 2008. **22**(3): p. 305-9.
76. Maréchal, A. and L. Zou, *DNA damage sensing by the ATM and ATR kinases*. Cold Spring Harb Perspect Biol, 2013. **5**(9).

77. Ray Chaudhuri, A. and A. Nussenzweig, *The multifaceted roles of PARP1 in DNA repair and chromatin remodelling*. Nat Rev Mol Cell Biol, 2017. **18**(10): p. 610-621.
78. Jeggo, P.A. and M. Löbrich, *DNA double-strand breaks: their cellular and clinical impact?* Oncogene, 2007. **26**(56): p. 7717-7719.
79. Nasirudeen, A.M., L. Wang, and D.X. Liu, *Induction of p53-dependent and mitochondria-mediated cell death pathway by dengue virus infection of human and animal cells*. Microbes Infect, 2008. **10**(10-11): p. 1124-32.
80. Chène, P., *Inhibiting the p53–MDM2 interaction: an important target for cancer therapy*. Nature Reviews Cancer, 2003. **3**(2): p. 102-109.
81. NCBI, *RAD17 RAD17 checkpoint clamp loader component [Homo sapiens (human)]*. 2023, National Library of Medicine: ncbi.nlm.nih/gov.
82. Liebermann, D.A. and B. Hoffman, *Gadd45 in stress signaling*. Journal of Molecular Signaling, 2008. **3**(1): p. 15.
83. Hollander, M.C., et al., *Genomic instability in Gadd45a-deficient mice*. Nat Genet, 1999. **23**(2): p. 176-84.
84. Smith, M.L., et al., *p53-mediated DNA repair responses to UV radiation: studies of mouse cells lacking p53, p21, and/or gadd45 genes*. Mol Cell Biol, 2000. **20**(10): p. 3705-14.
85. Pua, L.J.W., et al., *Functional Roles of JNK and p38 MAPK Signaling in Nasopharyngeal Carcinoma*. International Journal of Molecular Sciences, 2022. **23**(3): p. 1108.
86. Tell, G., et al., *The many functions of APE1/Ref-1: not only a DNA repair enzyme*. Antioxid Redox Signal, 2009. **11**(3): p. 601-20.
87. Sun, H., et al., *The FEN1 L209P mutation interferes with long-patch base excision repair and induces cellular transformation*. Oncogene, 2017. **36**(2): p. 194-207.
88. Kohutova, A., et al., *Ligase 3-mediated end-joining maintains genome stability of human embryonic stem cells*. Faseb j, 2019. **33**(6): p. 6778-6788.
89. Jiricny, J., *Postreplicative mismatch repair*. Cold Spring Harb Perspect Biol, 2013. **5**(4): p. a012633.
90. Roy, R., J. Chun, and S.N. Powell, *BRCA1 and BRCA2: different roles in a common pathway of genome protection*. Nat Rev Cancer, 2011. **12**(1): p. 68-78.
91. Liu, J., et al., *Characterization of BRCA1-deficient premalignant tissues and cancers identifies Plekha5 as a tumor metastasis suppressor*. Nature Communications, 2020. **11**(1): p. 4875.
92. Wen, W.X. and C.O. Leong, *Association of BRCA1- and BRCA2-deficiency with mutation burden, expression of PD-L1/PD-1, immune infiltrates, and T cell-inflamed signature in breast cancer*. PLoS One, 2019. **14**(4): p. e0215381.
93. Institute, N.C. *BRCA Gene Mutations: Cancer Risk and Genetic Testing*. Available from: <https://www.cancer.gov/about-cancer/causes-prevention/genetics/brca-fact-sheet#r1>.
94. Qiu, S. and J. Huang, *MRN complex is an essential effector of DNA damage repair*. J Zhejiang Univ Sci B, 2021. **22**(1): p. 31-37.
95. Krejci, L., et al., *Homologous recombination and its regulation*. Nucleic Acids Res, 2012. **40**(13): p. 5795-818.

96. Wang, R., et al., *DNA polymerase δ compensates for Fanconi anemia pathway deficiency by countering DNA replication stress*. Proc Natl Acad Sci U S A, 2020. **117**(52): p. 33436-33445.
97. Petta, T.B., et al., *Human DNA polymerase δ protects cells against oxidative stress*. Embo j, 2008. **27**(21): p. 2883-95.
98. Mun, M.J., et al., *One-step multiplex real-time RT-PCR for detection and typing of dengue virus*. Mol Cell Probes, 2019. **43**: p. 86-91.
99. Laguette, N., et al., *Premature activation of the SLX4 complex by Vpr promotes G2/M arrest and escape from innate immune sensing*. Cell, 2014. **156**(1-2): p. 134-45.
100. Lai, M., et al., *Activation of the ATR pathway by human immunodeficiency virus type 1 Vpr involves its direct binding to chromatin in vivo*. J Virol, 2005. **79**(24): p. 15443-51.
101. Tachiwana, H., et al., *HIV-1 Vpr induces DNA double-strand breaks*. Cancer Res, 2006. **66**(2): p. 627-31.
102. Zimmerman, E.S., et al., *Human immunodeficiency virus type 1 Vpr induces DNA replication stress in vitro and in vivo*. J Virol, 2006. **80**(21): p. 10407-18.
103. Philpott, S.M. and G.C. Buehring, *Defective DNA repair in cells with human T-cell leukemia/bovine leukemia viruses: role of tax gene*. J Natl Cancer Inst, 1999. **91**(11): p. 933-42.
104. Baydoun, H.H., et al., *HTLV-I tax increases genetic instability by inducing DNA double strand breaks during DNA replication and switching repair to NHEJ*. PLoS One, 2012. **7**(8): p. e42226.
105. Chandhasin, C., et al., *Human T-cell leukemia virus type 1 tax attenuates the ATM-mediated cellular DNA damage response*. J Virol, 2008. **82**(14): p. 6952-61.
106. Machida, K., et al., *Hepatitis C virus infection activates the immunologic (type II) isoform of nitric oxide synthase and thereby enhances DNA damage and mutations of cellular genes*. J Virol, 2004. **78**(16): p. 8835-43.
107. Machida, K., et al., *Hepatitis C virus inhibits DNA damage repair through reactive oxygen and nitrogen species and by interfering with the ATM-NBS1/Mre11/Rad50 DNA repair pathway in monocytes and hepatocytes*. J Immunol, 2010. **185**(11): p. 6985-98.
108. Machida, K., et al., *Hepatitis C virus triggers mitochondrial permeability transition with production of reactive oxygen species, leading to DNA damage and STAT3 activation*. J Virol, 2006. **80**(14): p. 7199-207.
109. Ariumi, Y., et al., *The DNA damage sensors ataxia-telangiectasia mutated kinase and checkpoint kinase 2 are required for hepatitis C virus RNA replication*. J Virol, 2008. **82**(19): p. 9639-46.
110. Lai, C.K., et al., *Hepatitis C virus NS3/4A protein interacts with ATM, impairs DNA repair and enhances sensitivity to ionizing radiation*. Virology, 2008. **370**(2): p. 295-309.
111. Xu, L.H., et al., *Coronavirus infection induces DNA replication stress partly through interaction of its nonstructural protein 13 with the p125 subunit of DNA polymerase δ* . J Biol Chem, 2011. **286**(45): p. 39546-59.

112. Li, N., et al., *Influenza infection induces host DNA damage and dynamic DNA damage responses during tissue regeneration*. Cell Mol Life Sci, 2015. **72**(15): p. 2973-88.
113. Vijaya Lakshmi, A.N., et al., *Detection of influenza virus induced DNA damage by comet assay*. Mutat Res, 1999. **442**(1): p. 53-8.
114. Clavarino, G., et al., *Induction of GADD34 is necessary for dsRNA-dependent interferon- β production and participates in the control of Chikungunya virus infection*. PLoS Pathog, 2012. **8**(5): p. e1002708.
115. Nargi-Aizenman, J.L., et al., *Rapid activation of poly(ADP-ribose) polymerase contributes to Sindbis virus and staurosporine-induced apoptotic cell death*. Virology, 2002. **293**(1): p. 164-71.
116. Verbruggen, P., et al., *Interferon antagonist NSs of La Crosse virus triggers a DNA damage response-like degradation of transcribing RNA polymerase II*. J Biol Chem, 2011. **286**(5): p. 3681-92.
117. Baer, A., et al., *Induction of DNA damage signaling upon Rift Valley fever virus infection results in cell cycle arrest and increased viral replication*. J Biol Chem, 2012. **287**(10): p. 7399-410.
118. Lin, P.Y., et al., *Avian reovirus S1133-induced DNA damage signaling and subsequent apoptosis in cultured cells and in chickens*. Arch Virol, 2011. **156**(11): p. 1917-29.
119. Shen, X., et al., *Borna disease virus 1 impairs DNA double-strand break repair through the ATR/Chk1 signalling pathway, resulting in learning and memory impairment in rats*. J Gen Virol, 2022. **103**(12).
120. Hammack, C., et al., *Zika Virus Infection Induces DNA Damage Response in Human Neural Progenitors That Enhances Viral Replication*. J Virol, 2019. **93**(20).

CHAPTER 3: DISCUSSION AND FUTURE DIRECTIONS

Discussion and conclusions

Overall, these results suggest global repression of DNA repair and DNA damage response genes post-dengue infection. Specifically, we report suppression of key homologous recombination, mismatch repair, Fanconi anemia, non-homologous end joining, base excision repair, nucleotide excision repair, direct reversal of DNA damage, and DNA damage response and cellular stress response genes. In addition to this, we see an increase in the mutagenic translesion synthesis polymerase, POL η . Further, these deficient repair pathways may lead to an accumulation of toxic DNA damage and, ultimately, genome instability in host cells post-DENV infection. Together, these results suggest significant genome instability post-dengue infection. The long-term effects of this genome instability remain unknown. Further, it is unknown how long these markers of genome instability last post-infection.

We also report the therapeutic potential of JH-RE-06.NaOH in dengue infection. We observed a significant decrease in DENV-4 levels in cells pre-treated with JH-RE-06. This observation suggests a significant link between RNA virus proliferation and the mutagenic translesion synthesis pathway and highlights the anti-viral potential of JH-RE-06. Whether REV1 TLS polymerase directly interacts with DENV remains unknown and will be of significant interest in our future studies.

While the distinct mechanisms by which DENV propels these phenotypes are unknown, there is literature to suggest DNA damage and the ensuing DNA damage responses can cause global transcriptional repression. Studies have shown that p53 can act as a transcriptional repressor to repress the expression of ribosomal genes (reference needed here). Interestingly, another study has shown that in response to DNA damage, p53 levels may increase in conjunction with the decrease of MYC levels leading to cell cycle arrest [121, 122]. Further, limited evidence suggests that DENV can modulate apoptosis response in host cells. One study observed that dengue can activate mTORC2 signaling to inhibit virus-induced apoptosis and promote the survival of the host cell [123]. In contrast, studies have also shown that all four serotypes of DENV can trigger apoptosis both in vitro and in vivo [124]. However, an exact mechanism is lacking. Whether our observed DNA repair genes expression modulation is linked to a specific cell death pathway remains unknown.

Furthermore, in addition to DENV-dependent apoptosis, DENV infection has been shown to increase senescence in human umbilical vein endothelial cells (HUVECs) [125]. Senescence is a state of irreversible cellular growth arrest that is often modulated by DNA damage and the DNA damage response. Interestingly, endothelial cell senescence is associated with disrupted cell-cell junctions which may be a factor in dengue-dependent vascular leakage and overall disease pathogenesis [126]. Further, repression of DNA repair genes is also associated with cellular senescence and could be leading to some of the repression of DNA repair pathways we have observed [127].

Study Limitations

There are several limitations to this study. This study was carried out primarily in Vero E6, African green monkey kidney cells. More experiments must be done to determine whether there are similar results in human cell lines, as well as in animal models and patient populations. Additionally, this study only examined the DENV-4 serotype. Whether serotypes 1-3 trigger similar genome instability in host cells is unknown. Western blotting was not performed for all genes tested due to the time restraints of this project. Western blots should be performed to determine whether protein expression aligns with transcript expression levels. Finally, this study only examines genome instability markers up to 5 DPI, and it is unknown if these genome instability markers persist past this time point.

Future Directions

As this is a preliminary study to lay the groundwork for investigating DENV-dependent genome instability, this project has several future directions. First, full genome instability analysis will be carried out on JH-RE-06.NaOH-treated samples to further determine whether the small molecule inhibitor can suppress genome instability phenotypes, as previously seen with SARS-CoV-2 infection [58]. This would include western blot analysis to assess γ H2AX protein expression, DNA damage response and DNA repair gene expression, telomere length assays, and HPRT mutagenesis assays. Further, analysis of cell death pathways including apoptosis, senescence, and autophagy

markers will be assessed following DENV infection to further delineate the mechanism by which DENV may be modulating host cell genome instability pathways.

Next, microsatellite instability testing should be performed post-DENV infection due to the repression of the mismatch repair pathway. Deficient MMR and MSI are distinct hallmarks of certain cancers and should be evaluated further.

As mentioned in the study limitation section, this thesis only evaluated DENV-4 infection in Vero E6 cells. For a more comprehensive understanding of dengue infection in the context of genome instability, human cell lines and patient sera samples should be evaluated with each of the four dengue serotypes.

Chapter 3 References

58. Victor, J., et al., *SARS-CoV-2 hijacks host cell genome instability pathways*. Res Sq, 2022.
121. Porter, J.R., et al., *Global Inhibition with Specific Activation: How p53 and MYC Redistribute the Transcriptome in the DNA Double-Strand Break Response*. Mol Cell, 2017. **67**(6): p. 1013-1025.e9.
122. Hofmann, J.W., et al., *Reduced expression of MYC increases longevity and enhances healthspan*. Cell, 2015. **160**(3): p. 477-88.
123. Carter, C.C., et al., *Dengue activates mTORC2 signaling to counteract apoptosis and maximize viral replication*. Front Cell Infect Microbiol, 2022. **12**: p. 979996.
124. Martins Sde, T., et al., *Dendritic cell apoptosis and the pathogenesis of dengue*. Viruses, 2012. **4**(11): p. 2736-53.
125. AbuBakar, S., et al., *Senescence affects endothelial cells susceptibility to dengue virus infection*. Int J Med Sci, 2014. **11**(6): p. 538-44.
126. Krouwer, V.J., et al., *Endothelial cell senescence is associated with disrupted cell-cell junctions and increased monolayer permeability*. Vasc Cell, 2012. **4**(1): p. 12.
127. Collin, G., et al., *Transcriptional repression of DNA repair genes is a hallmark and a cause of cellular senescence*. Cell Death Dis, 2018. **9**(3): p. 259.

COMPREHENSIVE BIBLIOGRAPHY

1. Fang, C.-B., et al., *Fanconi Anemia Pathway: Mechanisms of Breast Cancer Predisposition Development and Potential Therapeutic Targets*. *Frontiers in Cell and Developmental Biology*, 2020. **8**.
2. Education, N. *Dengue Viruses*. Scitable; Available from: <https://www.nature.com/scitable/topicpage/dengue-viruses-22400925/#:~:text=Discovery%20of%20the%20Dengue%20Viruses&text=In%201943%2C%20Ren%20Kimura%20and,independently%20isolated%20the%20dengue%20virus.>
3. *Dengue and severe dengue*. 2022 January 10, 2022; Available from: <https://www.who.int/news-room/fact-sheets/detail/dengue-and-severe-dengue>.
4. NIAID. *Dengue Fever*. Available from: <https://www.niaid.nih.gov/diseases-conditions/dengue-fever#:~:text=Worldwide%2C%20about%2050%20million%20cases,who%20have%20recently%20traveled%20abroad.>
5. Hasan, S., et al., *Dengue virus: A global human threat: Review of literature*. *J Int Soc Prev Community Dent*, 2016. **6**(1): p. 1-6.
6. Back, A.T. and A. Lundkvist, *Dengue viruses - an overview*. *Infect Ecol Epidemiol*, 2013. **3**.
7. Wang, E., et al., *Evolutionary relationships of endemic/epidemic and sylvatic dengue viruses*. *J Virol*, 2000. **74**(7): p. 3227-34.
8. Hanley, K.A.W., S.C., *Frontiers in dengue virus research*, ed. K.A.W. Hanley, S.C. 2010: Caister Academic Press.
9. Nanaware, N., et al., *Dengue Virus Infection: A Tale of Viral Exploitations and Host Responses*. *Viruses*, 2021. **13**(10).
10. Harapan, H., et al., *Dengue: A Minireview*. *Viruses*, 2020. **12**(8).
11. Póvoa, T.F., et al., *The pathology of severe dengue in multiple organs of human fatal cases: histopathology, ultrastructure and virus replication*. *PLoS One*, 2014. **9**(4): p. e83386.
12. Begum, F., et al., *Insight into the Tropism of Dengue Virus in Humans*. *Viruses*, 2019. **11**(12).
13. van der Schaar, H.M., et al., *Dissecting the cell entry pathway of dengue virus by single-particle tracking in living cells*. *PLoS Pathog*, 2008. **4**(12): p. e1000244.
14. Cruz-Oliveira, C., et al., *Receptors and routes of dengue virus entry into the host cells*. *FEMS Microbiol Rev*, 2015. **39**(2): p. 155-70.
15. Ang, F., et al., *Small interference RNA profiling reveals the essential role of human membrane trafficking genes in mediating the infectious entry of dengue virus*. *Virology*, 2010. **7**: p. 24.
16. Kaksonen, M. and A. Roux, *Mechanisms of clathrin-mediated endocytosis*. *Nat Rev Mol Cell Biol*, 2018. **19**(5): p. 313-326.
17. Singh, B., et al., *Defective Mitochondrial Quality Control during Dengue Infection Contributes to Disease Pathogenesis*. *J Virol*, 2022. **96**(20): p. e0082822.

18. Simula, M.P. and V. De Re, *Hepatitis C virus-induced oxidative stress and mitochondrial dysfunction: a focus on recent advances in proteomics*. *Proteomics Clin Appl*, 2010. **4**(10-11): p. 782-93.
19. Dan Dunn, J., et al., *Reactive oxygen species and mitochondria: A nexus of cellular homeostasis*. *Redox Biol*, 2015. **6**: p. 472-485.
20. Zhang, Z., L. Rong, and Y.P. Li, *Flaviviridae Viruses and Oxidative Stress: Implications for Viral Pathogenesis*. *Oxid Med Cell Longev*, 2019. **2019**: p. 1409582.
21. Prevention, C.f.D.C.a. *Dengue Clinical Presentation*. For Healthcare Providers; Available from: <https://www.cdc.gov/dengue/healthcare-providers/clinical-presentation.html>.
22. Institute, N.C., in *NCI Dictionary of Cancer Terms*. cancer.gov.
23. Yao, Y. and W. Dai, *Genomic Instability and Cancer*. *J Carcinog Mutagen*, 2014. **5**.
24. Terabayashi, T. and K. Hanada, *Genome instability syndromes caused by impaired DNA repair and aberrant DNA damage responses*. *Cell Biology and Toxicology*, 2018. **34**(5): p. 337-350.
25. Negrini, S., V.G. Gorgoulis, and T.D. Halazonetis, *Genomic instability — an evolving hallmark of cancer*. *Nature Reviews Molecular Cell Biology*, 2010. **11**(3): p. 220-228.
26. O'Sullivan, R.J. and J. Karlseder, *Telomeres: protecting chromosomes against genome instability*. *Nat Rev Mol Cell Biol*, 2010. **11**(3): p. 171-81.
27. Yang, J., et al., *ATM, ATR and DNA-PK: initiators of the cellular genotoxic stress responses*. *Carcinogenesis*, 2003. **24**(10): p. 1571-80.
28. Chatterjee, N. and G.C. Walker, *Mechanisms of DNA damage, repair, and mutagenesis*. *Environ Mol Mutagen*, 2017. **58**(5): p. 235-263.
29. Fuchs, R.P., et al., *Crosstalk between repair pathways elicits double-strand breaks in alkylated DNA and implications for the action of temozolomide*. *eLife*, 2021. **10**: p. e69544.
30. Kulke, M.H., et al., *O6-methylguanine DNA methyltransferase deficiency and response to temozolomide-based therapy in patients with neuroendocrine tumors*. *Clin Cancer Res*, 2009. **15**(1): p. 338-45.
31. Mehrgou, A. and M. Akouchekian, *The importance of BRCA1 and BRCA2 genes mutations in breast cancer development*. *Med J Islam Repub Iran*, 2016. **30**: p. 369.
32. Krokan, H.E. and M. Bjørås, *Base excision repair*. *Cold Spring Harb Perspect Biol*, 2013. **5**(4): p. a012583.
33. Hegde, M.L., T.K. Hazra, and S. Mitra, *Early steps in the DNA base excision/single-strand interruption repair pathway in mammalian cells*. *Cell Research*, 2008. **18**(1): p. 27-47.
34. Kim, Y.J. and D.M. Wilson, 3rd, *Overview of base excision repair biochemistry*. *Curr Mol Pharmacol*, 2012. **5**(1): p. 3-13.
35. Kusakabe, M., et al., *Mechanism and regulation of DNA damage recognition in nucleotide excision repair*. *Genes and Environment*, 2019. **41**(1): p. 2.

36. Gomez, V. and A. Hergovich, *Chapter 14 - Cell-Cycle Control and DNA-Damage Signaling in Mammals*, in *Genome Stability*, I. Kovalchuk and O. Kovalchuk, Editors. 2016, Academic Press: Boston. p. 227-242.
37. de Boer, J. and J.H.J. Hoeijmakers, *Nucleotide excision repair and human syndromes*. *Carcinogenesis*, 2000. **21**(3): p. 453-460.
38. Moldovan, G.L. and A.D. D'Andrea, *How the fanconi anemia pathway guards the genome*. *Annu Rev Genet*, 2009. **43**: p. 223-49.
39. Rageul, J. and H. Kim, *Fanconi anemia and the underlying causes of genomic instability*. *Environ Mol Mutagen*, 2020. **61**(7): p. 693-708.
40. Ohashi, A., et al., *Fanconi anemia complementation group D2 (FANCD2) functions independently of BRCA2- and RAD51-associated homologous recombination in response to DNA damage*. *J Biol Chem*, 2005. **280**(15): p. 14877-83.
41. Liu, W., et al., *Fanconi anemia pathway as a prospective target for cancer intervention*. *Cell & Bioscience*, 2020. **10**(1): p. 39.
42. Davis, A.J. and D.J. Chen, *DNA double strand break repair via non-homologous end-joining*. *Transl Cancer Res*, 2013. **2**(3): p. 130-143.
43. Mao, Z., et al., *Comparison of nonhomologous end joining and homologous recombination in human cells*. *DNA Repair (Amst)*, 2008. **7**(10): p. 1765-71.
44. Woodbine, L., A.R. Gennery, and P.A. Jeggo, *The clinical impact of deficiency in DNA non-homologous end-joining*. *DNA Repair (Amst)*, 2014. **16**: p. 84-96.
45. Pećina-Šlaus, N., et al., *Mismatch Repair Pathway, Genome Stability and Cancer*. *Front Mol Biosci*, 2020. **7**: p. 122.
46. Preston, B.D., T.M. Albertson, and A.J. Herr, *DNA replication fidelity and cancer*. *Semin Cancer Biol*, 2010. **20**(5): p. 281-93.
47. Hsieh, P. and K. Yamane, *DNA mismatch repair: molecular mechanism, cancer, and ageing*. *Mech Ageing Dev*, 2008. **129**(7-8): p. 391-407.
48. Institute, N.C., *mismatch repair deficiency*, in *NCI Dictionary of Cancer Terms*. National Cancer Institute: cancer.gov.
49. Pino, M.S., et al., *Deficient DNA mismatch repair is common in Lynch syndrome-associated colorectal adenomas*. *J Mol Diagn*, 2009. **11**(3): p. 238-47.
50. Yamanaka, K., et al., *Inhibition of mutagenic translesion synthesis: A possible strategy for improving chemotherapy?* *PLoS Genet*, 2017. **13**(8): p. e1006842.
51. Wojtaszek, J.L., et al., *A Small Molecule Targeting Mutagenic Translesion Synthesis Improves Chemotherapy*. *Cell*, 2019. **178**(1): p. 152-159 e11.
52. Sail, V., et al., *Identification of Small Molecule Translesion Synthesis Inhibitors That Target the Rev1-CT/RIR Protein-Protein Interaction*. *ACS Chem Biol*, 2017. **12**(7): p. 1903-1912.
53. Dash, R.C., et al., *Virtual Pharmacophore Screening Identifies Small-Molecule Inhibitors of the Rev1-CT/RIR Protein-Protein Interaction*. *ChemMedChem*, 2019. **14**(17): p. 1610-1617.
54. Chatterjee, N., et al., *REVI inhibitor JH-RE-06 enhances tumor cell response to chemotherapy by triggering senescence hallmarks*. *Proc Natl Acad Sci U S A*, 2020. **117**(46): p. 28918-28921.
55. Wendel, S.O., et al., *HPV 16 E7 alters translesion synthesis signaling*. *Virology*, 2022. **19**(1): p. 165.

56. Dyson, O.F., J.S. Pagano, and C.B. Whitehurst, *The Translesion Polymerase Pol η Is Required for Efficient Epstein-Barr Virus Infectivity and Is Regulated by the Viral Deubiquitinating Enzyme BPLF1*. J Virol, 2017. **91**(19).
57. Victor, J., et al., *SARS-CoV-2 triggers DNA damage response in Vero E6 cells*. Biochem Biophys Res Commun, 2021. **579**: p. 141-145.
58. Victor, J., et al., *SARS-CoV-2 hijacks host cell genome instability pathways*. Res Sq, 2022.
59. Lu, W., et al., *Telomeres-structure, function, and regulation*. Exp Cell Res, 2013. **319**(2): p. 133-41.
60. Rodenhuis-Zybert, I.A., J. Wilschut, and J.M. Smit, *Dengue virus life cycle: viral and host factors modulating infectivity*. Cellular and Molecular Life Sciences, 2010. **67**(16): p. 2773-2786.
61. Barve, A., et al., *DNA Repair Repertoire of the Enigmatic Hydra*. Front Genet, 2021. **12**: p. 670695.
62. Wood, R.D., *Nucleotide excision repair in mammalian cells*. J Biol Chem, 1997. **272**(38): p. 23465-8.
63. Williams, G.J., et al., *Structural insights into NHEJ: building up an integrated picture of the dynamic DSB repair super complex, one component and interaction at a time*. DNA Repair (Amst), 2014. **17**: p. 110-20.
64. Ryan, E.L., R. Hollingworth, and R.J. Grand, *Activation of the DNA Damage Response by RNA Viruses*. Biomolecules, 2016. **6**(1): p. 2.
65. Reuter, S., et al., *Oxidative stress, inflammation, and cancer: how are they linked?* Free Radic Biol Med, 2010. **49**(11): p. 1603-16.
66. Cherupanakkal, C., et al., *Lipid peroxidation, DNA damage, and apoptosis in dengue fever*. IUBMB Life, 2018. **70**(11): p. 1133-1143.
67. Poetsch, A.R., *The genomics of oxidative DNA damage, repair, and resulting mutagenesis*. Comput Struct Biotechnol J, 2020. **18**: p. 207-219.
68. Klaunig, J.E., L.M. Kamendulis, and B.A. Hocevar, *Oxidative stress and oxidative damage in carcinogenesis*. Toxicol Pathol, 2010. **38**(1): p. 96-109.
69. Ivanov, A.V., et al., *Oxidative stress, a trigger of hepatitis C and B virus-induced liver carcinogenesis*. Oncotarget, 2017. **8**(3): p. 3895-3932.
70. Chien, Y.W., et al., *Risk of Leukemia after Dengue Virus Infection: A Population-Based Cohort Study*. Cancer Epidemiol Biomarkers Prev, 2020. **29**(3): p. 558-564.
71. Ammerman, N.C., M. Beier-Sexton, and A.F. Azad, *Growth and maintenance of Vero cell lines*. Curr Protoc Microbiol, 2008. **Appendix 4**: p. Appendix 4E.
72. Sène, M.-A., Y. Xia, and A.A. Kamen, *Overview of recent advances in Vero cells genomic characterization and engineering for high-throughput vaccine manufacturing*. Clinical and Translational Discovery, 2022. **2**(2): p. e40.
73. Kasai, F., et al., *HuH-7 reference genome profile: complex karyotype composed of massive loss of heterozygosity*. Hum Cell, 2018. **31**(3): p. 261-267.
74. McCormick, K.D., et al., *Development of a robust cytopathic effect-based high-throughput screening assay to identify novel inhibitors of dengue virus*. Antimicrob Agents Chemother, 2012. **56**(6): p. 3399-401.
75. Kuo, L.J. and L.X. Yang, *Gamma-H2AX - a novel biomarker for DNA double-strand breaks*. In Vivo, 2008. **22**(3): p. 305-9.

76. Maréchal, A. and L. Zou, *DNA damage sensing by the ATM and ATR kinases*. Cold Spring Harb Perspect Biol, 2013. **5**(9).
77. Ray Chaudhuri, A. and A. Nussenzweig, *The multifaceted roles of PARP1 in DNA repair and chromatin remodelling*. Nat Rev Mol Cell Biol, 2017. **18**(10): p. 610-621.
78. Jeggo, P.A. and M. Löbrich, *DNA double-strand breaks: their cellular and clinical impact?* Oncogene, 2007. **26**(56): p. 7717-7719.
79. Nasirudeen, A.M., L. Wang, and D.X. Liu, *Induction of p53-dependent and mitochondria-mediated cell death pathway by dengue virus infection of human and animal cells*. Microbes Infect, 2008. **10**(10-11): p. 1124-32.
80. Chène, P., *Inhibiting the p53–MDM2 interaction: an important target for cancer therapy*. Nature Reviews Cancer, 2003. **3**(2): p. 102-109.
81. NCBI, *RAD17 RAD17 checkpoint clamp loader component [Homo sapiens (human)]*. 2023, National Library of Medicine: ncbi.nlm.nih/gov.
82. Liebermann, D.A. and B. Hoffman, *Gadd45 in stress signaling*. Journal of Molecular Signaling, 2008. **3**(1): p. 15.
83. Hollander, M.C., et al., *Genomic instability in Gadd45a-deficient mice*. Nat Genet, 1999. **23**(2): p. 176-84.
84. Smith, M.L., et al., *p53-mediated DNA repair responses to UV radiation: studies of mouse cells lacking p53, p21, and/or gadd45 genes*. Mol Cell Biol, 2000. **20**(10): p. 3705-14.
85. Pua, L.J.W., et al., *Functional Roles of JNK and p38 MAPK Signaling in Nasopharyngeal Carcinoma*. International Journal of Molecular Sciences, 2022. **23**(3): p. 1108.
86. Tell, G., et al., *The many functions of APE1/Ref-1: not only a DNA repair enzyme*. Antioxid Redox Signal, 2009. **11**(3): p. 601-20.
87. Sun, H., et al., *The FEN1 L209P mutation interferes with long-patch base excision repair and induces cellular transformation*. Oncogene, 2017. **36**(2): p. 194-207.
88. Kohutova, A., et al., *Ligase 3-mediated end-joining maintains genome stability of human embryonic stem cells*. Faseb j, 2019. **33**(6): p. 6778-6788.
89. Jiricny, J., *Postreplicative mismatch repair*. Cold Spring Harb Perspect Biol, 2013. **5**(4): p. a012633.
90. Roy, R., J. Chun, and S.N. Powell, *BRCA1 and BRCA2: different roles in a common pathway of genome protection*. Nat Rev Cancer, 2011. **12**(1): p. 68-78.
91. Liu, J., et al., *Characterization of BRCA1-deficient premalignant tissues and cancers identifies Plekha5 as a tumor metastasis suppressor*. Nature Communications, 2020. **11**(1): p. 4875.
92. Wen, W.X. and C.O. Leong, *Association of BRCA1- and BRCA2-deficiency with mutation burden, expression of PD-L1/PD-1, immune infiltrates, and T cell-inflamed signature in breast cancer*. PLoS One, 2019. **14**(4): p. e0215381.
93. Institute, N.C. *BRCA Gene Mutations: Cancer Risk and Genetic Testing*. Available from: <https://www.cancer.gov/about-cancer/causes-prevention/genetics/brca-fact-sheet#r1>.
94. Qiu, S. and J. Huang, *MRN complex is an essential effector of DNA damage repair*. J Zhejiang Univ Sci B, 2021. **22**(1): p. 31-37.

95. Krejci, L., et al., *Homologous recombination and its regulation*. Nucleic Acids Res, 2012. **40**(13): p. 5795-818.
96. Wang, R., et al., *DNA polymerase ι compensates for Fanconi anemia pathway deficiency by countering DNA replication stress*. Proc Natl Acad Sci U S A, 2020. **117**(52): p. 33436-33445.
97. Petta, T.B., et al., *Human DNA polymerase ι protects cells against oxidative stress*. Embo j, 2008. **27**(21): p. 2883-95.
98. Mun, M.J., et al., *One-step multiplex real-time RT-PCR for detection and typing of dengue virus*. Mol Cell Probes, 2019. **43**: p. 86-91.
99. Laguette, N., et al., *Premature activation of the SLX4 complex by Vpr promotes G2/M arrest and escape from innate immune sensing*. Cell, 2014. **156**(1-2): p. 134-45.
100. Lai, M., et al., *Activation of the ATR pathway by human immunodeficiency virus type 1 Vpr involves its direct binding to chromatin in vivo*. J Virol, 2005. **79**(24): p. 15443-51.
101. Tachiwana, H., et al., *HIV-1 Vpr induces DNA double-strand breaks*. Cancer Res, 2006. **66**(2): p. 627-31.
102. Zimmerman, E.S., et al., *Human immunodeficiency virus type 1 Vpr induces DNA replication stress in vitro and in vivo*. J Virol, 2006. **80**(21): p. 10407-18.
103. Philpott, S.M. and G.C. Buehring, *Defective DNA repair in cells with human T-cell leukemia/bovine leukemia viruses: role of tax gene*. J Natl Cancer Inst, 1999. **91**(11): p. 933-42.
104. Baydoun, H.H., et al., *HTLV-I tax increases genetic instability by inducing DNA double strand breaks during DNA replication and switching repair to NHEJ*. PLoS One, 2012. **7**(8): p. e42226.
105. Chandhasin, C., et al., *Human T-cell leukemia virus type 1 tax attenuates the ATM-mediated cellular DNA damage response*. J Virol, 2008. **82**(14): p. 6952-61.
106. Machida, K., et al., *Hepatitis C virus infection activates the immunologic (type II) isoform of nitric oxide synthase and thereby enhances DNA damage and mutations of cellular genes*. J Virol, 2004. **78**(16): p. 8835-43.
107. Machida, K., et al., *Hepatitis C virus inhibits DNA damage repair through reactive oxygen and nitrogen species and by interfering with the ATM-NBS1/Mre11/Rad50 DNA repair pathway in monocytes and hepatocytes*. J Immunol, 2010. **185**(11): p. 6985-98.
108. Machida, K., et al., *Hepatitis C virus triggers mitochondrial permeability transition with production of reactive oxygen species, leading to DNA damage and STAT3 activation*. J Virol, 2006. **80**(14): p. 7199-207.
109. Ariumi, Y., et al., *The DNA damage sensors ataxia-telangiectasia mutated kinase and checkpoint kinase 2 are required for hepatitis C virus RNA replication*. J Virol, 2008. **82**(19): p. 9639-46.
110. Lai, C.K., et al., *Hepatitis C virus NS3/4A protein interacts with ATM, impairs DNA repair and enhances sensitivity to ionizing radiation*. Virology, 2008. **370**(2): p. 295-309.
111. Xu, L.H., et al., *Coronavirus infection induces DNA replication stress partly through interaction of its nonstructural protein 13 with the p125 subunit of DNA polymerase δ* . J Biol Chem, 2011. **286**(45): p. 39546-59.

112. Li, N., et al., *Influenza infection induces host DNA damage and dynamic DNA damage responses during tissue regeneration*. Cell Mol Life Sci, 2015. **72**(15): p. 2973-88.
113. Vijaya Lakshmi, A.N., et al., *Detection of influenza virus induced DNA damage by comet assay*. Mutat Res, 1999. **442**(1): p. 53-8.
114. Clavarino, G., et al., *Induction of GADD34 is necessary for dsRNA-dependent interferon- β production and participates in the control of Chikungunya virus infection*. PLoS Pathog, 2012. **8**(5): p. e1002708.
115. Nargi-Aizenman, J.L., et al., *Rapid activation of poly(ADP-ribose) polymerase contributes to Sindbis virus and staurosporine-induced apoptotic cell death*. Virology, 2002. **293**(1): p. 164-71.
116. Verbruggen, P., et al., *Interferon antagonist NSs of La Crosse virus triggers a DNA damage response-like degradation of transcribing RNA polymerase II*. J Biol Chem, 2011. **286**(5): p. 3681-92.
117. Baer, A., et al., *Induction of DNA damage signaling upon Rift Valley fever virus infection results in cell cycle arrest and increased viral replication*. J Biol Chem, 2012. **287**(10): p. 7399-410.
118. Lin, P.Y., et al., *Avian reovirus S1133-induced DNA damage signaling and subsequent apoptosis in cultured cells and in chickens*. Arch Virol, 2011. **156**(11): p. 1917-29.
119. Shen, X., et al., *Borna disease virus 1 impairs DNA double-strand break repair through the ATR/Chk1 signalling pathway, resulting in learning and memory impairment in rats*. J Gen Virol, 2022. **103**(12).
120. Hammack, C., et al., *Zika Virus Infection Induces DNA Damage Response in Human Neural Progenitors That Enhances Viral Replication*. J Virol, 2019. **93**(20).
121. Porter, J.R., et al., *Global Inhibition with Specific Activation: How p53 and MYC Redistribute the Transcriptome in the DNA Double-Strand Break Response*. Mol Cell, 2017. **67**(6): p. 1013-1025.e9.
122. Hofmann, J.W., et al., *Reduced expression of MYC increases longevity and enhances healthspan*. Cell, 2015. **160**(3): p. 477-88.
123. Carter, C.C., et al., *Dengue activates mTORC2 signaling to counteract apoptosis and maximize viral replication*. Front Cell Infect Microbiol, 2022. **12**: p. 979996.
124. Martins Sde, T., et al., *Dendritic cell apoptosis and the pathogenesis of dengue*. Viruses, 2012. **4**(11): p. 2736-53.
125. AbuBakar, S., et al., *Senescence affects endothelial cells susceptibility to dengue virus infection*. Int J Med Sci, 2014. **11**(6): p. 538-44.
126. Krouwer, V.J., et al., *Endothelial cell senescence is associated with disrupted cell-cell junctions and increased monolayer permeability*. Vasc Cell, 2012. **4**(1): p. 12.
127. Collin, G., et al., *Transcriptional repression of DNA repair genes is a hallmark and a cause of cellular senescence*. Cell Death Dis, 2018. **9**(3): p. 259.

GLOSSARY

| | |
|-------------|----------------------------|
| DENV | Dengue Virus |
| HPI | Hours Post Infection |
| DPI | Days Post Infection |
| MOI | Multiplicity of Infection |
| HR | Homologous Recombination |
| NHEJ | Non-Homologous End Joining |
| MMR | Mismatch Repair |
| FA | Fanconi Anemia |
| DDR | DNA damage response |
| TLS | Translesion synthesis |